

AD-A273 036

Naval Command,
Control and Ocean
Surveillance Center

RDT&E Division

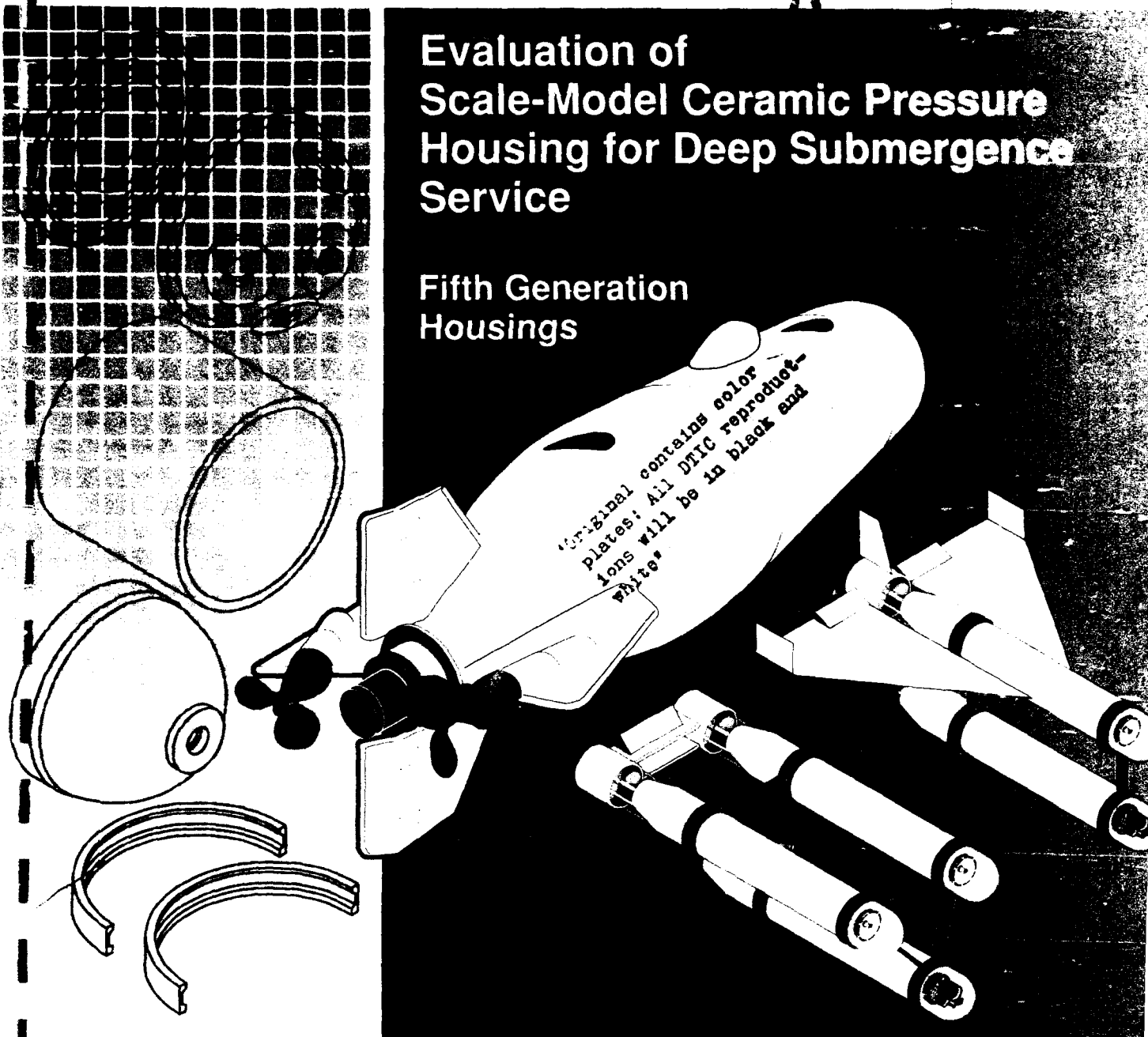
San Diego, CA
92152-5001

DTIC
1993 2 1993

2

Evaluation of Scale-Model Ceramic Pressure Housing for Deep Submergence Service

Fifth Generation Housings



J. D. Stachiw
R. P. Johnson
R. R. Kurkchubasche

Technical Report 1582
March 1993

Approved for public release; distribution is unlimited.

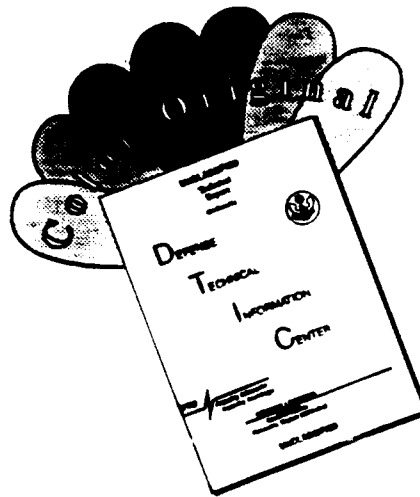


93 11 10 05 2

93-28401



DISCLAIMER NOTICE



THIS DOCUMENT IS BEST QUALITY AVAILABLE. THE COPY FURNISHED TO DTIC CONTAINED A SIGNIFICANT NUMBER OF COLOR PAGES WHICH DO NOT REPRODUCE LEGIBLY ON BLACK AND WHITE MICROFICHE.

Evaluation of Scale-Model Ceramic Pressure Housing for Deep Submergence Service

J. D. Stachiw
R. P. Johnson
R. R. Kurkchubasche

[illegible]

DTIC QUALITY INSPECTED 1

**NAVAL COMMAND, CONTROL AND
OCEAN SURVEILLANCE CENTER
RDT&E DIVISION
San Diego, California 92152-5001**

J. D. FONTANA, CAPT, USN
Commanding Officer

R. T. SHEARER
Executive Director

ADMINISTRATIVE INFORMATION

This work was performed by the Marine Materials Technical Staff, RDT&E Division of the Naval Command, Control and Ocean Surveillance Center, for the Naval Sea Systems Command, Washington, DC 20362.

Released by
J. D. Stachiw, Head
Marine Materials
Technical Staff

Under authority of
N. B. Estabrook, Head
Ocean Engineering
Division

ACKNOWLEDGMENT

Michael J. Plapp is acknowledged for his support with the finite element analysis (FEA) work done for the scale-model housing.

SUMMARY

There exists a potential requirement for large, one-atmosphere housings for deep submergence, unmanned vehicles of the U.S. Navy. Ceramics appear to be the optimum structural material for construction of such housings because of their high specific compressive strength, and modulus of elasticity. The designs for these pressure-resistant housings incorporate ceramics as the primary load-carrying material in both the cylindrical and hemispherical components of the housing structure. Only the central stiffener, joints, and penetration inserts are, at the present time, designed to be fabricated from titanium alloys.

Most of the features in the current series of housing designs have been validated in prior studies of ceramic pressure housings (references 1, 2, 3, and 4). Some, however, are new and need to be validated by testing prior to incorporating them into the current fifth-generation ceramic housing designs. These features are (1) coupling with integral stiffener for joining of cylinders, (2) hemispheres with integral cylindrical skirts, and (3) bearing gaskets of graphite fiber-reinforced (GFR) PEEK composite. To minimize costs, plans were formulated to validate the housing design by pressure testing a structural 1:2.075 scale model of the 26-inch-diameter external pressure housing assembly in the current ceramic housing program. All structural features and materials of construction were the same in both the scale-model and full-size housings. The weight-to-displacement ratio of both housings is 0.61 in seawater. In comparison, the weight-to-displacement ratio of a titanium housing assembly, with identical interior dimensions and design depth, is 0.868, representing a 42-percent increase in weight. As a result of its significantly lower weight-to-displacement ratio, the ceramic housing assembly can support a payload that is three (3) times heavier than the one carried by a titanium housing assembly.

The scale-model ceramic housing consisted of two 94-percent alumina 12.047-inch OD by 11.179-inch ID by 15.375-inch L monocoque cylinders joined by a single 12.53-inch OD by 9.88-inch ID by 2.166-inch W titanium coupling with integral T-ring

stiffener. As bulkheads served 94-percent alumina Type 1 5.717-inch ID by 0.18-inch thick and Type 2 5.717-inch ID by 0.271-inch-thick hemispheres rimmed by cylindrical skirts with 12.047-inch OD by 11.179-inch ID by 1.204-inch L dimensions. A single 2-inch ID penetration was incorporated into the pole of the Type 2 hemisphere. The ends of cylinders and hemispheres were protected with Naval Ocean Systems Center (NOSC) Type 1 titanium end caps bonded to ceramic surfaces with epoxy adhesives. A 0.04-inch-thick ring of GFR PEEK composite served as the bearing gasket between the ceramic and titanium ring plane bearing surfaces.

The 12-inch OD cylindrical scale-model ceramic housing assembly successfully withstood sustained proof testing to 10,000 psi and 100 pressure cycles to 9,000 psi design pressure. In addition, a spherical test assembly consisting of a Type 1 ceramic hemisphere mated to a titanium hemisphere successfully withstood 500 pressure cycles to 9,000 psi. When tested to destruction, the scale-model housing assembly imploded at 11,933 psi by elastic instability failure mode.

The design of the 26-inch-diameter external pressure housings assembled from 25-inch OD ceramic cylinders and hemispheres, the selection of materials, and the fabrication procedures have been validated for service to a maximum depth of 20,000 feet with a proven minimum 1.33 safety factor based on critical pressure at implosion. The safety factor can be increased to 1.87, if so required, without changing the dimensions of ceramic components. A minor modification consisting of decreasing the inner diameter of the titanium coupling stiffener from 9.88 to 8.75 inches will cause a safety factor increase. This results in a reduction of inner clear-bore diameter, which, in turn, may require the repackaging of potential payload for placement inside the cylinder assembly.

The 12-inch OD ceramic housing assembly, besides representing a 1:2.075 scale model of the ceramic hull in the 26-inch OD pressure housing assembly, can serve also as a ceramic hull with a 65-pound payload capability, for a small remotely operated deep-submergence vehicle.

CONTENTS

INTRODUCTION	1
SCALE-MODEL HOUSING	2
CONFIGURATION	2
STRESS AND STABILITY ANALYSES	2
FABRICATION	3
TESTING PROGRAM	4
INSTRUMENTATION	4
TEST ARRANGEMENTS	4
Spherical Housing Test Assembly	4
Cylindrical Housing Test Assembly	4
TEST SCHEDULE	5
Proof Testing	5
Fatigue Testing	5
Implosion Testing	5
TEST OBSERVATIONS	6
STRAINS	6
STRESSES	6
ACOUSTIC EMISSIONS	6
FATIGUE CRACKS	6
CATASTROPHIC FAILURE	6
DISCUSSION	7
STRESSES	7
ELASTIC STABILITY	7
CRACK FORMATION	8
FINDINGS	8
CONCLUSIONS	9

FEATURED RESEARCH

RECOMMENDATIONS	9
GLOSSARY	10
REFERENCES	11
APPENDIX A: ENGINEERING DRAWINGS OF SCALE-MODEL CERAMIC PRESSURE HOUSING	A-1
APPENDIX B: STRESS AND STABILITY ANALYSIS OF SCALE-MODEL CERAMIC PRESSURE HOUSING	B-1
APPENDIX C: FORMATION OF FATIGUE CRACKS IN PLANE-BEARING SURFACES OF CYLINDERS AND HEMISPHERES	C-1
APPENDIX D: EFFECT OF SACRIFICIAL END RINGS ON CYCLIC FATIGUE LIFE OF CERAMIC COMPONENTS	D-1

FIGURES

1. Components of the 12-inch OD scale-model ceramic external pressure housing assembly, Sheet 1	13
1. Components of the 12-inch OD scale-model ceramic external pressure housing assembly, Sheet 2	15
2. Ceramic hemispheres serving as bulkheads in the scale-model housing assembly (note the cylindrical skirt at the equator)	16
3. Type 2 ceramic hemisphere with 2-inch OD polar penetration	16
4. Ceramic cylinder with 12.097-inch OD by 15.375-inch L by 0.434-inch t dimensions serving as cylindrical components of the scale-model housing assembly	17
5. Titanium end caps for the ceramic cylinders	17
6. Titanium end caps for the ceramic hemispheres	18
7. Titanium coupling for the ceramic cylinders	18
8. GFR PEEK composite 0.04-inch-thick bearing gaskets for ceramic components	19
9. GFR PEEK composite gasket after bonding to the ceramic hemisphere	19
10. Cylindrical hull of the scale-model external pressure housing, assembled by adhesive-bonding two cylinders in a titanium coupling	20
11. The 0.25-inch-thick silicon rubber pads bonded to the exterior of the hemispheres serve to protect the ceramic surface against point impacts	20
12. Components of the penetrator insert and the associated bulkhead penetrator shell	21
13. Spherical test assembly consisting of a titanium hemisphere and Type 1 or 2 ceramic hemispheres joined with an aluminum spacer and fastened by a clamp band, Sheet 1	23

13. Spherical test assembly consisting of a titanium hemisphere and Type 1 or 2 ceramic hemispheres joined with an aluminum spacer and fastened by a clamp band, Sheet 2	25
14. Placement of the spherical test assembly into the pressure vessel at the Southwest Research Institute	21
15. Cylindrical housing assembly consisting of two ceramic cylinders joined by a coupling and closed off by Type 1 and 2 ceramic hemispheres, Sheet 1	27
15. Cylindrical housing assembly consisting of two ceramic cylinders joined by a coupling and closed off by Type 1 and 2 ceramic hemispheres, Sheet 2	29
16. Cylindrical housing assembly after instrumenting with electric-resistance strain gages	31
17. Placement of the cylindrical housing assembly into the pressure vessel at the Southwest Research Institute	31
18. Split retaining plate and hydraulic jack used for the removal of the ceramic hemisphere from the titanium end cap	32
19. Fatigue cracks on the plane-bearing surface of the Type 1 ceramic hemisphere after it has been subjected to 500 pressurizations to 9,000 psi	32
20. Hoop strains on the interior surface of ceramic cylinder A	33
21. Hoop strains on the interior flange of the titanium coupling	33
22. Hoop strains on the interior surface of ceramic cylinder B	34
23. Acoustic emissions generated during pressure cycling of the spherical test assembly with the Type 1 ceramic hemispheres	34
24. Acoustic emissions generated during pressure cycling of the scale-model housing assembly with both ceramic hemispheres	35
25. Metallic components of the scale-model housing assembly after catastrophic implosion at 11,933 psi	35
26. Central coupling whose buckling initiated the implosion of the housing	36
27. Detail of the buckled coupling	36
28. Detail of the buckled end cap on one of the cylinders	37
29. Interior dimensions of the end caps and central coupling after implosion of the housing	37
30. 12-inch ceramic cylinders equipped with Mod 0 and Mod 1 end caps	38
31. Dimensions of Mod 0 and Mod 1 end caps for 12-inch ceramic cylinder pressure cycle during the third generation ceramic housing study (Stachiw, 1993). Spalling was observed after 50 cycles on cylinders with Mod 0 end caps. Cylinders with Mod 1 end caps were free of spalls after 500 cycles to 9,000 psi hydrostatic loading. In both cases, a 0.02-inch-thick epoxy layer separated the ceramic bearing surfaces from metallic end caps	38

FEATURED RESEARCH

32. The ceramic cylinders on third and fourth generation housings were joined by the mechanical joint, while those in the fifth generation are joined by an adhesive-bonding coupling _____ 39

TABLES

1. Typical materials for construction of deep submergence pressure housings _____ 40
2. Comparison of alumina ceramic to titanium alloy _____ 41
3. Physical properties of selected ceramic compositions _____ 42
4. Acoustic emissions during hydrostatic testing, Sheet 1 _____ 43
4. Acoustic emissions during hydrostatic testing, Sheet 2 _____ 44
4. Acoustic emissions during hydrostatic testing, Sheet 3 _____ 45
5. Strains recorded during pressurization of the scale-model housing assembly to 9,500 psi, Sheet 1 _____ 46
5. Strains recorded during pressurization of the scale-model housing assembly to 9,500 psi, Sheet 2 _____ 47
5. Strains recorded during pressurization of the scale-model housing assembly to 9,500 psi, Sheet 3 _____ 48
5. Strains recorded during pressurization of the scale-model housing assembly to 9,500 psi, Sheet 4 _____ 49
5. Strains recorded during pressurization of the scale-model housing assembly to 9,500 psi, Sheet 5 _____ 50
5. Strains recorded during pressurization of the scale-model housing assembly to 9,500 psi, Sheet 6 _____ 51
5. Strains recorded during pressurization of the scale-model housing assembly to 9,500 psi, Sheet 7 _____ 52
5. Strains recorded during pressurization of the scale-model housing assembly to 9,500 psi, Sheet 8 _____ 53
5. Strains recorded during pressurization of the scale-model housing assembly to 9,500 psi, Sheet 9 _____ 54
5. Strains recorded during pressurization of the scale-model housing assembly to 9,500 psi, Sheet 10 _____ 55
5. Strains recorded during pressurization of the scale-model housing assembly to 9,500 psi, Sheet 11 _____ 56
6. Comparison of FEA calculations to test results on model housing components, Sheet 1 _____ 57
6. Comparison of FEA calculations to test results on model housing components, Sheet 2 _____ 58

INTRODUCTION

The United States Navy has a requirement for unmanned underwater vehicles (UUVs) with depth capabilities of 20,000 feet. Their complexity makes them heavy, such that UUVs must rely on their own displacement in water of syntactic foam to achieve neutral buoyancy.

Unmanned underwater vehicles require lightweight pressure hulls to optimize their performance (i.e., speed, range, and payload). To achieve these goals, the pressure hulls for deep-submergence vehicles require materials with high compressive strength, low density, high elastic modulus, high heat transfer, and outstanding resistance to corrosion. Ceramics appear to meet all of these criteria (table 1).¹

Since alumina ceramics are the least expensive, and the technology for their fabrication is well developed, they are the preferred choice for construction of large ceramic pressure housings. Two compositions are preferred for the fabrication of large cylinders and hemispheres from which a housing is subsequently assembled. The alumina compositions considered desirable for this application are 94- and 96-percent alumina ceramics, as they represent an optimum combination of physical properties and cost of fabrication (table 2). Their physical properties, except for fracture toughness and tensile strength, are superior to those of titanium (table 3) and, for this reason, the weight-to-displacement ratio of ceramic pressure housing assemblies is significantly lower than of pressure housings with the same dimensions and design depth.

Thus, the 6-, 12-, and 20-inch-diameter ceramic housings designed and tested in prior years by Dr. Stachiw and the 50-inch-diameter cylinder designed at Martin Marietta were fabricated from 94-percent alumina by COORS Ceramics, while the 96-percent alumina was utilized by WESGO for fabrication of the 16.5- and 22.5-inch-diameter ceramic housings for the Westinghouse Oceanic

Division. Since the difference between the structural properties of these two alumina compositions is less than 10 percent, they can be used interchangeably in the fabrication of ceramic housing components of the same design, provided that a 5- to 10-percent decrease in critical pressure associated with the 94-percent composition can be operationally tolerated.

Based on the successful performance of past Naval Ocean Systems Center (NOSC)² ceramic housings, two housings were selected to meet the projected payload and space requirements of potential deep-submergence, unmanned, autonomous vehicles for the Navy.

The design of the 25- and 32-inch-diameter ceramic cylinders and hemispheres for the 26- and 33-inch-diameter external pressure housing assemblies incorporates most of the structural features being validated in prior test programs on 6-, 12- and 20-inch-diameter ceramic housings (references 1, 2, 3, and 4). Those features are the (1) monocoque cylindrical shell, (2) metallic end caps with double flanges bonded to cylinders and hemispheres that not only protect the edges of the ceramics, but also serve as the mechanical joints between ceramic components, and (3) metallic ring stiffener that provides radial support to cylinder ends at midbay of cylindrical assembly.

In addition to the proven structural features, three new ones were introduced. The new features are (1) cylindrical skirts on the ceramic hemispheres, (2) metallic coupling with integral T-ring stiffener for joining ceramic cylinders with adhesive bonding at midbay, and (3) bearing gaskets of graphite fiber-reinforced (GFR) PEEK composite. A cylindrical skirt on the hemispheres reduces the axial stress on the hemisphere edge, and thus the propensity for initiation of fatigue cracks, by matching the thickness of the skirt to that of the cylinder. The coupling with integral T-ring stiffener is designed to minimize the weight of the joint, maximize the useful space inside the cylinder, and, at the same

1. Figures and tables are placed at the end of the text.

2. NOSC is now Naval Command, Control and Ocean Surveillance Center (NCCOSC), RDT&E Division (NRaD).

ceramic cylinders so that they do not buckle at pressures $\leq 11,250$ psi. The bearing gasket serves to reduce the propensity of the ceramic bearing surfaces to initiate cracks under repeated pressurizations of the housing.

Because of these new unproven structural design features, it was considered prudent to evaluate them experimentally before fabricating the 26- and 33-inch-diameter external pressure housing assemblies. The 26- and 33-inch-diameter ceramic cylindrical housings comprise the fifth generation of ceramic housings in the Navy's structural ceramics program. This evaluation was conducted with a scale model of the housing. Since fabrication tooling already existed from previous NCCOSC programs for 12-inch-diameter cylinders and hemispheres, this size was chosen for the scale-model housing.

SCALE-MODEL HOUSING

CONFIGURATION

The 12-inch OD ceramic housing configuration (figure 1) is an exact 1:2.075 scale copy of the structural components in the 26-inch-diameter external pressure housing assembly (reference 5). All pressure-resistant components of the large housing, after reduction in size, have been incorporated into the 12-inch housing (appendix A). Components of the 26-inch-diameter housing assembly, not serving as parts of the 25-inch-diameter ceramic pressure-resistant envelope, were omitted from the model for fabrication economy. Thus, the external plastic composite fairing for impact protection and the internal rails for payload package found on the large housings were omitted from the 12-inch-diameter scale-model housing.

STRESS AND STABILITY ANALYSES

Since the 12-inch OD housing is, in all aspects, a scale model of the full-size 26-inch OD external pressure housing assembly, there was no need to perform a detailed stress analysis of the scale-model housing, as one had already been performed for the 26-inch OD housing during its design (reference 5). Still, a general stress analysis and elastic stability analysis was performed to

check whether the geometric scaling-down process for the structural components of the 26-inch OD housing assembly was performed properly, and did not result in higher stresses in the scale model than in the full-size housing.

The results of the computer-generated analyses showed that the magnitude and orientation of stresses, as well as the elastic stability of the scale-model housing (appendix B) did not differ significantly from those calculated for the 26-inch OD full-size external pressure housing assembly (reference 5).

The finite element analysis (FEA) of the scale-model housing assembly showed that the stresses in ceramic and titanium components were within the design limits selected for large housings. Only at two locations did the calculated stresses significantly exceed the 100-percent safety margin of design stress levels (table 2): on the interior of Type 1 and 2 hemispheres at the transition zone from cylindrical to spherical surfaces, and at the edge of polar penetration in the Type 2 hemisphere. The calculated stresses at 9,000 psi external pressure exceeded the 150,000 psi compressive design stress at these locations, resulting in only a 66-percent safety margin for material failure. Since these stresses are compressive and of a local nature, the reduction of the safety margin from 100 to 66 was considered to be acceptable and no cause for concern.

The calculated stresses which caused some concern were the positive radial stresses on the plane-bearing surfaces of cylinders and hemispheres. Although their magnitude was less than 50 percent of the ceramic's Modulus of Rupture (MOR), there was no doubt that the radial stress of such magnitude will, during repeated pressurizations, initiate and support the propagation of circumferential fatigue cracks at right angles to the plane-bearing surface. It was hoped, however, that the growth rate of these fatigue cracks will not result in a catastrophic failure at less than 500 pressure cycles.

The prediction for a cyclic fatigue life in excess of 500 pressure cycles was based on the fact that the magnitude of calculated tensile radial stresses inside the edges of cylinders and hemispheres

declines rapidly with distance from the plane surface. Thus, according to the FEA, at a distance of approximately 0.5 of an inch from the plane surface, the radial stress becomes negative (i.e., compressive) and will not support further growth of circumferential cracks. Since the flanges on the titanium end caps extend approximately one inch beyond the predicted depth of the cracks in the plane-bearing surface, their presence reinforces the cracked portion of the ceramic, preventing the cracks from widening and deepening.

Based on the above considerations, it was postulated that the depth of the cracks, even after 500 pressure cycles, will not significantly increase beyond 0.5 of an inch. As a result of this postulated restraint on the extent of crack propagation, the catastrophic implosion due to the presence of cyclic fatigue cracks will not take place until the plastic composite bearing gasket has been worn out by repeated application of bearing stress. Tests performed on gasket material coupons of GFR PEEK composite between a block of 96-percent alumina and a titanium anvil have shown that the life of the test assembly is in excess of 500 cycles to 70,000 psi, 500 cycles to 80,000 psi, and 500 cycles to 90,000 psi axial bearing stress applied sequentially (reference 6).

FABRICATION

The ceramic components of the 12-inch OD scale-model housing were fabricated from 94-percent alumina ceramic by COORS Ceramics (figures 1 through 4). The fabrication process consisted of forming the green bodies by isostatic pressing, which were subsequently machined to rough dimensions prior to firing. After firing, the ceramic components were diamond ground to final dimensions. The COORS AD 94-percent alumina composition was used instead of the WESGO AL600 96-percent alumina composition from which the 25- and 32-inch-diameter ceramic cylinders and hemispheres for the 26- and 33-inch OD pressure housings are to be fabricated by WESGO. The reason for the substitution was schedule expediency, since the production of 94-percent ceramic components at COORS Ceramics was several months ahead of the production of 96-percent alu-

mina at WESGO. This substitution of materials was acceptable, as the testing of a scale-model housing fabricated from 94-percent alumina ceramic would generate conservative data because of its somewhat-lower mechanical properties (table 2).

The fabricated ceramic components were subjected to a series of quality-control tests to ensure their conformance to specifications. The quality-control tests included a dimensional check, dye penetrant application for detection of surface cracks, and sonic inspection for internal flaws. The sonic test utilized a 10-kHz 3-inch focused beam to generate a C-span by pulse-echo method. A ceramic witness specimen with 0.032-inch-diameter drilled blind holes was the calibration standard for the sonic equipment. The C-span detected only a single flaw smaller than 0.032-inch-diameter in each of the cylinders. No flaws were detected in the hemispheres.

The metallic components of the scale-model housing were machined from Ti-6Al-4V alloy; the same material used in metallic components of large housings (figures 5 through 7). The metallic components were bonded to the ceramic surfaces on ends of cylinders and hemispheres with the same epoxy compound used on large housings. The bonding process consisted of cleaning the metallic surfaces with methyl ethyl ketone to remove oil, followed by etching with SEMCO Passagel 107 to remove surface oxides. After cleaning the metallic surfaces, premixed adhesive was poured into the annular spaces in end caps and coupling. The adhesive was prepared by mixing 70 parts of CIBA Geigy 283 hardener with 100 parts of CIBA Geigy 6010 resin, followed by degassing under vacuum.

The ends of ceramic components were prepared for bonding by cleaning them with methyl ethyl ketone. Prior to insertion of the ceramic component into metallic seats, a .040-inch-thick GFR PEEK composite gasket was fastened to bearing surfaces by a bead of 5-minute epoxy applied to the chamfered edges of the ceramic component (figures 8 and 9). The bead of adhesive applied to the chamfered edge of the ceramic component sealed the interface between the plane ceramic, and composite gasket-bearing surfaces from

intrusion of epoxy adhesive during submersion of the ceramic component into the annular space of the epoxy-filled end cap. The reason for preventing the intrusion of resin between the plane-bearing surfaces of ceramic component and composite gasket is the hypothesis formulated by Dr. Stachiw that epoxy adhesive under compression in excess of its yield strength may flow like a viscous fluid into any minute crack in the ceramic surface, causing it to expand.

After pouring the adhesive into the annular space inside a metallic end cap, or coupling, the ends of ceramic cylinder or hemispheres were gradually immersed into the layer of adhesive on the bottom of annular space, causing the adhesive to extrude through the radial clearances between the ceramic component and the titanium flanges. To prevent cracking the ceramic components while inserting them to the bottom of the annular spaces of the end caps, caution was exercised. To ensure proper seating, a dead weight of 60 pounds was placed on top of the ceramic component, forcing it slowly down through the layer of epoxy. A water level placed on top of the dead weight provided real-time information on the ceramic component's departure from vertical. If the ceramic component departed from a vertical position, the dead load on top of the component was shifted to return it back to vertical. Placement of elastomer boot seals over the edges of the end caps and couplings completed the cylindrical assembly (figure 10).

After bonding the metallic components to the ceramic hemispheres and cylinders, the exterior surfaces of the hemispheres were protected from impacts by bonding 0.25-inch-thick patches of silicon rubber (figure 11). An insert was placed inside the polar penetration of the hemisphere to facilitate threading of bulkhead penetrators (figures 11 and 12).

TESTING PROGRAM

INSTRUMENTATION

The model housing assembly was instrumented with 50 biaxial strain gage rosettes. Their placement was guided by three principles: (1) detection of maximum stress, (2) validation of the finite-

element computer program, and (3) detection of incipient buckling. (For location of gages, see figure 15, drawing SK9402-035.) Since it was known from calculations that the catastrophic failure of the model housing assembly would be initiated by buckling of the midbay coupling, 15 gages were bonded to its exterior and interior surfaces. The rest of the gages were distributed over the two ceramic cylinders and hemispheres.

In addition to strain gage instrumentation, an acoustic emission detector was bonded to the exterior of the pressure vessel in which the scale-model housing was to be tested. The frequency response of the acoustic transducer was in the 50- to 200-kHz range.

TEST ARRANGEMENTS

Two kinds of test arrangements were used for pressure testing the scale-model housing. One test arrangement was specifically configured for testing the ceramic hemispheres individually, while the other test arrangement was configured for testing the whole scale-model housing assembly.

Spherical Housing Test Assembly

The spherical housing test assembly consisted of mating the ceramic hemisphere to a 12-inch-diameter titanium hemisphere by means of a spacer ring, and subsequently fastening them together with a split-wedge band (figure 13). The wedge band was equipped with ears to which nylon slings were attached for suspending the spherical test assembly below the pressure-vessel cover (figure 14). Nylon slings also were used to suspend a ballast weight below the test assembly. After successfully withstanding all the pressure tests scheduled for the ceramic hemispheres, the spherical housings were dismantled. After visual inspections, the ceramic hemispheres were integrated into the cylindrical housing test assembly.

Cylindrical Housing Test Assembly

The cylindrical housing test assembly consisted of the cylindrical hull capped at the ends with Type 1 and 2 hemispheres (figures 15 and 16). For proof and imposition testing, the cylindrical hull was capped at both ends with ceramic hemispheres.

For cyclic fatigue testing, the Type 1 ceramic hemisphere was replaced with a titanium hemisphere. In all cases, the hemispheres were fastened to the ends of the cylindrical hull with Marman clamps. Subsequently, two split-belly bands were tightened around the ends of the cylindrical body. These bands served as attachment points for four nylon slings. The upper pair of slings suspended the housing assembly vertically from the pressure-vessel end closure, while the lower pair of slings served as attachment points for ballast (figure 17). The testing arrangement was completed by feeding the instrumentation leads from the interior of the housing to the exterior of the pressure vessel cover by means of potted bulkhead penetrators.

TEST SCHEDULE

The following schedule was used for pressure testing the spherical and cylindrical model housing test assemblies.

Proof Testing

1. Spherical test assembly Type 1 (Type 1 ceramic hemisphere mated to titanium hemisphere)		0 - 10,000 psi; 60-minute hold
2. Spherical test assembly Type 2 (Type 2 ceramic hemisphere mated to titanium hemisphere)		0 - 10,000 psi; 60-minute hold
3. Cylindrical test assembly (Cylindrical ceramic hull capped by ceramic hemispheres Type 1 and 2)	Test #1	0 - 9,000 psi; 60-minute hold
	Test #2	0 - 9,500 psi; 60-minute hold
	Test #3	0 - 9,000 psi; 60-minute hold
	Test #4	0 - 10,000 psi; 60-minute hold
	Test #5	0 - 10,500 psi; 1-minute hold

Fatigue Testing

1. Spherical test assembly Type 1 Cycles 1 to 500 (Type 1 ceramic hemisphere mated to titanium hemisphere)	0 - 9,000 psi; 1-minute hold at peak pressures
2. Cylindrical test assembly Cycles 1 to 100 (Cylindrical ceramic hull capped at one end by Type 2 ceramic hemisphere and on the other end with titanium hemisphere)	0 - 9,000 psi; 1-minute hold at peak pressures

Implosion Testing

1. Cylindrical test assembly (Cylindrical ceramic hull capped by ceramic hemispheres Types 1 and 2)	0 - 11,938 psi
--	----------------

The Type 1 ceramic hemisphere was inspected for fatigue cracks after completion of 500 pressure cycles, but prior to proof testing it to 10,500 psi and, subsequently, to implosion at 11,933 psi. Since cracks were not visible on ceramic surfaces outside of the end cap flange, the end cap was removed and the plane-bearing surface was inspected where fatigue cracks would originate.

A special jig was designed to separate the titanium end cap from the ceramic hemisphere. A hydraulic jack applied axial force to the hemisphere while the titanium end cap was restrained from moving using a split retaining plate (figure 18). To facilitate removal of the hemisphere, the titanium end cap was heated to 572°F (300°C) for several hours prior to applying axial force.

The plane-bearing surfaces on the Type 1 ceramic hemisphere and the GFR PEEK gasket were inspected after removing the titanium end cap. The surface of the gasket was in good condition, showing no wear. Circumferential cracks with vertical orientation were found, however, on the ceramic plane-bearing surface (figure 19). An effort was made to establish the depth of cracks by means of ultrasonic nondestructive (ND) testing. With the aid of a 10 kHz pulse-echo applied at right angles to the external surface of the cylindrical skirt, the depth of the cracks was measured to be

FEATURED RESEARCH

approximately 0.5-to-0.75-inch. Cracks were not detected within 0.5 of an inch of the upper edge on the cylindrical skirt.

After ultrasonic inspection, the titanium end cap was re-bonded with epoxy to the Type 1 ceramic hemisphere. The refurbished Type 1 hemisphere assembly was reinstalled and the whole housing was subjected to a proof test of 10,500 psi. After successful proof test, the model housing was pressurized again, this time to implosion which occurred at 11,933 psi.

TEST OBSERVATIONS

STRAINS

Strains recorded at all locations on the ceramic surfaces were linear and of a negative nature in the whole range of pressures from 0 to 10,000 psi (table 3).

Strains recorded at all locations on titanium surfaces were all negative in hoop, and positive in axial direction. All strains were linear from 0 to 9,000 psi (figures 20 through 22). Minor deviation from linearity was observed in strains on the central coupling at pressures above 9,000 psi.

After depressurization from 10,000 psi proof pressure, the strains returned to within ± 50 micro inches/inch of strains at beginning of pressurization (table 4).

STRESSES

On ceramic surfaces the magnitude of compressive stresses calculated from recorded strains exceeded the 150,000 psi design stress at 10,000 psi proof pressure only on the concave surface at the pole of the Type 1 hemisphere. However, at 9,000 psi design pressure, all compressive stresses on the ceramic surfaces were below the design stress level (table 3). Tensile stresses were not found at any strain gage location on the ceramic surfaces.

On the titanium surfaces the magnitude of stresses calculated from recorded strains was below the 90,000 psi design stress level at 10,000 psi proof pressure. As a matter of fact, they were all below

the 60,000 psi level representing a safety factor (S.F.) of 2 based on yielding of titanium. Tensile stresses were observed only at the center of the titanium coupling, directly above and below the circumferential web joining the outer flange to the inner one. Their presence indicated that the flanges were deflecting with respect to the web of the stiffener.

ACOUSTIC EMISSIONS

The acoustic emissions recorded during pressure cycling of the Type 1 ceramic hemisphere displayed the typical Kaiser effect, i.e., the total number of events generated by each cycle progressively decreased with cycling from 515 events to approximately 15 after 50 cycles (figure 23). However, at about every tenth cycle, the number of events increased by one or more orders of magnitude followed immediately by cycles with less than 20 events.

Acoustic emissions were monitored only during the first three pressure cycles of the scale-model housing. The Kaiser effect was pronounced here as well (figure 24).

FATIGUE CRACKS

Fatigue cracks were observed on the plane-bearing surface of the Type 1 ceramic hemisphere after the titanium end cap was removed at the conclusion of the 500 cycles to 9,000 psi (figure 19). Their shallow depth (0.75 inch) after 500 cycles seems to indicate that they ceased to grow further in depth after having reached the location below the bearing surface where FEA has shown that only compressive stresses exist.

It is not known definitively when the first crack initiated, but it is surmised from the periodic bursts of acoustic emissions developed during the 8th, 13th, 22nd, 31st, 37th, and 42nd cycles that the cracks initiated in those early cycles and progressively grew in depth during the following cycles at irregular intervals.

CATASTROPHIC FAILURE

The catastrophic feature which took place at 11,933 psi during short-term pressurization at the conclusion of the testing program was initiated by

elastic instability (i.e., elastic buckling) of the central coupling with the integral stiffener. This can be seen from photographs of the failed coupling (figures 25 through 28). The coupling was deformed into a slight oval (figure 29) before the exterior flange was ripped apart at the location where the ceramic cylinder fractured. The flanges on the end caps for hemispheres displayed similar deformation to that on the central coupling.

DISCUSSION

STRESSES

The correlation between stresses calculated on the basis of measured strains, and stresses predicted by FEA is quite good (table 5). In most cases, the difference is less than 10 percent. In all cases, the stresses generated by FEA were higher than those calculated on the basis of strains. The reason for this difference lies in the fact that FEA values shown in table 5 were read from the upper, rather than the lower range of color bands on the computer-generated stress plots. The difference between the magnitudes of FEA and experimentally determined stresses is small enough and in the right direction to consider the FEA program validated for the model housing.

Since none of the stresses on ceramic surfaces exceed the -150,000 and +200,000 psi design stress limits at 9,000 psi design pressure loading, the ceramic structure can be considered well designed for its design pressure. None of the stresses on the titanium components exceed the 90,000 psi design stress level, indicating that the metallic components are also well designed for the 9,000 psi design pressure loading.

As a matter of fact, all the stresses recorded on both the ceramic and the titanium parts are less than 50 percent of the stress at which material failure is known to take place for these materials. This should not be interpreted as total absence of any peak stresses above the 50-percent level of material failure, as these are locations difficult to instrument (i.e., edge of penetration in the Type 2 hemisphere, and transition from spherical to cylindrical curvature on the inside of hemispheres)

where FEA predicts stresses in the 150,000- to 200,000-psi range.

ELASTIC STABILITY

The correlation between the 12,208-psi critical pressure predicted by the BOSOR4 computer program and the 11,933-psi implosion pressure at which the housing failed is very good. The 275 psi difference between the actual and calculated failure pressure is probably due to the fact that the calculated value was based on the elastic modulus of 44×10^6 psi obtained from the manufacturer's sales brochure for 94-percent alumina, while the elastic modulus in the fabricated ceramic component was probably only 43×10^6 psi.

The mode of buckling was as predicted; the housing failed by formation of lobes (i.e., it became noncircular) as can be seen from the somewhat elliptical shape of the failed central coupling with integral stiffener (figure 30). The plastic deformation of the coupling was not very severe since the force of the implosion of the housing was reduced significantly due to the fact that its interior was 80-percent filled with water prior to destructive testing.

The buckling of the housing was triggered by the buckling of the titanium coupling. This took place when the magnitude of radial loading upon the coupling, consisting of hydrostatic pressure and radial-bearing stress generated by radial contradiction of ceramic cylinder ends under pressure, exceeded the elastic stability of the coupling.

The radial support provided by the coupling to the cylinder ends was substantial (figures 20 through 22) as can be seen from the comparison of hoop strains at midbays of both cylinders with an internal flange of the coupling stiffener. At 9,000 psi pressure, the average hoop strain on the interior surface of cylinders at midbay was -2410 microinches/inch, while on the interior and external surfaces of the coupling flanges, it was only -1711 and -1071 microinches/inch, respectively. The strains were linear to 9,500 psi pressure. At higher pressures, the hoop strains on the coupling begin to depart from linearity. At 10,000-psi proof pressure, the departure from linearity is in the 5-percent range.

CRACK FORMATION

The use of NOSC Mod 1 end caps and GFR PEEK composite bearing gaskets resulted in a cyclic fatigue life (defined as absence of visible spalling above metallic end caps) in excess of 500 cycles to design pressure. Although some fatigue cracks were observed on the plane-bearing surfaces after removal of end caps at the conclusion of the 500 cycles, their depth did not exceed the height of the flanges on the end caps. As a result, there was no leakage or reduction in the load-carrying ability of the ceramic components. Destructive testing of the housing to implosion supports this postulate, as the housing imploded at a pressure calculated for a housing without any cracks.

Taking into account that (1) the maximum depth of the axial cracks on the bearing surface did not exceed 0.75 inch after 500 pressure cycles, (2) the height of the cap flanges extends 1.0 inch, and (3) the implosion pressure did not reflect the presence of cracks, it can be postulated that the ceramic component would not have failed even if the cycling was continued for an additional 100 to 500 cycles.

From the present data, it cannot be determined whether the long fatigue life can be attributed solely to the usage of composite gaskets, high cap flanges, or the 50-percent reduction in axial bearing stress resulting from addition of the cylindrical skirt to the hemispheres, or all of the above. A recently completed study at NRaD (appendix C) has shown that under repeated axial bearing stress of 75,000 psi on plane-bearing surfaces of 8-inch-diameter alumina-ceramic cylinders equipped with Mod 1 aluminum end caps, fatigue cracks have not been observed after 300 pressure cycles on surfaces that were resting on a 0.04-inch-thick GFR PEEK composite gasket.

Another NRaD study (reference 2) conducted with 12-inch-diameter cylinders has shown definitely that the fatigue life of ceramic bearing surfaces is a function of flange height on end caps; the higher the flanges, the longer the fatigue life (i.e., the rate of crack propagation is inversely related to height of flanges). In that study, ceramic cylinder ends protected by end caps with 1.3-inch-high flanges

and resting on a 0.01-inch-thick epoxy layer have demonstrated a cyclic fatigue life (defined as absence of visible spalling above metallic flanges) under 65,000 psi axial loading in excess of 500 pressure cycles, while those protected by end caps with 0.30-inch-high flanges failed at less than 100 cycles (figures 30 and 31).

Thus, it appears that the only firm conclusion that can be formulated on the basis of the data is that the initiation and propagation of cyclic fatigue cracks on the plane-ceramic bearing surface is not accelerated by the presence of the 0.04-inch-thick GFR PEEK composite gasket. However, a high probability exists that the GFR PEEK composite gasket does increase the fatigue life of ceramic bearing surfaces. To prove this would require, however, extensive (>1,000 cycles to 9,000 psi) pressure cycling of ceramic cylinders with, and without, GFR PEEK composite gaskets.

FINDINGS

1. The metallic coupling with integral ring stiffener is a cost effective way for permanently joining ceramic cylinders. It replaces four metallic components of a removable mechanical joint (figure 32) with a single one (i.e., two end caps, a central stiffener, and a split wedge band are replaced by a single coupling with integral ring stiffener).
2. The metallic coupling with integral ring stiffener is a weight effective way for providing radial support to an assembly of monocoque ceramic cylinders, provided that restrictions are not imposed on the height of the web connecting the stiffener flange to the coupling. In such a case, it is superior to the mechanical joint with separate stiffener ring, wedge band, and end caps.
3. In applications where access to the interior (i.e., clear ID of the housing) of the cylindrical housing is to be maximized, the coupling with an integral ring stiffener provides more radial support to the adjoining ceramic cylinders than a mechanical joint with a separate joint stiffener of the same height as the coupling.
4. The model housing design provides a proven 19-percent safety margin over the 10,000 psi

proof pressure. Since a 25-percent safety margin over proof pressure was specified for the 26- and 33-inch full-size ceramic housings, the couplings for the full-size housings need to be modified to raise the safety margin at proof pressure to the 25-percent level.

5. The cylindrical skirt on the ceramic hemispheres with the same thickness as the mating cylinder reduces the axial bearing stress in the hemisphere by 50 percent without introducing any tensile stresses at the transition from cylindrical to hemispherical shape. The 50-percent reduction in axial bearing stress has increased the cyclic fatigue life of the hemispheres to the same number of cycles as the monocoque ceramic cylinders (i.e., in excess of 500 cycles to 9,000 psi).

CONCLUSIONS

The 12-inch-diameter scale-model of the 26-inch-diameter alumina-ceramic pressure housing assembly consisting of a 25-inch-diameter ceramic

cylindrical hull with hemispherical ceramic bulkheads has met all the design requirements of pressure housings for unmanned, underwater vehicles with a maximum operational depth of 20,000 feet (6,096 meters).

The scale-model housing has demonstrated at 9,000 psi maximum working pressure a safety factor of 1.50 based on material strength, and 1.33 based on critical pressure by buckling. The cyclic fatigue has been found to be in excess of 500 pressurizations to maximum working pressure.

RECOMMENDATIONS

All design features of the scale-model housing should be incorporated into the 26-inch-diameter full-size external pressure housing assembly. The only change recommended is an 11-percent increase in width of coupling web and flanges in order to increase the critical pressure by buckling from 11,933 psi to 12,500 psi. This would provide the scale-model housing with a 25-percent safety margin over 10,000 psi proof pressure.

FEATURED RESEARCH

GLOSSARY

AUTB	Advanced Ultrasonic Test Bed	NDT	nondestructive test
FEA	finite element analysis	NDE	nondestructive evaluation
FEM	finite element model	ND	nondestructive
GFRP	graphite fiber-reinforced peek	NOSC	Naval Ocean Systems Center
ID	inner diameter	OD	outside diameter
IED	independent exploratory development	PEEK	poly-ether-ether-ketone
Kpsi	one thousand psi	rms	root mean square
L	length	SAM	Scanning Acoustic Microscopy
L/D	length/diameter	S.F.	stress factor
MEK	methyl ethyl ketone	t	ceramic shell thickness
MOR	Modulus of rupture	t/D	thickness diameter
		t/Ro	thickness external radius
		W	width
		W/D	weight-to-displacement

REFERENCES

1. Burke, M. A. 1991. "The Selection and Testing of a Gasket Material to Interface Between Ceramic and Metallic Pressure Vessel Components," Westinghouse Science and Technology Center Document No. 91-8TC3-GORDN-R1 (Aug).
2. Farnworth, S. K. 1992. "Ceramic-Metal Joint Screening Test Report," Westinghouse Electric Corporation Oceanic Division, Ocean Engineering Report 92 (Apr).
3. Johnson, R. P., R. R. Kurkchubasche, and J. D. Stachiw. 1993. "Design and Structural Analysis of Alumina Ceramic Housings For Deep Submergence Service—Fifth Generation Housings," NRaD TR 1583 (Mar), NCCOSC RDT&E Division, San Diego, CA.
4. Stachiw, J. D. and J. L. Held. 1987. "Exploratory Evaluation of Alumina Ceramic Housings for Deep Submergence Service—The Second Generation NOSC Ceramic Housings," NOSC TR 1176 (Sep), Naval Ocean Systems Center, San Diego, CA.
5. Stachiw, J. D. 1990. "Exploratory Evaluation of Alumina Ceramic Housings for Deep Submergence Service—Fourth Generation Housings," NOSC TR 1355 (Jun), Naval Ocean Systems Center, San Diego, CA.
6. Stachiw, J. D. 1992. "Adhesive Bonded Mod 1 Joint With Improved Cyclic Fatigue Life For Ceramic External Pressure Housings—Fourth Generation Housings," NRaD TR 1587 (Oct), NCCOSC RDT&E Division, San Diego, CA.
7. Stachiw, J. D. 1989. "Exploratory Evaluation of Alumina Ceramic Housings for Deep Submergence Service—Third Generation Housings," NOSC TR 1314 (Sep), Naval Ocean Systems Center, San Diego, CA.

	8	7	6	5	
					▼
	NOTES				
	<p>⚠ V-BAND COUPLING (ITEM 7) MAY BE PURCHASED FROM:</p> <p>CLAMPCO PRODUCTS, INC 145 RAINBOW ST. WADSWORTH, OH 44281 (216) 336-8857</p>				
D	<p>⚠ O-RINGS (ITEMS 18 & 19) MAY BE PURCHASED FROM:</p> <p>PARKER SEAL GROUP O-RING DIVISION 2360 PALUMBO DRIVE P.O. BOX 11751 LEXINGTON, KY 40512 (606) 269-2351</p>				
	<p>⚠ EPOXY RESIN AND HARDENER (ITEMS 22 & 23) AND PASA GELL 107 (ITEM 24) MAY BE PURCHASED FROM</p> <p>YALE ENTERPRISES 4055 PACIFIC HIGHWAY SAN DIEGO, CA 92110 (619) 299-7710</p>				
C	<p>⚠ 5 MINUTE EPOXY AND HARDENER (ITEM 26) MAY BE PURCHASED FROM</p> <p>DEVCON CORPORATION DANVERS, MA 01923</p>				
	<p>5. GASKET (ITEM 20) BONDING PROCEDURE:</p> <p>A. WIPE THE END OF THE CERAMIC CYLINDER (ITEM 17) WITH METHYL ETHYL KETONE UNTIL PAPER TOWEL SHOWS NO FURTHER DISCOLORATION</p> <p>B. CENTER GASKET ON CERAMIC CYLINDER END USING GASKET ASSEMBLY FIXTURE (ITEM 21). MIX EQUAL PARTS 5 MINUTE EPOXY AND HARDENER (ITEM 26) AND APPLY TO INTERFACE BETWEEN GASKET AND CERAMIC CYLINDER USING 5 MINUTE EPOXY MIXTURE. REMOVE GASKET ASSEMBLY FIXTURE AND SEAL ID INTERFERENCE BETWEEN GASKET AND CERAMIC CYLINDER USING 5 MINUTE EPOXY MIXTURE. EXCESS 5 MINUTE EPOXY MIXTURE SHOULD BE REMOVED WHILE EPOXY IS STILL SOFT.</p> <p>C. REPEAT THIS BONDING PROCEDURE FOR REMAINING CERAMIC CYLINDER ENDS AND CERAMIC HEMI ENDS.</p>				
	<p>6. ENDCAP AND CENTRAL STIFFENER (ITEMS 4, 5 & 6) BONDING PROCEDURE:</p> <p>A. WIPE THE INTERIOR OF THE CYLINDER ENDCAP (ITEM 4) WITH METHYL ETHYL KETONE UNTIL PAPER TOWEL SHOWS NO FURTHER DISCOLORATION</p> <p>B. PASSIVATE THE INTERIOR OF THE CYLINDER ENDCAP BY APPLYING A LAYER OF PASA GELL 107 (ITEM 25) AND ALLOWING IT TO ETCH THE TITANIUM SURFACE FOR 30 MINUTES. RINSE OFF INTERIOR OF CYLINDER ENDCAP AND ALLOW SURFACES OF TITANIUM TO AIR DRY. AIR DRYING CAN BE ACCELERATED WITH A FORCED AIR HEATER.</p> <p>C. LAY THE CYLINDER ENDCAP FLAT WITH ITS BEARING SURFACE FACING DOWN ON THE HORIZONTAL WORKING SURFACE. MIX 100 PARTS EPOXY RESIN AND HARDENER (ITEM 23) AND POUR A .50 INCH DEEP LAYER IN THE INTERIOR OF THE CYLINDER ENDCAP.</p> <p>D. LOWER THE END OF THE CERAMIC CYLINDER WITH BONDED GASKET INTO THE CYLINDER ENDCAP PARTIALLY FILLED WITH THE EPOXY MIXTURE SO IT IS CENTERED WITHIN THE CYLINDER ENDCAP. ALLOW THE CERAMIC CYLINDER TO SETTLE EVENLY INTO THE CYLINDER ENDCAP UNTIL THE CERAMIC CYLINDER RESTS ON THE BOTTOM OF THE CYLINDER ENDCAP. ADDITIONAL WEIGHT UP TO 50 LBS CAN BE PLACED ON TOP OF THE CERAMIC CYLINDER TO HELP IT SETTLE EVENLY THRU THE EPOXY MIXTURE. CARE SHOULD BE TAKEN TO ASSURE THE CERAMIC CYLINDER REMAINS CENTERED WITHIN THE CYLINDER ENDCAP AND THE CENTERLINE OF THE CERAMIC CYLINDER STAYS PERPENDICULAR TO THE WORKING SURFACE THROUGHOUT THE BONDING PROCEDURE.</p> <p>E. WIPE OFF ANY SURPLUS EPOXY MIXTURE FROM THE EXTERIOR OF THE CYLINDER ENDCAP THAT EXTRUDED OUT DURING THE BONDING PROCEDURE. ASSEMBLY AND ANY SETTLING WEIGHTS USED UNDISTURBED FOR AT LEAST 24 HOURS TO ALLOW THE EPOXY MIXTURE TO BEGIN TO CURE. ONCE CURE PERIOD HAS PASSED, ANY EXCESS EPOXY MIXTURE REMAINING ON THE EXTERIOR OF THE CYLINDER ENDCAP SHOULD BE COMPLETELY REMOVED. COAT OF SILICONE COMPOUND (ITEM 25) TO THE EXTERIOR SURFACES OF THE CYLINDER ENDCAP PRIOR TO BONDING THE CERAMIC CYLINDER MAY BE APPLIED TO THE EXTERIOR OF THE CYLINDER ENDCAP. DO NOT ALLOW SILICONE COMPOUND ON OR NEAR ANY BONDING SURFACES.</p> <p>F. REPEAT THIS BONDING PROCEDURE FOR THE REMAINING ENDCAPS AND CENTRAL STIFFENER</p>				
B	<p>7. APPLY A LIGHT FILM OF SILICONE COMPOUND (ITEM 25) TO O-RINGS (ITEMS 17, 18 & 19) PRIOR TO ASSEMBLY.</p>				
A					
	8	7	6	5	▲

SUMMARY
CLASSIFICATION: C
CHARACTERISTICS
DOD-STD-2101 (C)
CRITICAL: NONE
MAJOR: NONE

Figure 1. Components of the 12-inch OD scale-model ceramic external pressure housing assembly, Sheet 1.

5		4		3		2		1	
SHEET NO.		REV. STATUS		ZONE		DESCRIPTION		DATE	
SK9402-044		REV. STATUS		ZONE		DESCRIPTION		DATE	
						ADD OVERALL DIMENSION TO SHEET 2		8/19/92	
						UPDATE NOTES AND PARTS LIST		10/23/92	
						UPDATE ASSEMBLY NOTES		11/27/92	
						UPDATE TITLE BLOCK		12/11/93	
						5 MINUTE EPOXY AND HARDENER		26	
						SILICONE COMPOUND		ML-S-8560	
						PASA GELL 107		24	
						CIBA GEIGY 283 HARDENER		23	
						CIBA GEIGY 6010 EPOXY RESIN		22	
1		55910		SK9402-078		GASKET ASSY FIXTURE, MOD HOUS.		21	
6		55910		0128902		GASKET, MODEL HOUSING		20	
2				2-226		O-RING		19	
1				2-219		O-RING		18	
2		55910		SK9402-045		O-RING, MODEL HOUSING		17	
2		55910		SK9402-042		JACKET, HEMISPHERE, MOD HOUS		16	
2		55910		SK9402-041		JACKET, CYLINDER, MOD HOUS		15	
2		55910		SK9402-040-2		SEAL, HEMISPHERE, MOD. HOUS		14	
4		55910		SK9402-039-3		SEAL, CYLINDER, MOD HOUS.		13	
1		55910		SK9402-032-2		PADS, PENETRATION, MOD. HOUS		12	
1		55910		SK9402-032-1		PADS, PENETRATION, MODEL HOUS		11	
1		55910		SK9402-038		ELECTRICAL FEEDTHRU		10	
1		55910		SK9402-031-2		PENETRATION, ELEC FEEDTHRU		9	
1		55910		SK9402-031-1		PENETRATION, ELEC. FEEDTHRU		8	
2				V0119300N-129852		V-BAND COUPLING		7	
1		55910		SK9402-007		CENTRAL STIFFENER, MOD HOUS		6	
2		55910		SK9402-006		HEMISPHERE ENDCAP, MOD. HOUS.		5	
2		55910		SK9402-005		CYLINDER ENDCAP, MOD. HOUS.		4	
1		55910		SK0226923		CERAMIC HEMI, TYPE 2, MOD HOUS.		3	
1		55910		SK0226922		CERAMIC HEMI, TYPE 1, MOD HOUS.		2	
2		55910		SK0226921		CERAMIC CYLINDER, MOD HOUS.		1	
1		55910		SK0226920		CERAMIC CYLINDER, MOD HOUS.		1	
1		55910		SK0226919		CERAMIC CYLINDER, MOD HOUS.		1	
1		55910		SK0226918		CERAMIC CYLINDER, MOD HOUS.		1	
1		55910		SK0226917		CERAMIC CYLINDER, MOD HOUS.		1	
1		55910		SK0226916		CERAMIC CYLINDER, MOD HOUS.		1	
1		55910		SK0226915		CERAMIC CYLINDER, MOD HOUS.		1	
1		55910		SK0226914		CERAMIC CYLINDER, MOD HOUS.		1	
1		55910		SK0226913		CERAMIC CYLINDER, MOD HOUS.		1	
1		55910		SK0226912		CERAMIC CYLINDER, MOD HOUS.		1	
1		55910		SK0226911		CERAMIC CYLINDER, MOD HOUS.		1	
1		55910		SK0226910		CERAMIC CYLINDER, MOD HOUS.		1	
1		55910		SK0226909		CERAMIC CYLINDER, MOD HOUS.		1	
1		55910		SK0226908		CERAMIC CYLINDER, MOD HOUS.		1	
1		55910		SK0226907		CERAMIC CYLINDER, MOD HOUS.		1	
1		55910		SK0226906		CERAMIC CYLINDER, MOD HOUS.		1	
1		55910		SK0226905		CERAMIC CYLINDER, MOD HOUS.		1	
1		55910		SK0226904		CERAMIC CYLINDER, MOD HOUS.		1	
1		55910		SK0226903		CERAMIC CYLINDER, MOD HOUS.		1	
1		55910		SK0226902		CERAMIC CYLINDER, MOD HOUS.		1	
1		55910		SK0226901		CERAMIC CYLINDER, MOD HOUS.		1	
1		55910		SK0226900		CERAMIC CYLINDER, MOD HOUS.		1	
1		55910		SK0226899		CERAMIC CYLINDER, MOD HOUS.			

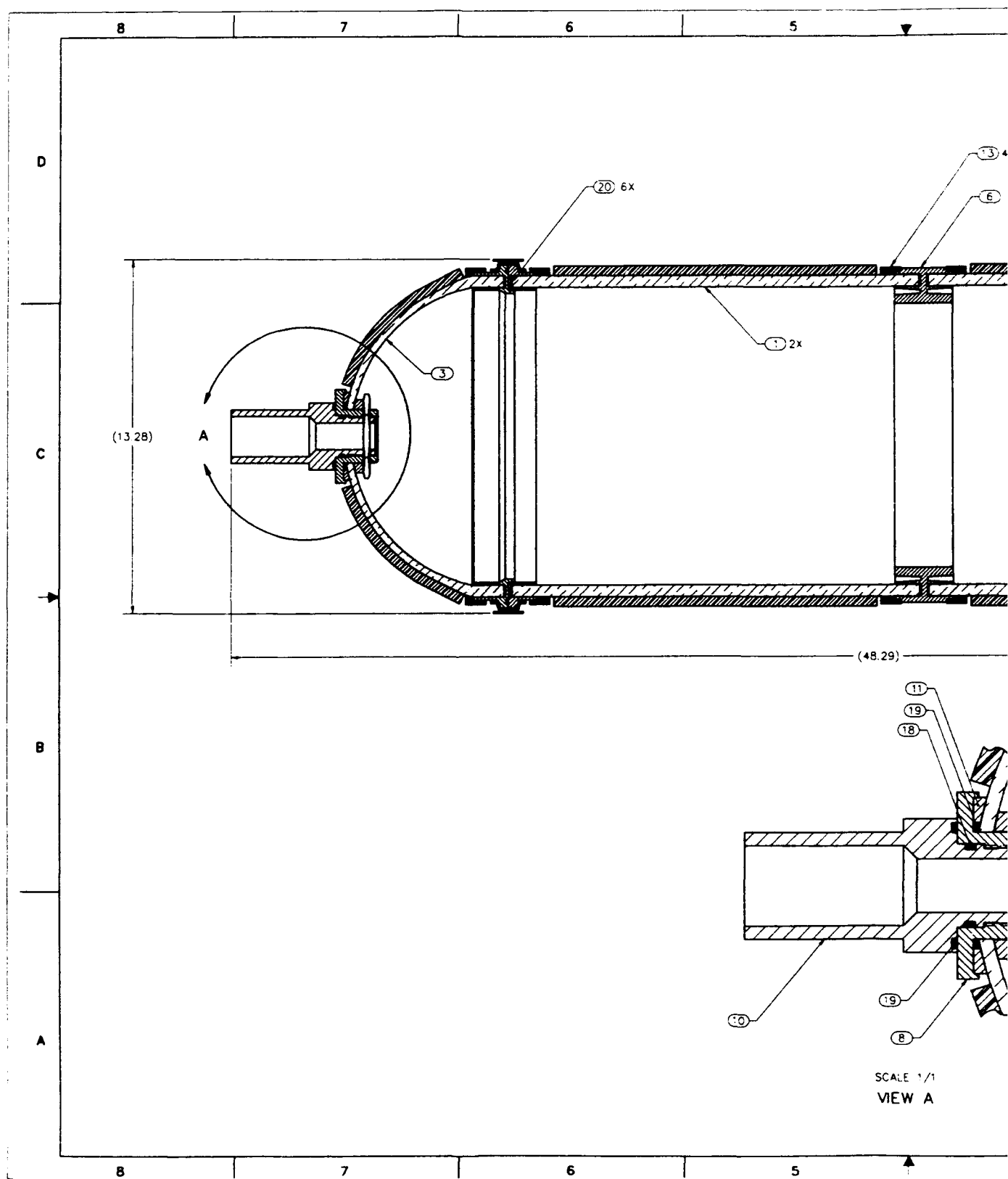
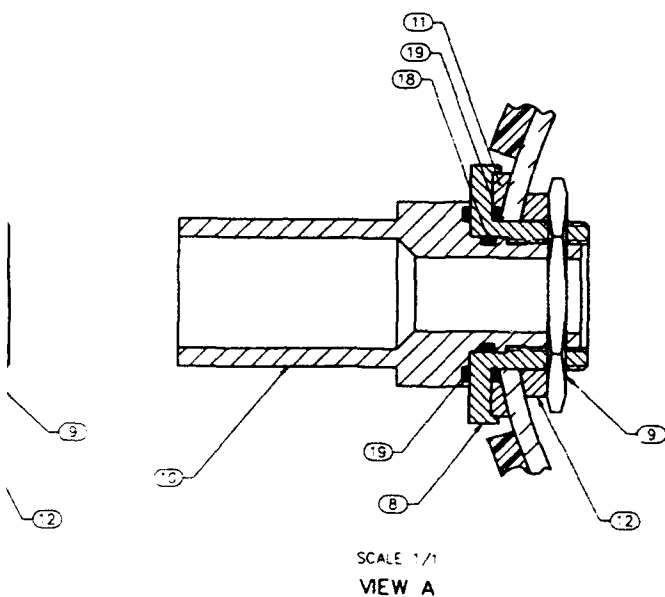
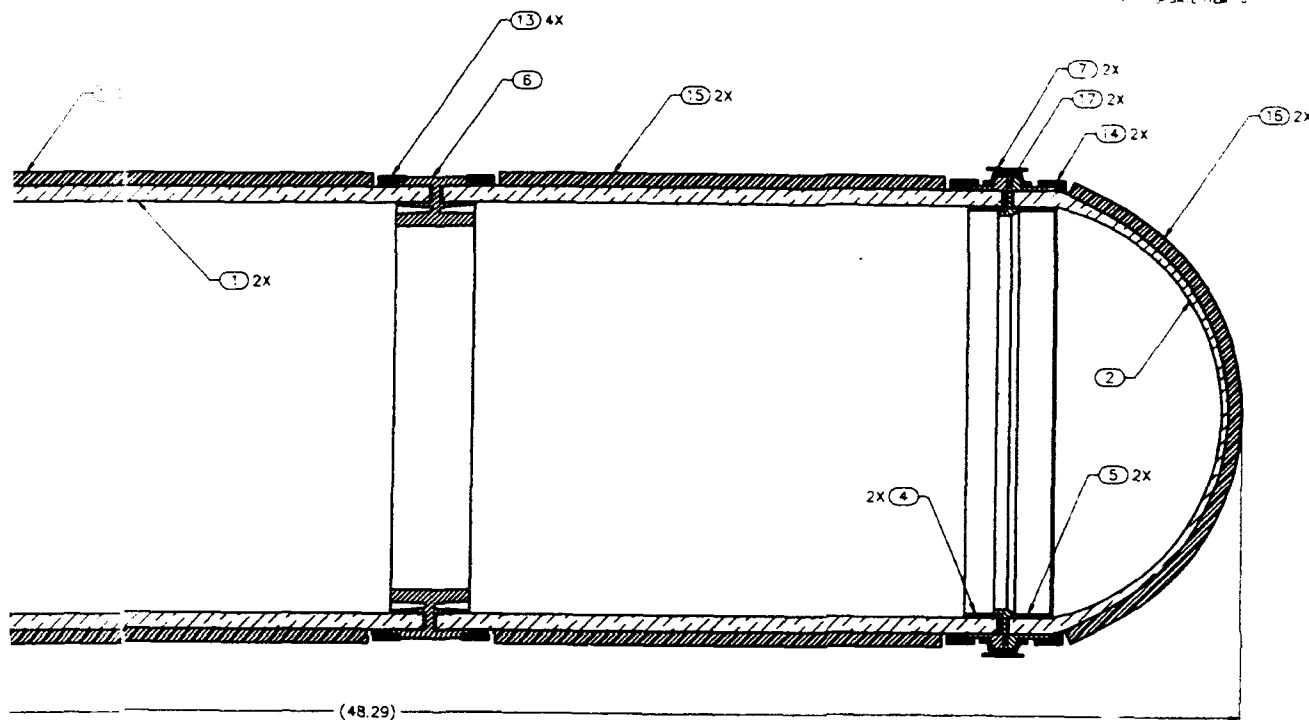


Figure 1. Components of the 12-inch OD scale-model ceramic external pressure housing assembly, Sheet 2.

DWG NO SK9402-044

REVISIONS			
ZONE	TR	DESCRIPTION	DATE
1		ADD OVERALL DIMENSION	8/20/92
2		UPDATE CYLINDER JACKET	10/13/92
3		REMOVE ITEM 2	11/7/92
4		UPDATE ITEM 10	11/16/92
			3/11/93



SIZE	CAGE CODE	DRAWING NUMBER
D	55910	SK9402-044
SCALE	1/2	SHEET 2

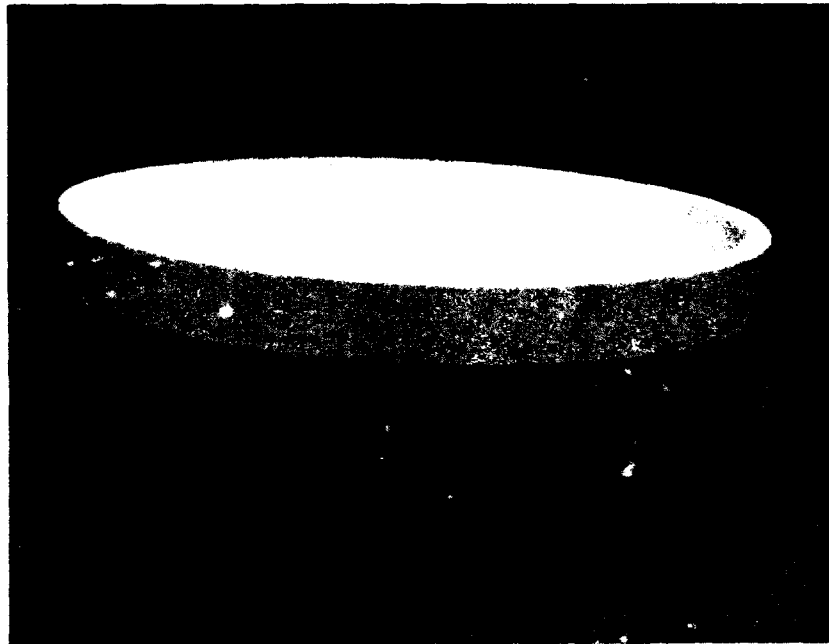


Figure 2. Ceramic hemispheres serving as bulkheads in the scale-model housing assembly (note the cylindrical skirt at the equator.)

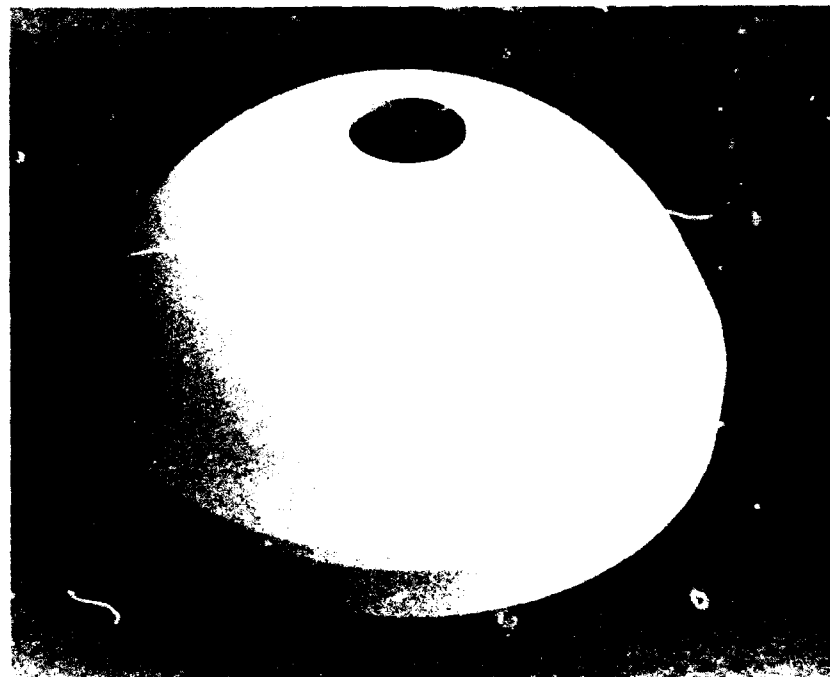


Figure 3. Type 2 ceramic hemisphere with 2-inch OD polar penetration.



Figure 4. Ceramic cylinder with 12.097-inch OD by 15.375-inch L by 0.434-inch t dimensions serving as cylindrical components of the scale-model housing assembly.



Figure 5. Titanium end caps for the ceramic cylinders.



Figure 6. Titanium end caps for the ceramic hemispheres.



Figure 7. Titanium coupling for the ceramic cylinders.

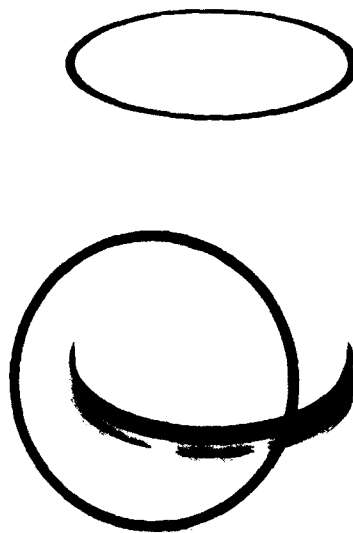


Figure 8. GFR PEEK composite 0.04-inch-thick bearing gaskets for ceramic components



Figure 9. GFR PEEK composite gasket after bonding to the ceramic hemisphere.



Figure 10. Cylindrical hull of the scale-model external pressure housing, assembled by adhesive-bonding two cylinders in a titanium coupling.



Figure 11. The 0.25-inch-thick silicon rubber pads bonded to the exterior of the hemispheres serve to protect the ceramic surface against point impacts.

FEATURED RESEARCH



Figure 12. Components of the penetrator insert and the associated bulkhead penetrator shell.



Figure 14. Placement of the spherical test assembly into the pressure vessel at the Southwest Research Institute.

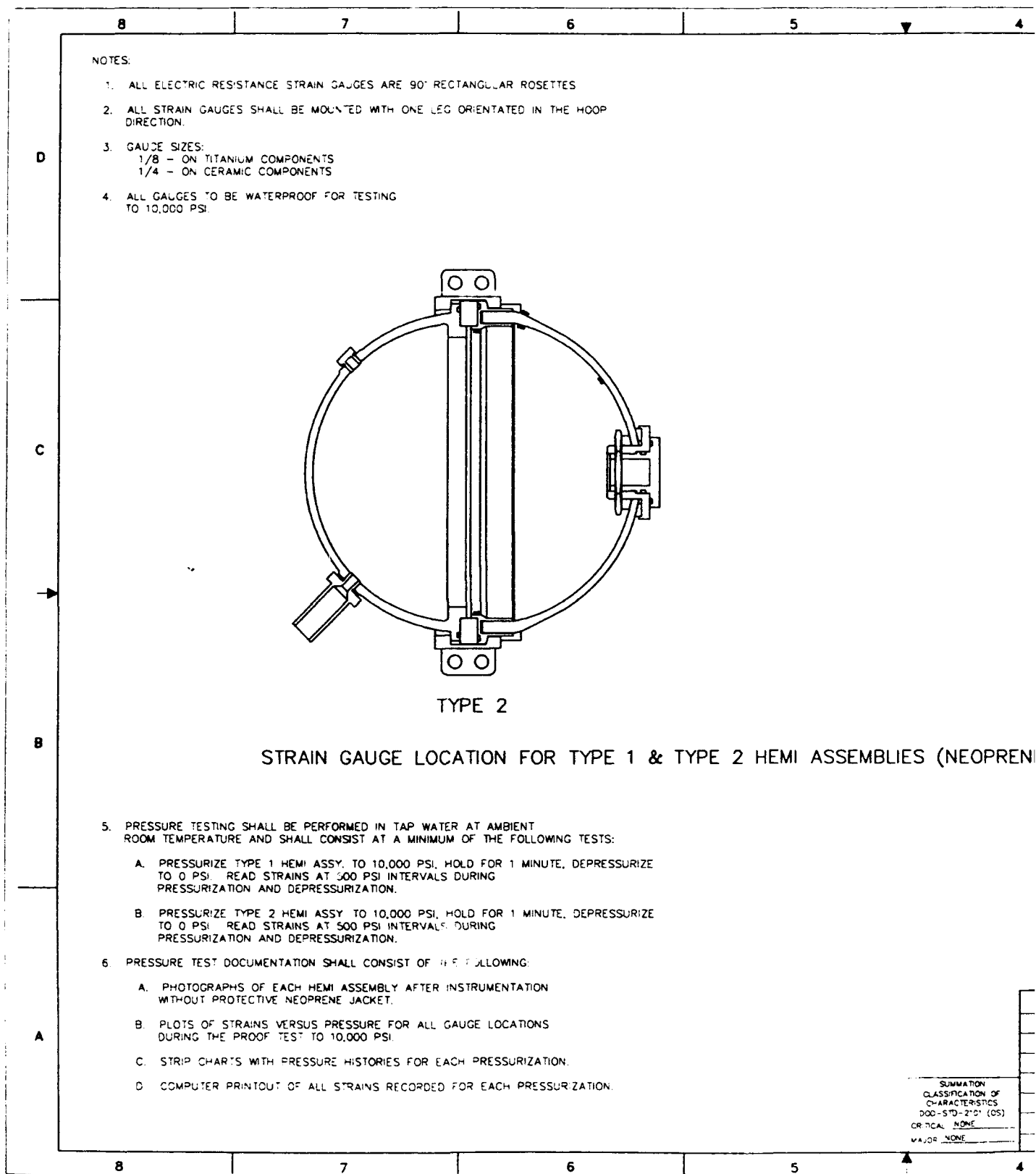
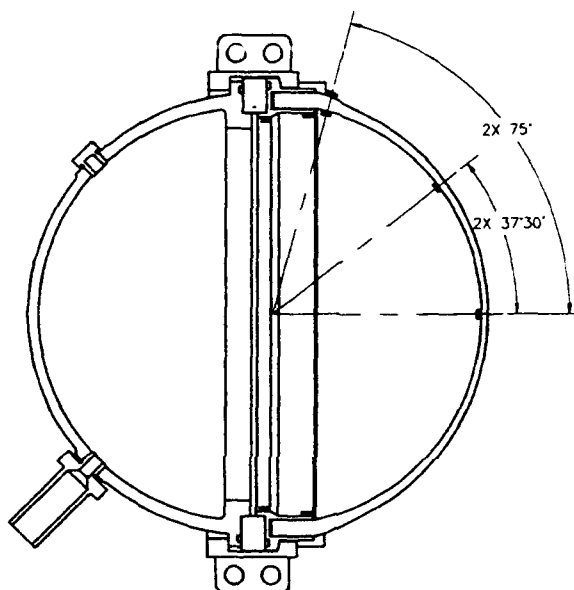


Figure 13. Spherical test assembly consisting of a titanium hemisphere and Type 1 or 2 ceramic hemispheres joined with an aluminum spacer and fastened by a clamp band, Sheet 1.

FEATURED RESEARCH

5	4	3	2	1
DWG NO. SK9402-080			REV. NO.	
REV. STATUS OF SHEETS			REVISIONS	
ZONE			DESCRIPTION	DATE
			UPDATE TITLE BLOCK	11/17/92
				3/11/93



TYPE 1

JACKETS
MI ASSEMBLIES (NEOPRENE JACKETS REMOVED FOR CLARITY)

QTY REQD	CAGE CODE	PART OR IDENTIFYING NUMBER	DESCRIPTION OR NOMENCLATURE	MATERIAL/SPEC/REF DESG	FIND NO.
PARTS LIST					
INTERPRET DRAWING IN ACCORDANCE WITH DOD-STD-100			NAVAL COMMAND, CONTROL, AND OCEAN SURVEILLANCE CENTER RESEARCH, DEVELOPMENT, TEST AND EVALUATION DIVISION SAN DIEGO, CA 92152-5000		
DO NOT SCALE THIS DRAWING			TEST CONFIGURATION, MODEL HEMISPHERES		
UNLESS OTHERWISE SPECIFIED: DIMENSIONS ARE IN INCHES BREAK ALL EDGES REMOVE ALL BURRS TOLERANCES ARE: XX ± XXX ± ANGLES ± MAX FILLETS MAX SURFACE ROUGHNESS ✓			APPROVED: J. STACHIV	SIZE: D 55910	
NEXT ASSY USED ON APPLICATION RELEASED DATE			CHECKED: R. KURKCHUB	DRAWING NUMBER: SK9402-080	
SUMMATION CLASSIFICATION OF CHARACTERISTICS DOD-STD-2101 (OS) CRITICAL: NONE MAJOR: NONE			PREPARED: R. JOHNSON	SCALE: 1/2 94020801 SHEET 1 OF 2	
BY: DIRECTION			APPROVED FOR:		

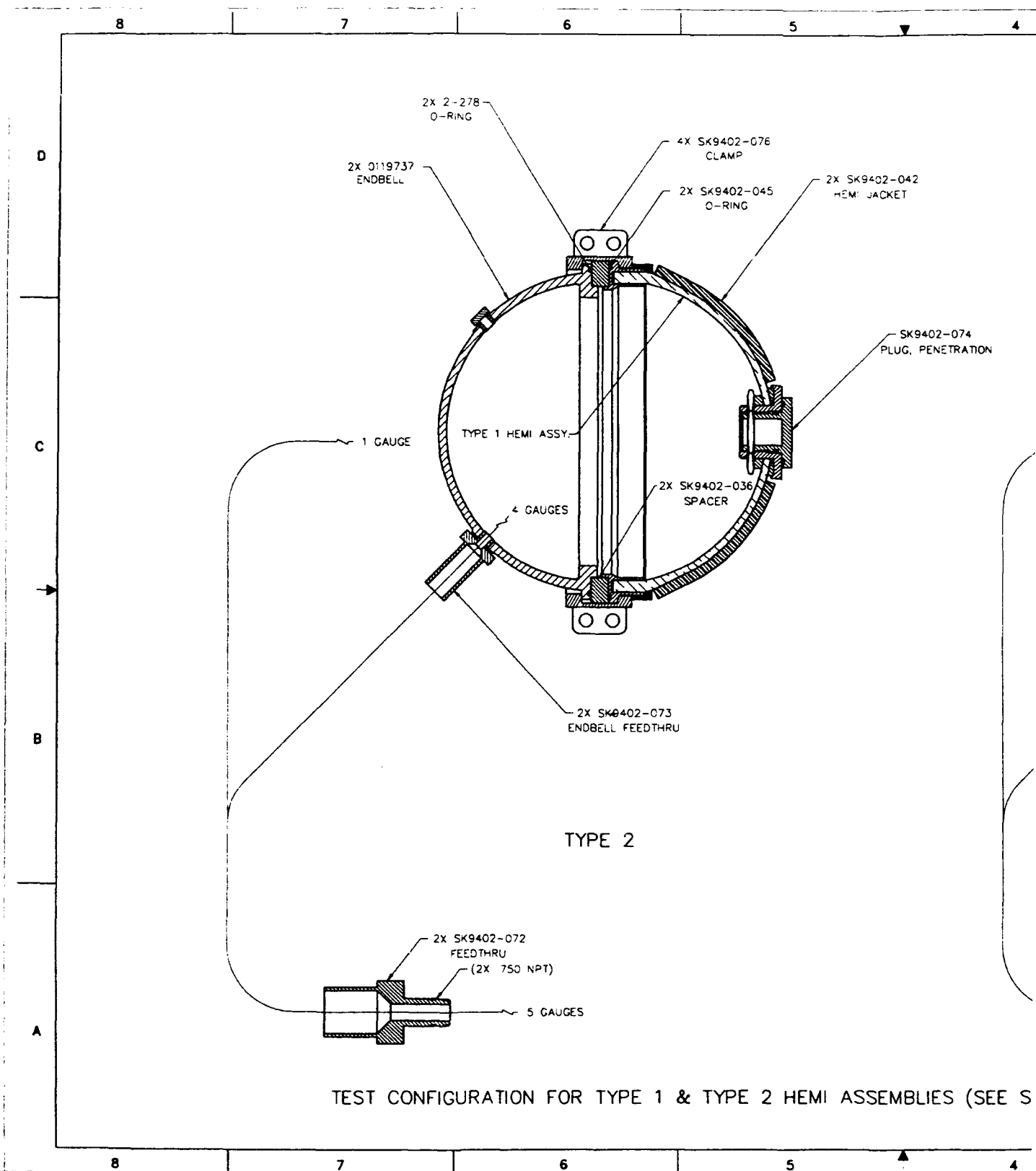


Figure 13. Spherical test assembly consisting of a titanium hemisphere and Type 1 or 2 ceramic hemispheres joined with an aluminum spacer and fastened by a clamp band, Sheet 2.

DWG NO SK9402-080

REVISIONS		DATE	APPROVAL
ZONE	LTR		
1	1	11/7/92	
		12/11/93	
UPDATE TITLE BLOCK			

-076

-045 2X SK9402-042
HEMI JACKET

SK9402-074
PLUG, PENETRATION

1 GAUGE

TYPE 2 HEMI ASSY.

7 GAUGES

(2X 15.19)

TYPE 1

8 GAUGES

2 HEMI ASSEMBLIES (SEE SHEET 1 FOR STRAIN GAUGE LOCATIONS)

T 1 FOR

SIZE	CAGE CODE	DRAWING NUMBER
D	55910	SK9402-080
SCALE	1/2	94020802 SHEET 2

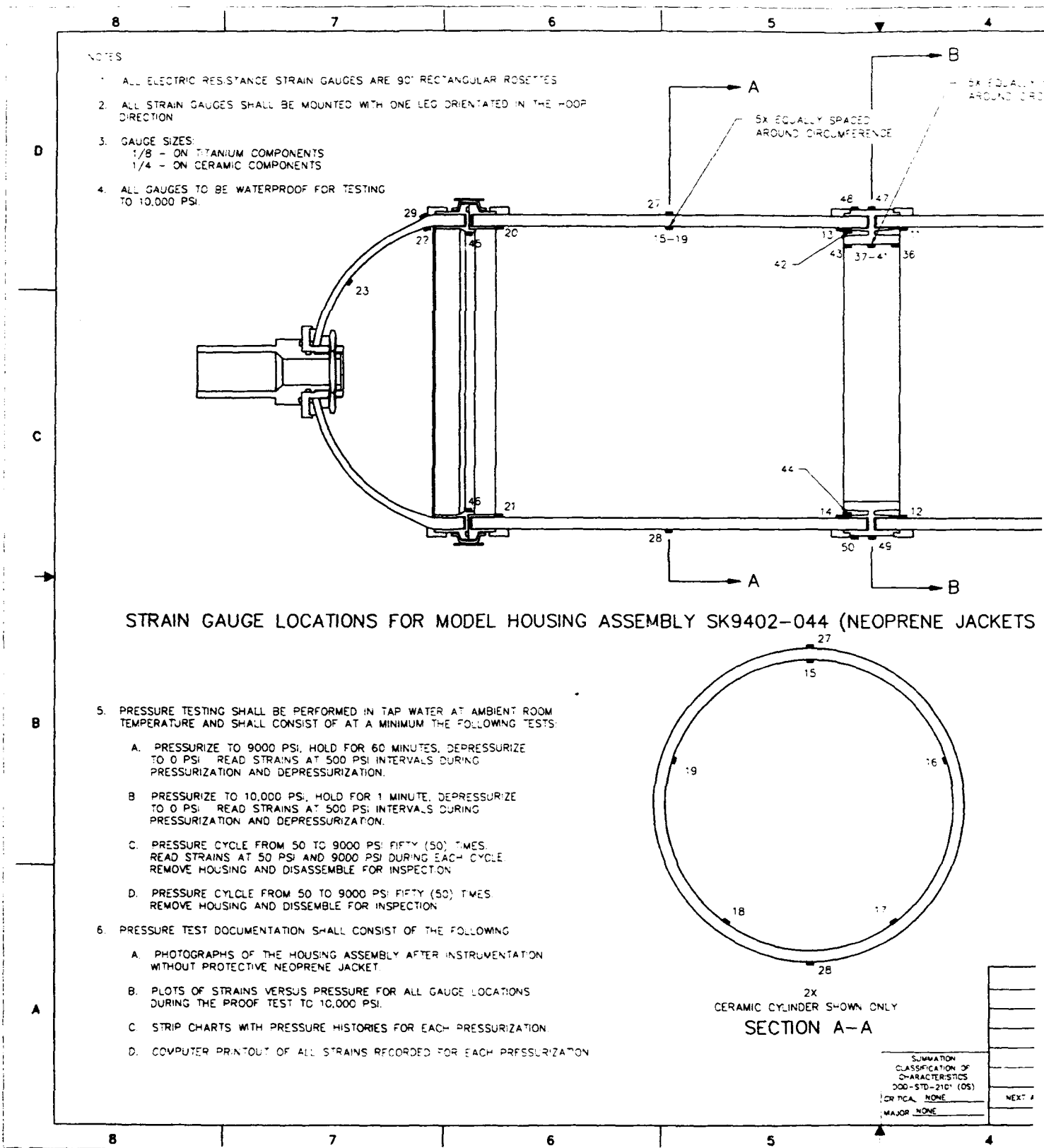
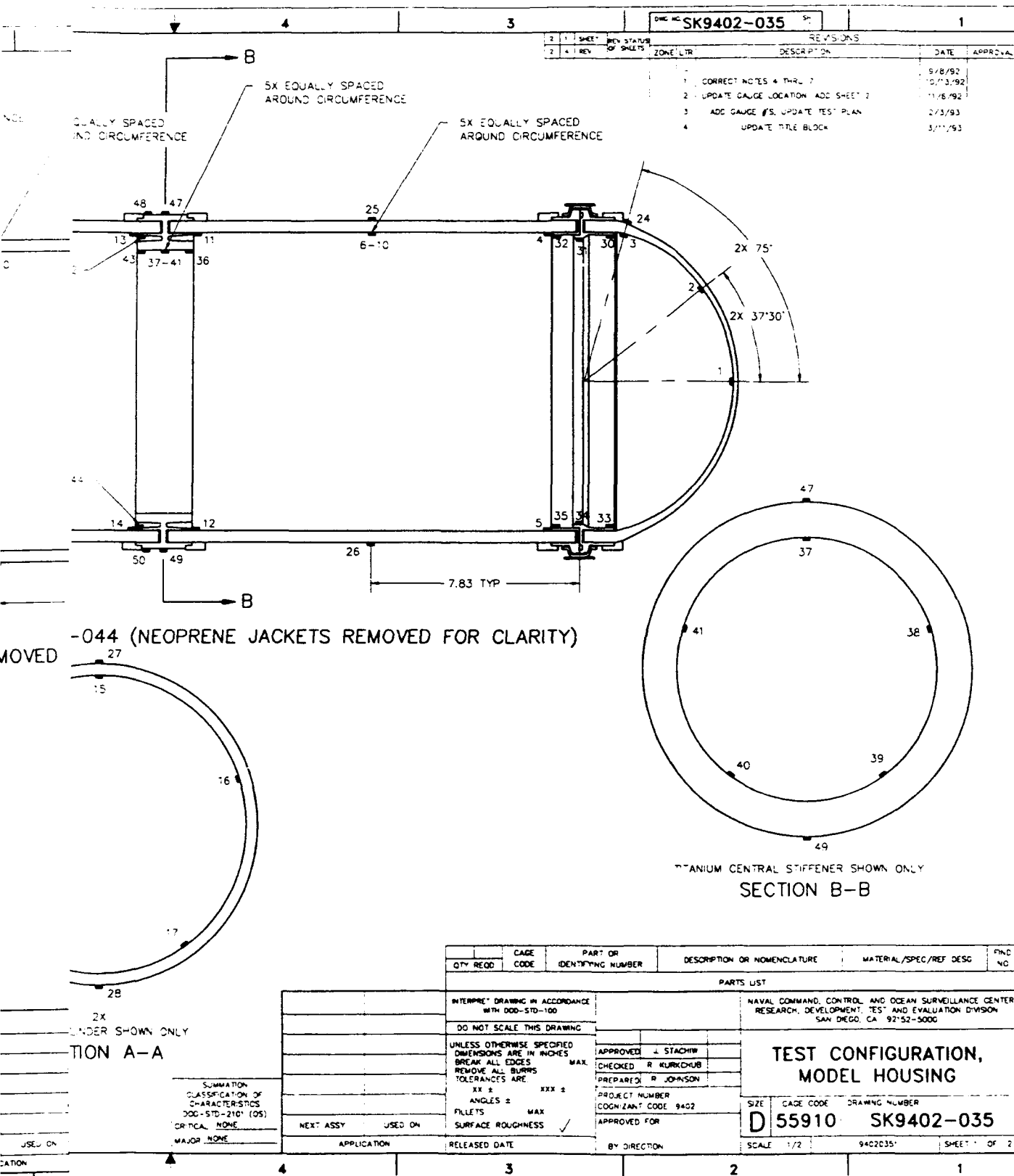


Figure 15. Cylindrical housing assembly consisting of two ceramic cylinders joined by a coupling and closed off by Type 1 and 2 ceramic hemispheres, Sheet 1.



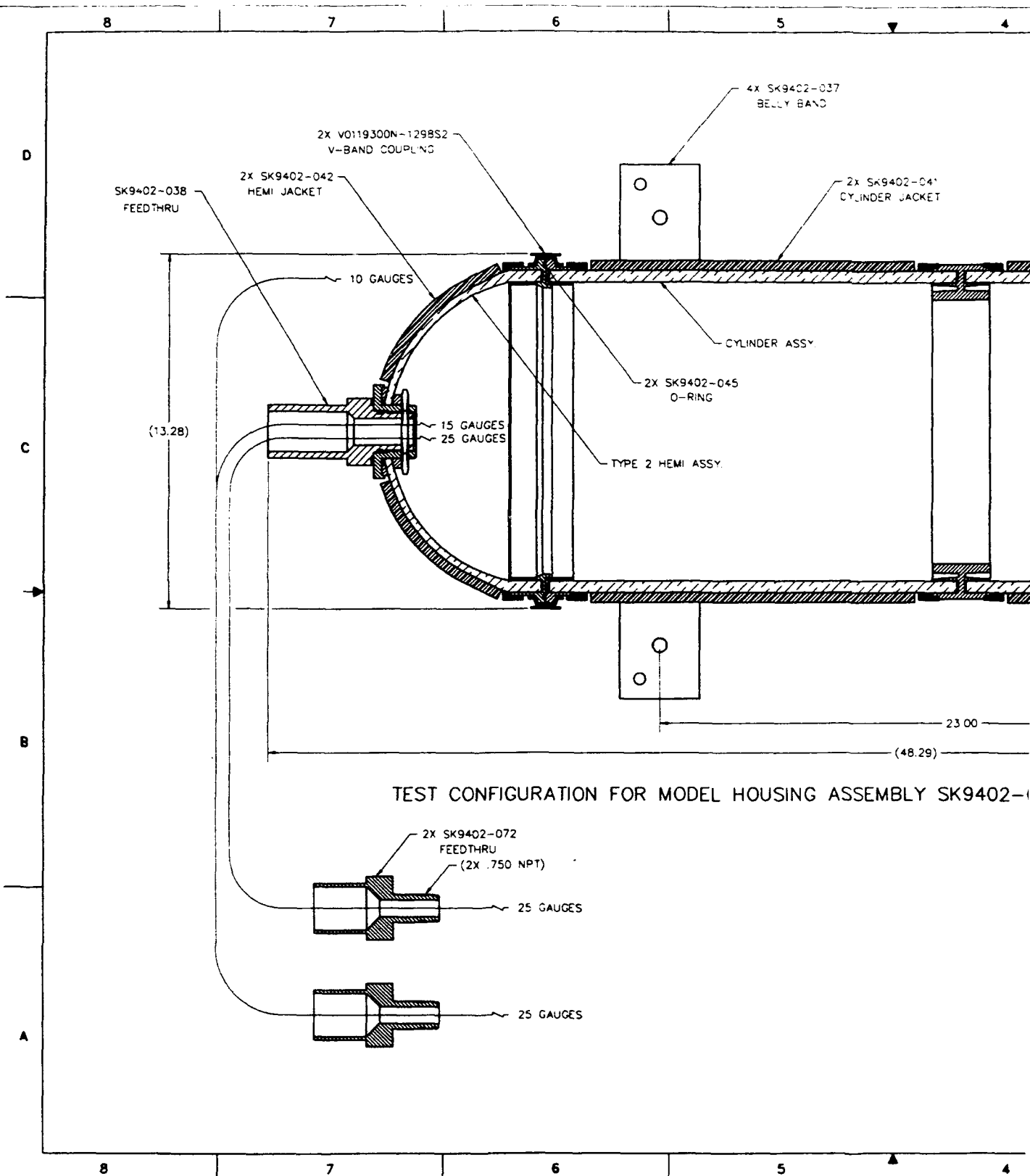


Figure 15. Cylindrical housing assembly consisting of two ceramic cylinders joined by a coupling and closed off by Type 1 and 2 ceramic hemispheres, Sheet 2.

DWG NO SK9402-035

REV		DESCRIPTION	DATE	APPROVAL
1			1/1/52	
2		CORRECT TYPE DESIGNATORS FOR HEMISPHERES	2/3/52	
3		UPDATE FEEDBACK	3/11/53	

4X SK9402-037
BELLY BAND

2X SK9402-041
CYLINDER JACKET

CYLINDER ASSY.

2-045
NO

SEY

TYPE 1 HEMI ASSY.

(2X 20.00)

23.00

(48.29)

EL HOUSING ASSEMBLY SK9402-044 (SEE SHEET 1 FOR STRAIN GAUGE LOCATIONS)

(SEE 1)

SIZE	CAGE CODE	DRAWING NUMBER
D	55910	SK9402-035
SCALE	1/2	94020952 SHEET 2

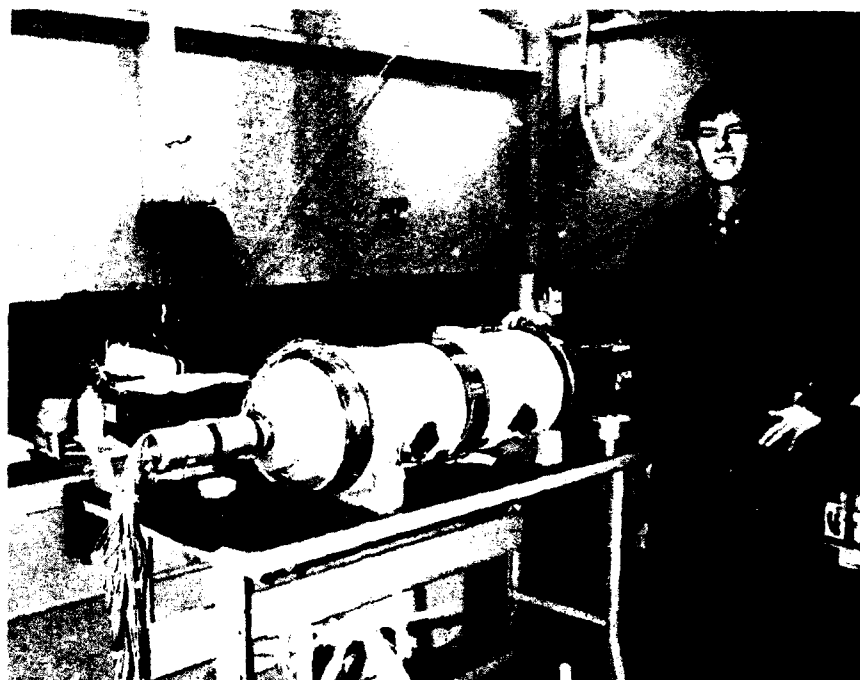


Figure 16. Cylindrical housing assembly after instrumenting with electric-resistance strain gages.

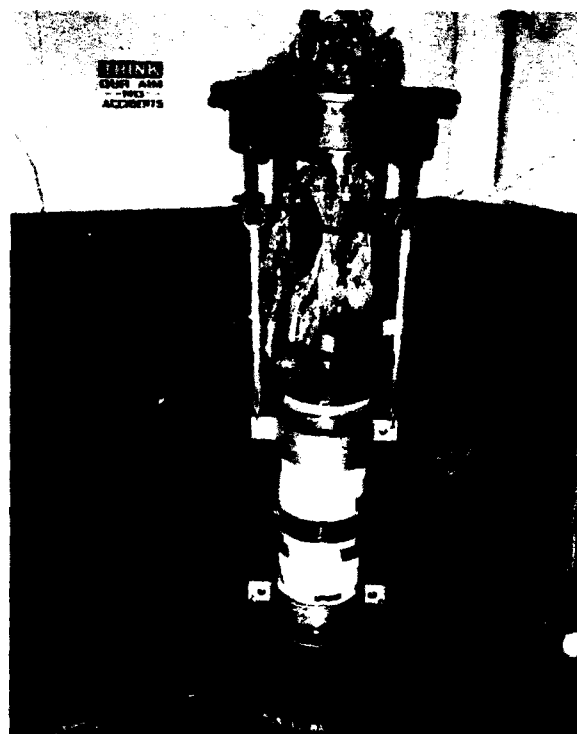


Figure 17. Placement of the cylindrical housing assembly into the pressure vessel at the Southwest Research Institute.

FEATURED RESEARCH



Figure 18. Split retaining plate and hydraulic jack used for the removal of the ceramic hemisphere from the titanium end cap.

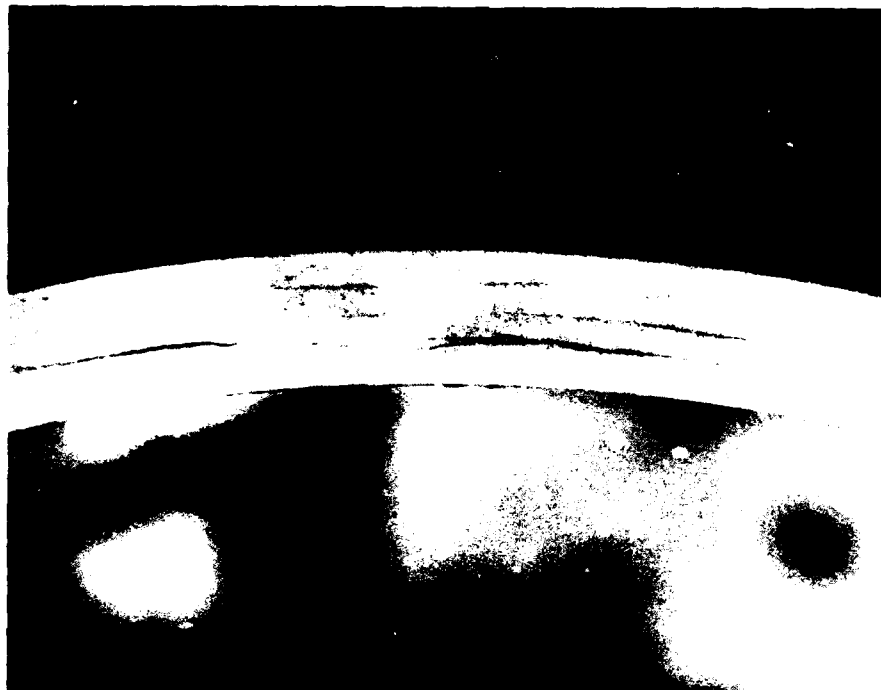


Figure 19. Fatigue cracks on the plane-bearing surface of the Type 1 ceramic hemisphere after it has been subjected to 500 pressurizations to 9,000 psi.

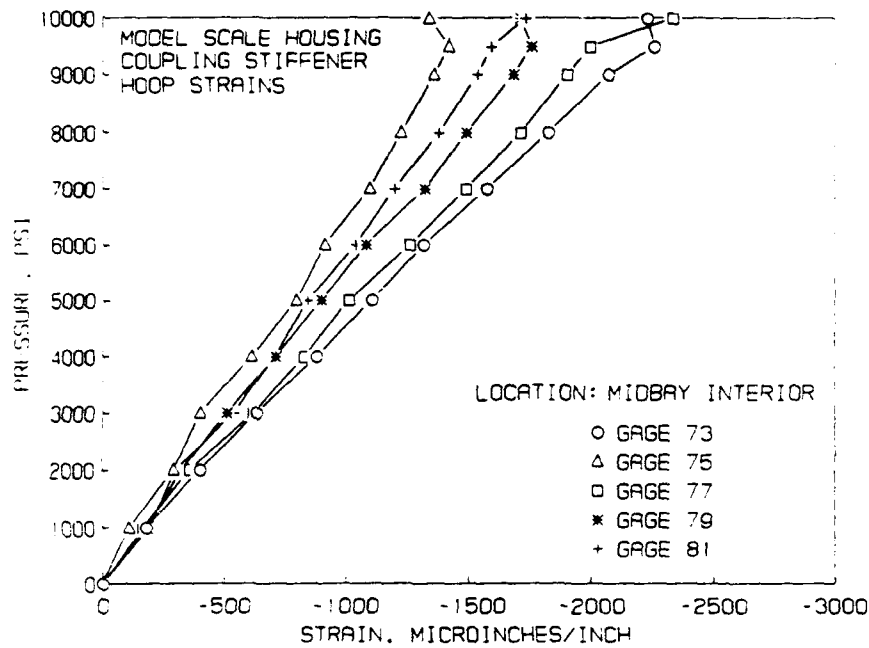


Figure 20. Hoop strains on the interior surface of ceramic cylinder A.

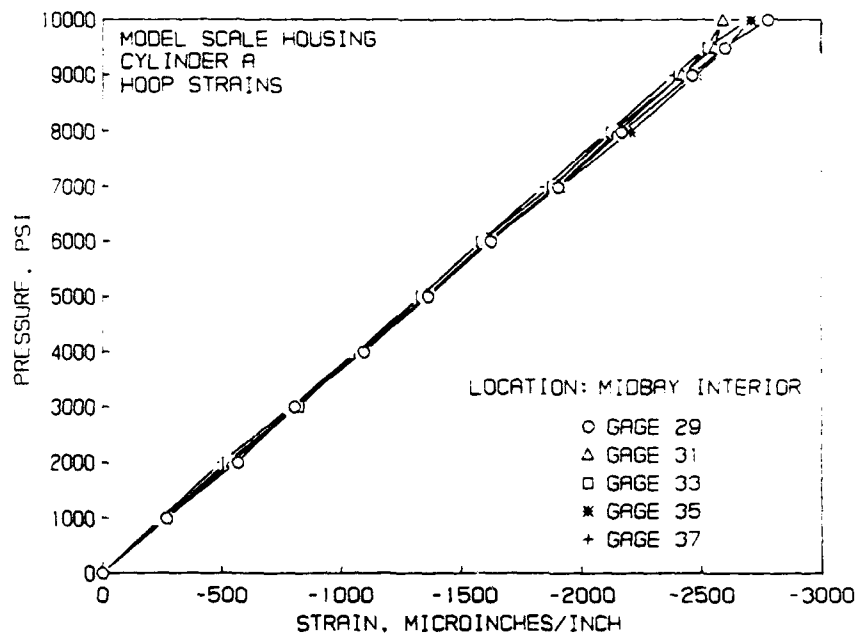


Figure 21. Hoop strains on the interior flange of the titanium coupling.

FEATURED RESEARCH

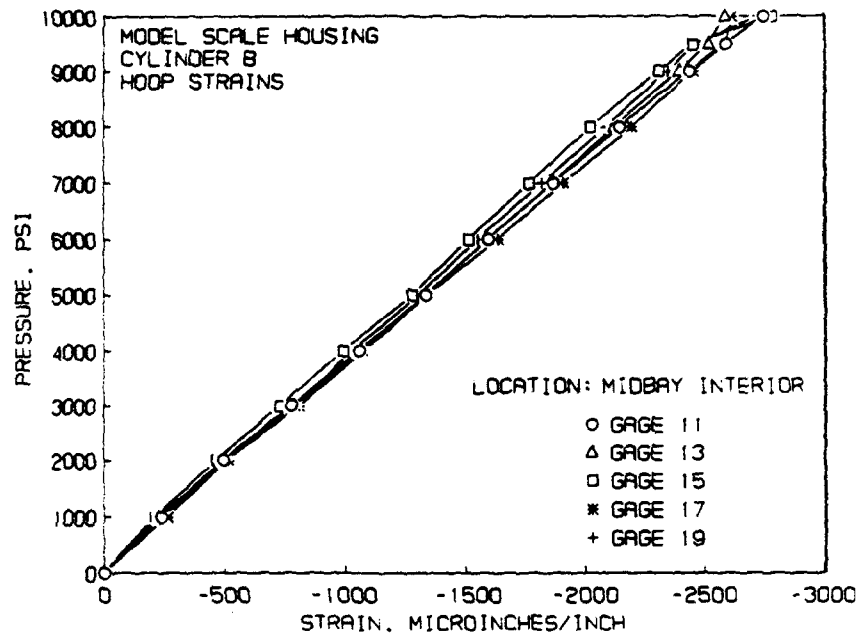


Figure 22. Hoop strains on the interior surface of ceramic cylinder B.

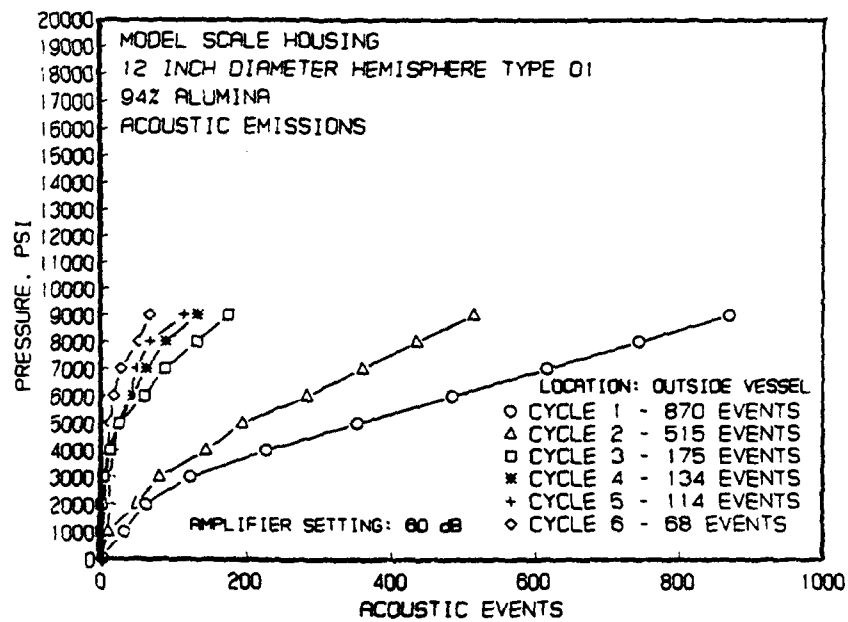


Figure 23. Acoustic emissions generated during pressure cycling of the spherical test assembly with the Type 1 ceramic hemispheres.

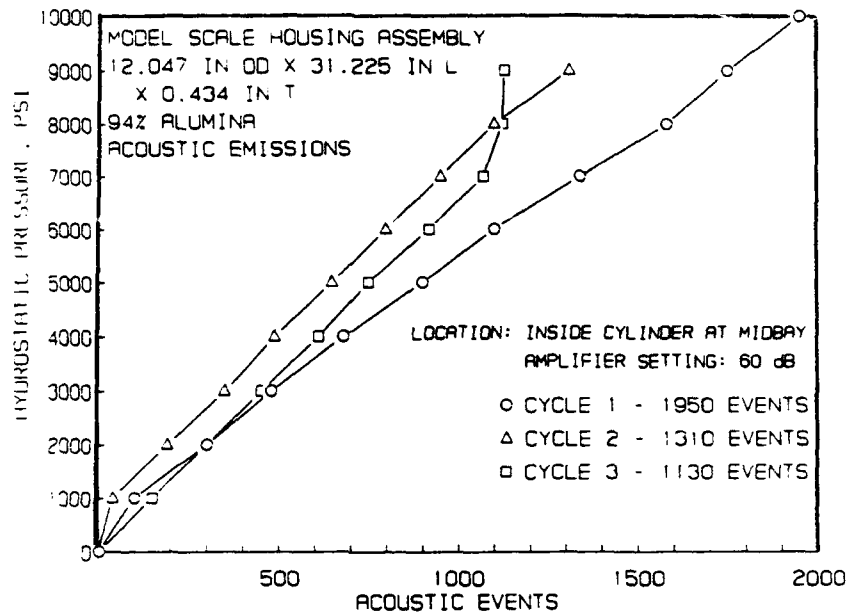


Figure 24. Acoustic emissions generated during pressure cycling of the scale-model housing assembly with both ceramic hemispheres.

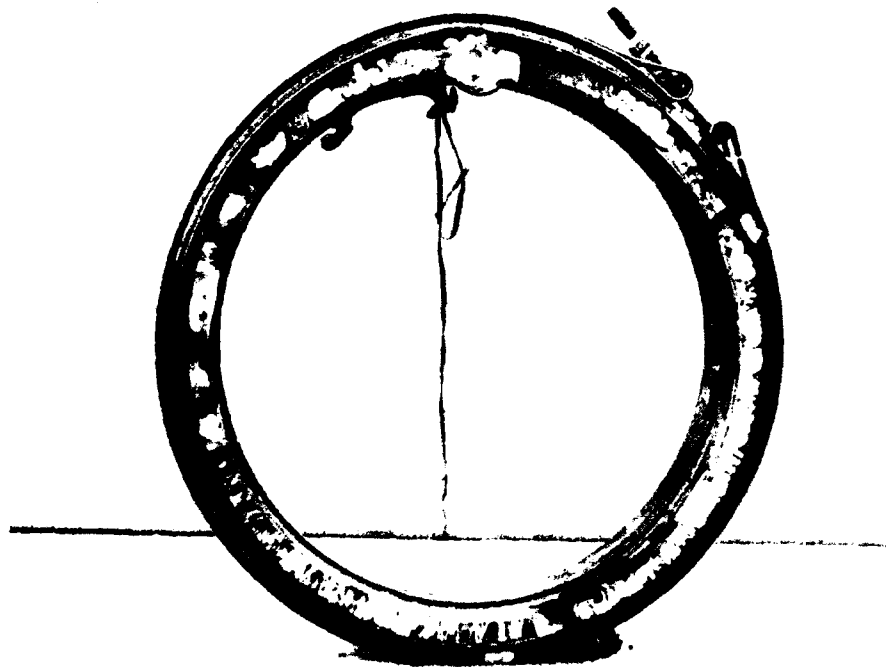


Figure 25. Metallic components of the scale-model housing assembly after catastrophic implosion at 11,933 psi.

FEATURED RESEARCH

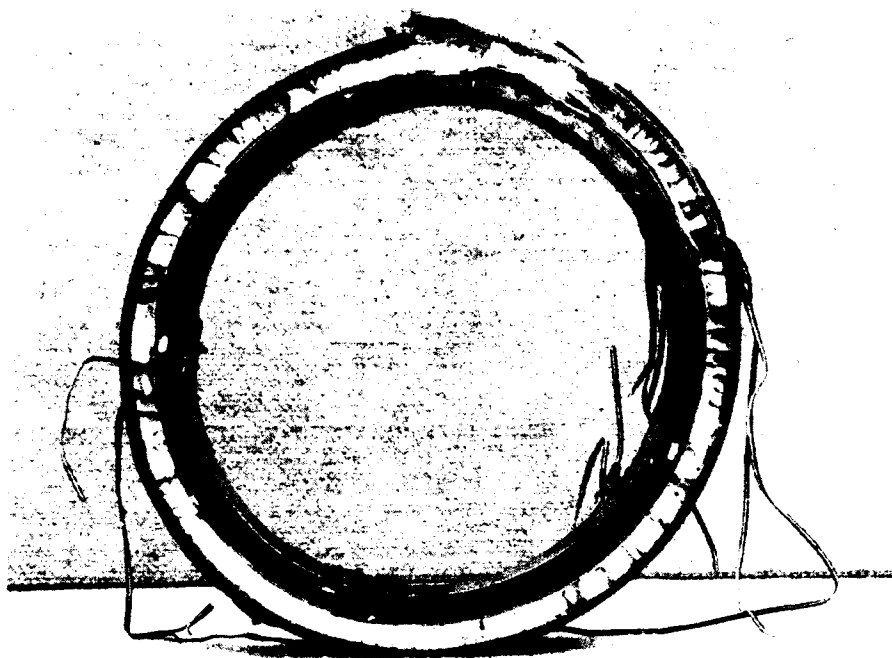


Figure 26. Central coupling whose buckling initiated the implosion of the housing.



Figure 27. Detail of the buckled coupling.



Figure 28. Detail of the buckled end cap on one of the cylinders.

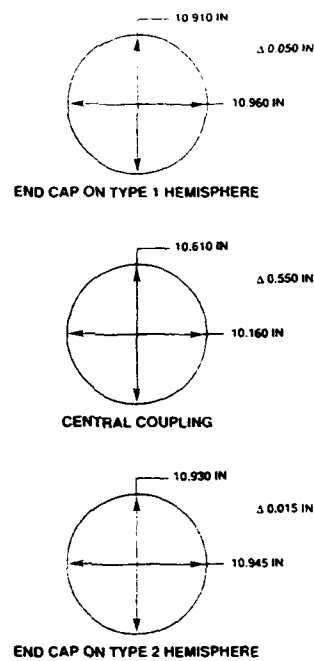


Figure 29. Interior dimensions of the end caps and central coupling after implosion of the housing.



Figure 30. 12-inch ceramic cylinders equipped with Mod 0 and Mod 1 end caps.

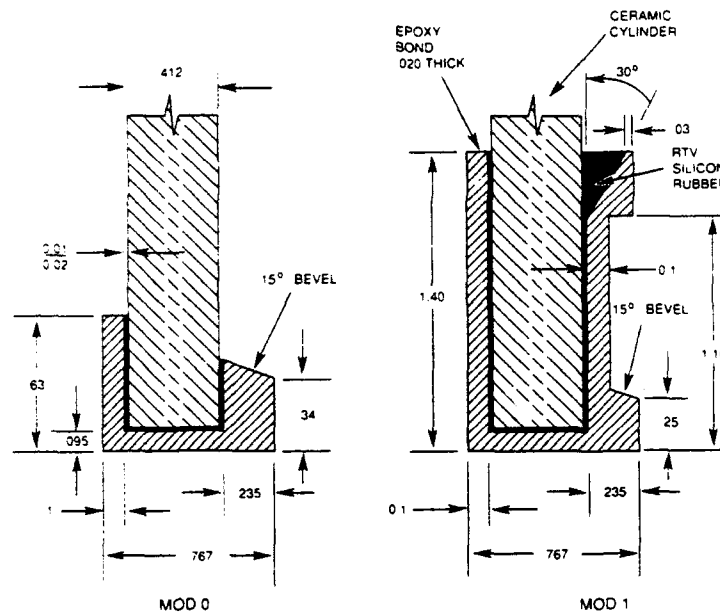


Figure 31. Dimensions of Mod 0 and Mod 1 end caps for 12-inch ceramic cylinder pressure cycled during the third generation ceramic housing study (Stachiw, 1993). Spalling was observed after 50 cycles on cylinders with Mod 0 end caps. Cylinders with Mod 1 end caps were free of spalls after 500 cycles to 9,000 psi hydrostatic loading. In both cases, a 0.02-inch-thick epoxy layer separated the ceramic bearing surfaces from metallic end caps.

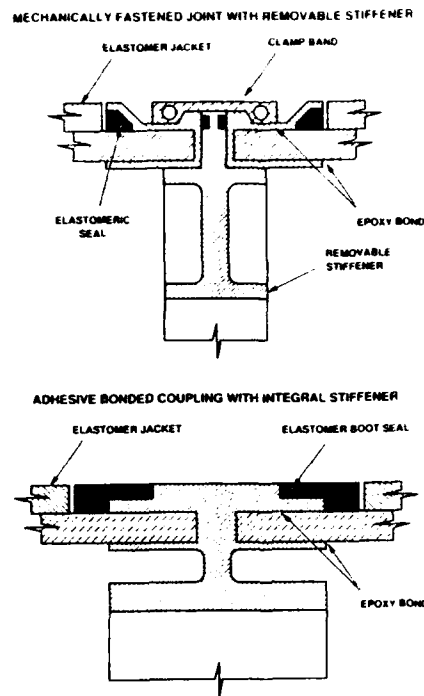


Figure 32. The ceramic cylinders on third and fourth generation housings were joined by the mechanical joint, while those in the fifth generation are joined by an adhesive-bonding coupling.

FEATURED RESEARCH

Table 1. Typical materials for construction of deep submergence pressure housings.

Material	Weight (lb/in ³)	Modulus of Elasticity (Mpsi)	Elasticity Weight	Compressive Strength (kpsi)	Strength Weight
Steel (HY80)	0.283	30	106	80	280
Steel (HY 130)	0.283	30	106	130	460
Aluminum (7075-T6)	0.100	10	100	73	730
Titanium (6Al-4V)	0.160	16	100	125	780
Glass (Pyrex)	0.080	9	112	100	1250
Glass Composite	0.075	3.5	47	100	1330
Graphite Composite	0.057	16	280	100	1750
Beryllia Ceramic 99%	0.104	51	490	300	2885
Alumina Ceramic 94%	0.130	44	338	300	2310
Glass Ceramic (Pyroceram 9606)	0.093	17.5	188	350	3760
Silicon Carbide	0.114	59	517	450	3947
Boron Carbide	0.089	63	707	400	4494
Alumina/SiC Composite (Lanxide 90-X-089)	0.124	43	346	300	2419
B ₄ C/Al Composite (Dow Chemical)	0.093	45	483	350	3763
Silicon Nitride	0.119	44	370	400	3361

Table 2. Comparison of alumina ceramic to titanium alloy.

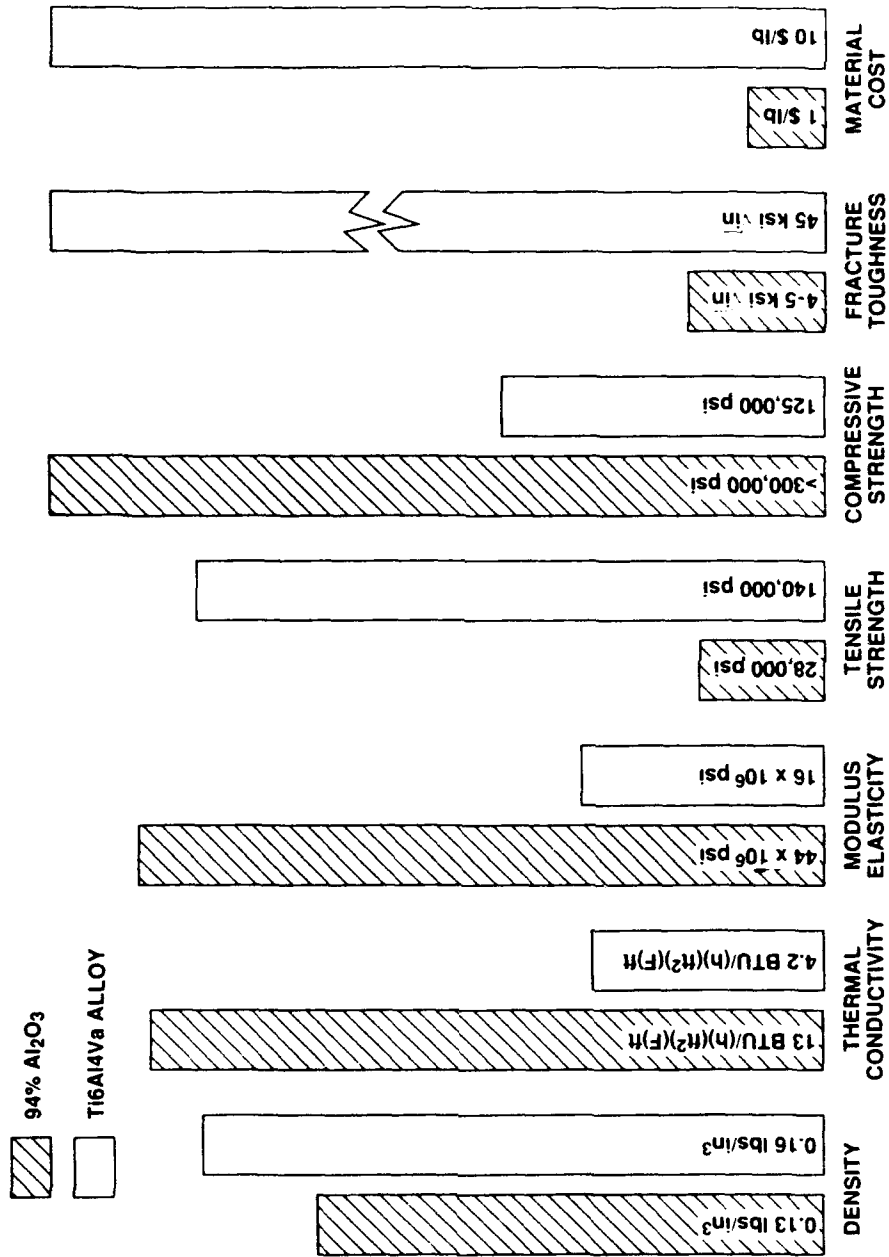


Table 3. Physical properties of selected ceramic compositions.

Properties*	Units	Test	Alumina					99.5% SiC	SiC Whisker Reinforced Al ₂ O ₃	SiC Direct Sintered	B ₄ C Direct Sintered
			85%	90%	94%	96%	99.5%				
Specific Gravity		ASTM C20-70	3.41	3.60	3.62	3.72	3.89	3.10	3.80	3.10	2.50
Hardness	Rockwell A and GPa	ASTM E18-67 100 g load	73	79	78	78	83	8.9	-	8.9	79.4
Surface Finish	Micrometres (micrometres)	Profilometer (0.75mm cut)	1.6 (63) 1.0 (39) 0.2 (8.9)	1.6 (63) 0.5 (20) 0.1 (3.9)	1.6 (63) 1.3 (51) 0.3 (12)	1.6 (63) 1.3 (51) 0.3 (12)	0.9 (35) 0.5 (20) 0.1 (3.9)	2.0 (100) 38 (10.3) 05 (2)	-	2.0 (100) 38 (10.3) 05 (2)	-
Crystal Size	Micrometres (micrometres)		2-12 (79-473) 6 (236)	2-10 (79-394) 4 (158)	2-25 (79-985) 12 (473)	2-20 (79-786) 11 (433)	5-50 (197-1970) 16 (640)	4.6	-	4.6	-
Water Absorp		ASTM C373-072	None	None	None	None	None	None	None	None	None
Gas Perm			None	None	None	None	None	None	None	None	None
Color			White	White	White	White	Ivory	Black	Green	Black	Black
Compressive Strength	25 C 1000 C	ASTM C773-74	1930 (280) - (-)	2482 (360) 517 (75)	2103 (305) 345 (50)	2068 (300) - (-)	2620 (380) - (-)	2137 (310)	2068 (300)	3900 (560)	7000 (1000)
Flexural Strength	TYP 25 C MIN 25 C TYP 1000 C MIN 1000 C	ASTM F417-75T	296 (43) 269 (39) 172 (25) 138 (20)	338 (49) 303 (44) - (-) - (-)	352 (51) 317 (46) 138 (20) 117 (17)	358 (52) 324 (47) 172 (25) 138 (20)	379 (55) 324 (47) - (-) - (-)	275 (40) 241 (35) - (-)	414 (60)	462 (67)	350 (51)
Tensile Strength	25 C 1000 C	ACMA Test 4	155 (22) - (-)	221 (32) 103 (15)	193 (28) 103 (15)	193 (28) 96 (14)	282 (36) - (-)	138 (20) 34 (5)	-	307 (44.5)	200 (29)
Mod of Elasti			221 (32)	276 (40)	283 (41)	303 (44)	372 (54)	351 (51)	344 (50)	410 (59)	350 (51)
Shear Modulus			96 (14)	117 (17)	117 (17)	124 (18)	152 (22)	138 (20)	-	166 (24)	-
Bulk Modulus			138 (20)	158 (23)	165 (24)	172 (25)	228 (33)	241 (35)	-	212 (31)	-
Trans. Sonic Vel			8.2 (27)x10 ³	8.8 (29)x10 ³	8.9 (29)x10 ³	9.1 (30)x10 ³	9.8 (32)x10 ³	11.1 (36)x10 ³	-	-	-
Poisson's Ratio			0.22	0.22	0.21	0.21	0.22	0.26	-	0.14	0.17
Max Use Temp No-load conds			1400 (2550)	1500 (2730)	1700 (3100)	1700 (3100)	1750 (3180)	1848 (3360)	1750 (3182)	1650 (3000)	-
Coefficient of Linear Thermal Expansion	200-25 C 25-100 C 25-500 C 25-800 C 25-1000 C 25-1200 C	ASTM C372-56	3.4 (1.9) 5.3 (3.0) 6.2 (3.5) 6.9 (3.9) 7.2 (4.0) 7.5 (4.2)	3.4 (1.9) 6.1 (3.4) 7.0 (3.9) 7.7 (4.3) 8.1 (4.5) 8.4 (4.7)	3.4 (1.9) 6.3 (3.5) 7.1 (4.0) 7.6 (4.3) 7.9 (4.4) 8.1 (4.5)	3.4 (1.9) 6.0 (3.4) 7.1 (4.0) 8.0 (4.5) 8.2 (4.6) 8.4 (4.7)	3.4 (1.9) 6.0 (3.4) 7.1 (4.0) 8.0 (4.5) 8.2 (4.6) 8.4 (4.7)	2.4 (1.3) 6.4 (3.6) 7.1 (4.0) 8.5 (4.7) 8.9 (4.9) 9.4 (5.2)	-	4.0 (2.20)	-
Thermal Conductivity	20 C 100 C 400 C 800 C	ASTM C408-58	14.6 (0.035) 12.1 (0.029) 6.7 (0.016) 4.2 (0.010)	16.7 (0.040) 13.4 (0.032) 7.9 (0.017) 5.0 (0.010)	18.0 (0.043) 14.2 (0.035) 7.9 (0.017) 5.0 (0.010)	24.7 (0.059) 18.8 (0.045) 10.0 (0.028) 5.4 (0.013)	35.6 (0.085) 25.9 (0.062) 12.1 (0.028) 6.3 (0.015)	281 (0.67) 201 (0.48) 84 (0.20) 30 (0.07)	35 (0.083)	110 (0.26)	33 (0.08)
Specific Heat	100 C	ASTM C351-61	920 (0.22)	920 (0.22)	880 (0.21)	880 (0.21)	880 (0.21)	1299 (0.31)	-	2807 (0.67)	-

Table 4. Acoustic emissions during hydrostatic testing, Sheet 1.

Test Date: 12/21/92

ACOUSTIC EMISSIONS DURING HYDROSTATIC TESTING
OF
12 IN CERAMIC HEMISPHERE TYPE 01

Pressure	PRESSURE CYCLE					
	1	2	3	4	5	6
1000	31	10	0	2	10	3
2000	61	48	0	3	12	5
3000	123	80	3	6	13	8
4000	227	144	13	10	18	9
5000	352	195	25	25	23	12
6000	485	283	59	44	40	18
7000	616	366	87	63	49	26
8000	744	436	132	90	68	51
9000	870	515	175	134	114	68

LOCATION OF TRANSDUCER: OUTSIDE VESSEL

- Notes: 1. Transducer: AET AC175 SN# 7039
50 to 200 KHZ
2. Amplifier Setting:
Rate: T Gain: 60 DB
Threshold: Automatic
Function: Events
Scale: 1
3. Recorder:
Channel "A" Events,
400 Full Range,
Channel "B" Rms,
50 MV Full Scale,
0.5 CM/Min Chart Speed

FEATURED RESEARCH

Table 4. Acoustic emissions during hydrostatic testing, Sheet 2.

Test Date: 12/21/92

ACOUSTIC EMISSIONS DURING HYDROSTATIC TESTING
OF
12 IN CERAMIC HEMISPHERE TYPE O1
(CONTINUED)

Cycle No.	1000 psi	3000 psi
7	0	48
8	0	1467
9	4	30
10	3	30
11	0	38
12	3	16
13	4	2953
14	5	19
15	7	25
16	5	20
17	7	32
18	1	18
19	1	13
20	4	28
21	2	19
26	5	2100
27	7	19
28	8	21
29	6	32
30	10	16
31	5	1990

LOCATION OF TRANSDUCER: OUTSIDE VESSEL

- Notes: 1. Transducer: AET AC175 SN# 7039
50 to 200 KHZ
2. Amplifier Setting:
Rate: T Gain: 60 DB
Threshold: Automatic
Function: Events
Scale: 1
3. Recorder:
Channel "A" Events,
400 Full Range,
Channel "B" Rms,
50 MV Full Scale,
0.5 CM/Min Chart Speed

Table 4. Acoustic emissions during hydrostatic testing, Sheet 3.

ACOUSTIC EMISSIONS DURING HYDROSTATIC TESTING
OF MODEL SCALE HOUSING ASSEMBLY

Cycles	1	2	3
Pressure	Events		
0000	0	0	0
1000	100	40	150
2000	300	190	300
3000	480	350	450
4000	680	490	610
5000	900	650	750
6000	1100	800	920
7000	1340	950	1070
8000	1580	1100	1122
9000	1750	1310	1130
10000	1950		

- Notes: 1. Transducer: AET AC175 SN# 7664
50 to 200 KHZ
2. Amplifier Setting:
Rate: T Gain: 60 DB
Threshold: Automatic
Function: Events
Scale: 1
3. Recorder:
Channel "A" Events,
400 Full Range,
Channel "B" Rms,
50 MV Full Scale,
0.5 CM/Min Chart Speed

FEATURED RESEARCH

Table 5. Strains recorded during pressurization of the scale-model housing assembly to 9,500 psi, Sheet 1.

16:25:45
12-17-1992

SCAN NUMBER 40
PRESSURE = 1000.000

	CHANNEL	UE	CHANNEL	UE	STRESS(HOOP)	STRESS(LONG)
2 GAGE ROSETTE 1	1	-258	2	-287	-14669	-15713
2 GAGE ROSETTE 2	3	-215	4	-200	-11815	-11277
2 GAGE ROSETTE 3	5	-89	6	-289	-6904	-14155
2 GAGE ROSETTE 4	7	-271	8	-56	-13024	-5192
2 GAGE ROSETTE 5	9	-215	10	56	-9340	510
2 GAGE ROSETTE 6	11	-236	12	-67	-11508	-5365
2 GAGE ROSETTE 7	13	-225	14	-23	-10561	-3212
2 GAGE ROSETTE 8	15	-210	16	-45	-10089	-4085
2 GAGE ROSETTE 9	17	-261	18	-100	-13000	-7128
2 GAGE ROSETTE 10	19	-246	20	-80	-12085	-6060
2 GAGE ROSETTE 11	21	-257	22	-79	-12590	-6124
2 GAGE ROSETTE 12	23	-260	24	-45	-12403	-4605
2 GAGE ROSETTE 13	25	-246	26	-45	-11746	-4444
2 GAGE ROSETTE 14	27	-235	28	-34	-11125	-3828
2 GAGE ROSETTE 15	29	-270	30	-100	-13377	-7207
2 GAGE ROSETTE 16	31	-271	32	-68	-13143	-5761
2 GAGE ROSETTE 17	33	-273	34	-91	-13436	-6823
2 GAGE ROSETTE 18	35	-261	36	-69	-12697	-5685
2 GAGE ROSETTE 19	37	-249	38	-68	-12103	-5542
2 GAGE ROSETTE 20	39	-274	40	23	-12410	-1600
2 GAGE ROSETTE 21	41	-316	42	-101	-15536	-7686
2 GAGE ROSETTE 22	43	-226	44	-235	-12657	-12920
2 GAGE ROSETTE 23	45	-144	46	-170	-8246	-9190
2 GAGE ROSETTE 24	47	-46	48	34	-1778	1118
2 GAGE ROSETTE 25	49	-271	50	-125	-13692	-8377
2 GAGE ROSETTE 26	51	-236	52	-125	-12068	-8036
2 GAGE ROSETTE 27	53	-258	54	-80	-12663	-6160
2 GAGE ROSETTE 28	55	-271	56	-91	-13363	-6807
2 GAGE ROSETTE 29	57	-125	58	-123	-6943	-6864
2 GAGE ROSETTE 30	59	-270	60	79	-4447	-81
2 GAGE ROSETTE 31	61	-203	62	-11	-3754	-1350
2 GAGE ROSETTE 32	63	-180	64	45	-3006	-186
2 GAGE ROSETTE 33	65	-175	66	-67	-3548	-2198
2 GAGE ROSETTE 34	67	-183	68	80	-2873	423
2 GAGE ROSETTE 35	69	-306	70	119	-4885	436
2 GAGE ROSETTE 36	71	-153	72	84	-2307	656
2 GAGE ROSETTE 37	73	-179	74	284	-1655	4147
2 GAGE ROSETTE 38	75	-107	76	257	-492	4062
2 GAGE ROSETTE 39	77	-163	78	330	-1108	5071
2 GAGE ROSETTE 40	79	-182	80	284	-1699	4134
2 GAGE ROSETTE 41	81	-188	82	182	-2382	2243
2 GAGE ROSETTE 42	83	-266	84	-19	-4939	-1850
2 GAGE ROSETTE 43	85	-196	86	88	-3065	490
2 GAGE ROSETTE 44	87	-273	88	96	-4419	207
2 GAGE ROSETTE 45	89	-152	90	39	-2543	-145
2 GAGE ROSETTE 46	91	-201	92	134	-2892	1300
2 GAGE ROSETTE 47	93	-48	94	123	-187	1952
2 GAGE ROSETTE 48	95	-137	96	-10	-2546	-948
2 GAGE ROSETTE 49	97	-114	98	19	-1842	73
2 GAGE ROSETTE 50	99	-87	100	19	-1462	-141

Table 5. Strains recorded during pressurization of the scale-model housing assembly to 9,500 psi, Sheet 2.

12-17-1992

SCAN NUMBER 41 2000.000
PRESSURE = 2000.00

	CHANNEL	UE	CHANNEL	UE	STRESS (HOOP)	STRESS (LONG)
2 GAGE ROSETTE 1	1	-562	2	-596	-31620	-32876
2 GAGE ROSETTE 2	3	-475	4	-455	-26248	-25546
2 GAGE ROSETTE 3	5	-190	6	-522	-13786	-25861
2 GAGE ROSETTE 4	7	-509	8	-101	-24379	-9543
2 GAGE ROSETTE 5	9	-486	10	22	-22150	-3663
2 GAGE ROSETTE 6	11	-494	12	-134	-24049	-10948
2 GAGE ROSETTE 7	13	-506	14	-102	-24254	-9568
2 GAGE ROSETTE 8	15	-464	16	-134	-22643	-10653
2 GAGE ROSETTE 9	17	-512	18	-178	-25262	-13123
2 GAGE ROSETTE 10	19	-503	20	-183	-24905	-13280
2 GAGE ROSETTE 11	21	-503	22	-124	-24338	-10580
2 GAGE ROSETTE 12	23	-531	24	-102	-25436	-9843
2 GAGE ROSETTE 13	25	-469	25	-90	-22463	-8672
2 GAGE ROSETTE 14	27	-491	28	-79	-23387	-8392
2 GAGE ROSETTE 15	29	-562	30	-178	-27574	-13609
2 GAGE ROSETTE 16	31	-542	32	-159	-26506	-12568
2 GAGE ROSETTE 17	33	-523	34	-171	-25716	-12903
2 GAGE ROSETTE 18	35	-523	36	-160	-25615	-12423
2 GAGE ROSETTE 19	37	-497	38	-159	-24425	-12131
2 GAGE ROSETTE 20	39	-549	40	23	-25042	-4253
2 GAGE ROSETTE 21	41	-599	42	-168	-29188	-13501
2 GAGE ROSETTE 22	43	-384	44	-444	-21979	-24161
2 GAGE ROSETTE 23	45	-298	46	-328	-16671	-17966
2 GAGE ROSETTE 24	47	-172	48	57	-7349	943
2 GAGE ROSETTE 25	49	-497	50	-205	-24865	-14224
2 GAGE ROSETTE 26	51	-483	52	-182	-23995	-13041
2 GAGE ROSETTE 27	53	-517	54	-159	-25326	-12321
2 GAGE ROSETTE 28	55	-497	56	-159	-24425	-12131
2 GAGE ROSETTE 29	57	-284	58	-179	-14808	-10973
2 GAGE ROSETTE 30	59	-404	60	45	-7084	-1455
2 GAGE ROSETTE 31	61	-316	62	23	-5613	-1367
2 GAGE ROSETTE 32	63	-315	64	0	-5707	-1769
2 GAGE ROSETTE 33	65	-262	66	-77	-5187	-2863
2 GAGE ROSETTE 34	67	-321	68	150	-4971	922
2 GAGE ROSETTE 35	69	-574	70	59	-10079	-2150
2 GAGE ROSETTE 36	71	-268	72	167	-3919	1528
2 GAGE ROSETTE 37	73	-398	74	474	-4565	6352
2 GAGE ROSETTE 38	75	-291	76	476	-2608	6997
2 GAGE ROSETTE 39	77	-356	78	573	-3231	8394
2 GAGE ROSETTE 40	79	-325	80	464	-3291	6592
2 GAGE ROSETTE 41	81	-300	82	430	-3025	6122
2 GAGE ROSETTE 42	83	-463	84	49	-8134	-1725
2 GAGE ROSETTE 43	85	-343	86	127	-5515	371
2 GAGE ROSETTE 44	87	-490	88	115	-8244	-664
2 GAGE ROSETTE 45	89	-352	90	147	-5563	689
2 GAGE ROSETTE 46	91	-383	92	249	-5544	2360
2 GAGE ROSETTE 47	93	-203	94	283	-2091	3990
2 GAGE ROSETTE 48	95	-255	96	-77	-5062	-2837
2 GAGE ROSETTE 49	97	-218	98	-10	-4008	-1403
2 GAGE ROSETTE 50	99	-260	100	29	-4549	-942

FEATURED RESEARCH

Table 5. Strains recorded during pressurization of the scale-model housing assembly to 9,500 psi, Sheet 3.

12-17-1992

SCAN NUMBER 42
PRESSURE = 3000.00

	CHANNEL	UE	CHANNEL	UE	STRESS (HOOP)	STRESS (LONG)
2 GAGE ROSETTE 1	1	-820	2	-861	-46076	-47572
2 GAGE ROSETTE 2	3	-667	4	-711	-37560	-39161
2 GAGE ROSETTE 3	5	-313	6	-733	-21481	-36762
2 GAGE ROSETTE 4	7	-768	8	-156	-36882	-14626
2 GAGE ROSETTE 5	9	-735	10	-22	-34027	-8134
2 GAGE ROSETTE 6	11	-775	12	-201	-37626	-16748
2 GAGE ROSETTE 7	13	-786	14	-192	-38056	-16444
2 GAGE ROSETTE 8	15	-729	16	-223	-35705	-17327
2 GAGE ROSETTE 9	17	-807	18	-267	-39725	-20070
2 GAGE ROSETTE 10	19	-793	20	-263	-39046	-19771
2 GAGE ROSETTE 11	21	-737	22	-203	-35900	-16489
2 GAGE ROSETTE 12	23	-768	24	-136	-36689	-13706
2 GAGE ROSETTE 13	25	-726	26	-124	-34614	-12707
2 GAGE ROSETTE 14	27	-737	28	-113	-35026	-12328
2 GAGE ROSETTE 15	29	-798	30	-267	-39293	-19979
2 GAGE ROSETTE 16	31	-802	32	-250	-39348	-19266
2 GAGE ROSETTE 17	33	-818	34	-239	-39979	-18899
2 GAGE ROSETTE 18	35	-807	36	-229	-39359	-18327
2 GAGE ROSETTE 19	37	-791	38	-239	-38718	-18634
2 GAGE ROSETTE 20	39	-789	40	-34	-36647	-9205
2 GAGE ROSETTE 21	41	-859	42	-190	-17042	-41367
2 GAGE ROSETTE 22	43	-588	44	-611	-32952	-33795
2 GAGE ROSETTE 23	45	-409	46	-486	-23503	-26316
2 GAGE ROSETTE 24	47	-309	48	23	-13992	-1944
2 GAGE ROSETTE 25	49	-723	50	-284	-36037	-20071
2 GAGE ROSETTE 26	51	-719	52	-273	-35733	-19507
2 GAGE ROSETTE 27	53	-697	54	-250	-34479	-18244
2 GAGE ROSETTE 28	55	-723	56	-273	-35927	-19548
2 GAGE ROSETTE 29	57	-352	58	-268	-18811	-15746
2 GAGE ROSETTE 30	59	-506	60	23	-9046	-2433
2 GAGE ROSETTE 31	61	-520	62	80	-8984	-1480
2 GAGE ROSETTE 32	63	-461	64	-11	-8421	-2797
2 GAGE ROSETTE 33	65	-388	66	-134	-7801	-4615
2 GAGE ROSETTE 34	67	-522	68	210	-8289	879
2 GAGE ROSETTE 35	69	-737	70	79	-12919	-2705
2 GAGE ROSETTE 36	71	-450	72	149	-7321	168
2 GAGE ROSETTE 37	73	-628	74	682	-7550	8845
2 GAGE ROSETTE 38	75	-398	76	714	-3208	10714
2 GAGE ROSETTE 39	77	-615	78	845	-6412	11867
2 GAGE ROSETTE 40	79	-507	80	767	-4883	11069
2 GAGE ROSETTE 41	81	-535	82	650	-6042	8795
2 GAGE ROSETTE 42	83	-759	84	146	-12954	-1627
2 GAGE ROSETTE 43	85	-549	86	195	-8868	452
2 GAGE ROSETTE 44	87	-688	88	135	-11728	-1428
2 GAGE ROSETTE 45	89	-524	90	196	-8396	615
2 GAGE ROSETTE 46	91	-574	92	268	-8907	1632
2 GAGE ROSETTE 47	93	-319	94	386	-3611	5219
2 GAGE ROSETTE 48	95	-392	96	-68	-7499	-3434
2 GAGE ROSETTE 49	97	-379	98	108	-6268	-173
2 GAGE ROSETTE 50	99	-452	100	10	-8145	-2369

Table 5. Strains recorded during pressurization of the scale-model housing assembly to 9,500 psi, Sheet 4.

12-17-1992

SCAN NUMBER 43
PRESSURE = 4000.00

	CHANNEL	UE	CHANNEL	UE	STRESS(HOOP)	STRESS(LONG)
2 GAGE ROSETTE 1	1	-1101	2	-1104	-61353	-61469
2 GAGE ROSETTE 2	3	-904	4	-922	-50523	-51167
2 GAGE ROSETTE 3	5	-402	6	-922	-27419	-46316
2 GAGE ROSETTE 4	7	-1006	8	-190	-48129	-18462
2 GAGE ROSETTE 5	9	-983	10	-45	-45688	-11572
2 GAGE ROSETTE 6	11	-1056	12	-313	-51634	-24604
2 GAGE ROSETTE 7	13	-1067	14	-271	-51749	-22801
2 GAGE ROSETTE 8	15	-994	16	-324	-48875	-24516
2 GAGE ROSETTE 9	17	-1080	18	-355	-53141	-26796
2 GAGE ROSETTE 10	19	-1028	20	-320	-50396	-24670
2 GAGE ROSETTE 11	21	-994	22	-249	-48162	-21053
2 GAGE ROSETTE 12	23	-1028	24	-182	-49092	-18312
2 GAGE ROSETTE 13	25	-972	26	-213	-46794	-19219
2 GAGE ROSETTE 14	27	-983	28	-124	-46446	-15223
2 GAGE ROSETTE 15	29	-1090	30	-311	-53168	-24847
2 GAGE ROSETTE 16	31	-1074	32	-330	-52601	-25550
2 GAGE ROSETTE 17	33	-1068	34	-364	-52698	-27071
2 GAGE ROSETTE 18	35	-1080	36	-320	-52800	-25175
2 GAGE ROSETTE 19	37	-1062	38	-341	-52191	-25964
2 GAGE ROSETTE 20	39	-1052	40	-57	-48973	12800
2 GAGE ROSETTE 21	41	-1130	42	-279	-54715	-23777
2 GAGE ROSETTE 22	43	-791	44	-822	-44355	-45474
2 GAGE ROSETTE 23	45	-552	46	-701	-32186	-37586
2 GAGE ROSETTE 24	47	-389	48	11	-17785	-3238
2 GAGE ROSETTE 25	49	-972	50	-375	-48359	-26660
2 GAGE ROSETTE 26	51	-955	52	-364	-47472	-25974
2 GAGE ROSETTE 27	53	-977	54	-341	-48287	-25144
2 GAGE ROSETTE 28	55	-983	56	-330	-48440	-24677
2 GAGE ROSETTE 29	57	-512	58	-313	-26568	-19340
2 GAGE ROSETTE 30	59	-607	60	-45	-11261	-4232
2 GAGE ROSETTE 31	61	-678	62	148	-11471	-1132
2 GAGE ROSETTE 32	63	-663	64	-11	-12090	-3934
2 GAGE ROSETTE 33	65	-476	66	-182	-9655	-5974
2 GAGE ROSETTE 34	67	-714	68	320	-11159	1795
2 GAGE ROSETTE 35	69	-1014	70	198	-17283	-2107
2 GAGE ROSETTE 36	71	-603	72	288	-9315	1836
2 GAGE ROSETTE 37	73	-877	74	900	-10842	11397
2 GAGE ROSETTE 38	75	-612	76	904	-6013	12967
2 GAGE ROSETTE 39	77	-827	78	1107	-8775	15434
2 GAGE ROSETTE 40	79	-708	80	985	-7303	13892
2 GAGE ROSETTE 41	81	-704	82	880	-7815	12011
2 GAGE ROSETTE 42	83	-976	84	233	-16398	-1261
2 GAGE ROSETTE 43	85	-745	86	254	-12099	411
2 GAGE ROSETTE 44	87	-924	88	212	-15571	-1358
2 GAGE ROSETTE 45	89	-695	90	255	-11173	719
2 GAGE ROSETTE 46	91	-756	92	364	-11667	2345
2 GAGE ROSETTE 47	93	-425	94	462	-5115	5989
2 GAGE ROSETTE 48	95	-569	96	-97	-10866	-4953
2 GAGE ROSETTE 49	97	-502	98	186	-8061	556
2 GAGE ROSETTE 50	99	-567	100	-38	-10505	-3881

FEATURED RESEARCH

Table 5. Strains recorded during pressurization of the scale-model housing assembly to 9,500 psi, Sheet 5.

12-17-1992

SCAN NUMBER 44
PRESSURE = 5000.00

	CHANNEL	UE	CHANNEL	UE	STRESS (HOOP)	STRESS (LONG)
2 GAGE ROSETTE 1	1	-1371	2	-1413	-76752	-78307
2 GAGE ROSETTE 2	3	-1130	4	-1166	-63287	-64598
2 GAGE ROSETTE 3	5	-514	6	-1155	-34815	-58130
2 GAGE ROSETTE 4	7	-1266	8	-235	-60525	-23031
2 GAGE ROSETTE 5	9	-1243	10	-112	-58303	-17187
2 GAGE ROSETTE 6	11	-1337	12	-380	-65210	-30404
2 GAGE ROSETTE 7	13	-1337	14	-362	-65034	-29568
2 GAGE ROSETTE 8	15	-1281	16	-402	-62846	-30891
2 GAGE ROSETTE 9	17	-1341	18	-422	-65819	-32390
2 GAGE ROSETTE 10	19	-1307	20	-412	-64134	-31580
2 GAGE ROSETTE 11	21	-1218	22	-294	-58882	-25293
2 GAGE ROSETTE 12	23	-1288	24	-239	-61605	-23440
2 GAGE ROSETTE 13	25	-1206	26	-236	-57808	-22521
2 GAGE ROSETTE 14	27	-1229	28	-170	-58194	-19679
2 GAGE ROSETTE 15	29	-1359	30	-400	-66438	-31543
2 GAGE ROSETTE 16	31	-1356	32	-386	-66155	-30897
2 GAGE ROSETTE 17	33	-1330	34	-443	-65501	-33261
2 GAGE ROSETTE 18	35	-1364	36	-412	-66765	-32132
2 GAGE ROSETTE 19	37	-1333	38	-443	-65664	-33295
2 GAGE ROSETTE 20	39	-1303	40	-80	-60773	-16284
2 GAGE ROSETTE 21	41	-1379	42	-313	-66482	-27722
2 GAGE ROSETTE 22	43	-972	44	-1022	-54610	-56423
2 GAGE ROSETTE 23	45	-663	46	-848	-38688	-45416
2 GAGE ROSETTE 24	47	-515	48	-11	-23793	-5494
2 GAGE ROSETTE 25	49	-1198	50	-409	-59092	-30414
2 GAGE ROSETTE 26	51	-1225	52	-443	-60653	-32243
2 GAGE ROSETTE 27	53	-1213	54	-421	-59916	-31088
2 GAGE ROSETTE 28	55	-1209	56	-443	-59942	-32093
2 GAGE ROSETTE 29	57	-602	58	-369	-31293	-22790
2 GAGE ROSETTE 30	59	-741	60	-79	-13898	-5606
2 GAGE ROSETTE 31	61	-870	62	216	-14573	-976
2 GAGE ROSETTE 32	63	-888	64	45	-15847	-4167
2 GAGE ROSETTE 33	65	-592	66	-191	-11823	-6803
2 GAGE ROSETTE 34	67	-934	68	380	-14809	1649
2 GAGE ROSETTE 35	69	-1272	70	297	-21412	-1762
2 GAGE ROSETTE 36	71	-784	72	344	-12299	1825
2 GAGE ROSETTE 37	73	-1106	74	1127	-13720	14233
2 GAGE ROSETTE 38	75	-796	76	1142	-8022	16247
2 GAGE ROSETTE 39	77	-1009	78	1398	-10450	19692
2 GAGE ROSETTE 40	79	-899	80	1231	-9389	17285
2 GAGE ROSETTE 41	81	-844	82	1167	-8753	16426
2 GAGE ROSETTE 42	83	-1203	84	262	-20348	-2008
2 GAGE ROSETTE 43	85	-932	86	264	-15425	-460
2 GAGE ROSETTE 44	87	-1178	88	279	-19810	-1569
2 GAGE ROSETTE 45	89	-809	90	343	-12749	1678
2 GAGE ROSETTE 46	91	-985	92	488	-15133	3310
2 GAGE ROSETTE 47	93	-580	94	518	-7602	6146
2 GAGE ROSETTE 48	95	-745	96	-97	-14069	-5946
2 GAGE ROSETTE 49	97	-654	98	275	-10314	1307
2 GAGE ROSETTE 50	99	-759	100	-67	-14155	-5481

Table 5. Strains recorded during pressurization of the scale-model housing assembly to 9,500 psi, Sheet 6.

12-17-1982

SCAN NUMBER 45
PRESSURE = 6000.00

	CHANNEL	UE	CHANNEL	UE	STRESS (HOOP)	STRESS (LONG)
2 GAGE ROSETTE 1	1	-1640	1	-1689	-91832	-93620
2 GAGE ROSETTE 2	3	-1070	4	-1099	-77505	-77845
2 GAGE ROSETTE 3	5	-614	5	-1366	-41482	-69814
2 GAGE ROSETTE 4	7	-1526	8	-279	-72920	-27600
2 GAGE ROSETTE 5	9	-1503	10	-135	-70484	-20734
2 GAGE ROSETTE 6	11	-1595	12	-469	-77967	-37015
2 GAGE ROSETTE 7	13	-1595	14	-441	-77693	-35707
2 GAGE ROSETTE 8	15	-1513	16	-469	-74167	-36217
2 GAGE ROSETTE 9	17	-1637	18	-500	-80174	-38826
2 GAGE ROSETTE 10	19	-1553	20	-492	-76218	-37639
2 GAGE ROSETTE 11	21	-1441	22	-339	-69601	-29533
2 GAGE ROSETTE 12	23	-1526	24	-284	-72968	-27827
2 GAGE ROSETTE 13	25	-1452	26	-292	-69662	-27482
2 GAGE ROSETTE 14	27	-1474	28	-215	-69942	-24135
2 GAGE ROSETTE 15	29	-1618	30	-500	-79298	-38642
2 GAGE ROSETTE 16	31	-1605	32	-489	-78587	-38009
2 GAGE ROSETTE 17	33	-1580	34	-512	-77671	-38817
2 GAGE ROSETTE 18	35	-1614	36	-480	-78939	-37707
2 GAGE ROSETTE 19	37	-1582	38	-500	-77656	-38314
2 GAGE ROSETTE 20	39	-1555	40	-149	-73015	-21874
2 GAGE ROSETTE 21	41	-1661	42	-369	-80026	-33024
2 GAGE ROSETTE 22	43	-1153	44	-1244	-65079	-68395
2 GAGE ROSETTE 23	45	-795	46	-1017	-46426	-54499
2 GAGE ROSETTE 24	47	-572	48	-34	-26643	-7087
2 GAGE ROSETTE 25	49	-1446	50	-523	-71634	-38050
2 GAGE ROSETTE 26	51	-1416	52	-512	-70103	-37228
2 GAGE ROSETTE 27	53	-1427	54	-489	-70400	-36290
2 GAGE ROSETTE 28	55	-1424	55	-466	-70045	-35215
2 GAGE ROSETTE 29	57	-705	58	-424	-36542	-26350
2 GAGE ROSETTE 30	59	-820	60	-158	-15770	-7483
2 GAGE ROSETTE 31	61	-1096	62	284	-18290	-1009
2 GAGE ROSETTE 32	63	-1135	64	57	-20268	-5351
2 GAGE ROSETTE 33	65	-767	66	-258	-15371	-9001
2 GAGE ROSETTE 34	67	-1136	68	471	-17957	2151
2 GAGE ROSETTE 35	69	-1502	70	367	-25187	-1795
2 GAGE ROSETTE 36	71	-909	72	446	-13981	2979
2 GAGE ROSETTE 37	73	-1315	74	1411	-15917	18212
2 GAGE ROSETTE 38	75	-913	76	1352	-8958	19391
2 GAGE ROSETTE 39	77	-1259	78	1622	-13729	22339
2 GAGE ROSETTE 40	79	-1081	80	1421	-11621	19700
2 GAGE ROSETTE 41	81	-1041	82	1368	-11197	18963
2 GAGE ROSETTE 42	83	-1479	84	379	-24702	-1447
2 GAGE ROSETTE 43	85	-1108	85	342	-18189	-37
2 GAGE ROSETTE 44	87	-1329	86	346	-22168	-1196
2 GAGE ROSETTE 45	89	-1009	90	441	-15825	2333
2 GAGE ROSETTE 46	91	-1186	92	564	-18748	3568
2 GAGE ROSETTE 47	93	-867	94	641	-8491	7860
2 GAGE ROSETTE 48	95	-863	95	-57	-16150	-6433
2 GAGE ROSETTE 49	97	-748	98	255	-12143	416
2 GAGE ROSETTE 50	99	-694	100	-76	-16650	-6410

FEATURED RESEARCH

Table 5. Strains recorded during pressurization of the scale-model housing assembly to 9,500 psi, Sheet 7.

12-17-1982

SCAN NUMBER 46
PRESSURE = 7000.00

	CHANNEL	UE	CHANNEL	UE	STRESS (HOOF)	STRESS (LONG)
2 GAGE ROSETTE 1	1	-1932	2	-1954	-107839	-108642
2 GAGE ROSETTE 2	3	-1582	4	-1633	-88602	-90437
2 GAGE ROSETTE 3	5	-715	6	-1577	-48149	-79499
2 GAGE ROSETTE 4	7	-1785	8	-335	-85424	-32683
2 GAGE ROSETTE 5	9	-1740	10	-191	-81950	-25613
2 GAGE ROSETTE 6	11	-1865	12	-558	-91242	-43734
2 GAGE ROSETTE 7	13	-1865	14	-509	-90759	-41434
2 GAGE ROSETTE 8	15	-1767	16	-558	-86721	-42785
2 GAGE ROSETTE 9	17	-1910	18	-577	-93482	-45041
2 GAGE ROSETTE 10	19	-1821	20	-595	-89553	-44967
2 GAGE ROSETTE 11	21	-1709	22	-407	-82596	-35245
2 GAGE ROSETTE 12	23	-1774	24	-318	-84741	-31800
2 GAGE ROSETTE 13	25	-1720	26	-326	-82327	-31624
2 GAGE ROSETTE 14	27	-1709	28	-260	-81176	-28483
2 GAGE ROSETTE 15	29	-1899	30	-589	-93085	-45446
2 GAGE ROSETTE 16	31	-1898	32	-580	-92990	-45035
2 GAGE ROSETTE 17	33	-1876	34	-625	-92374	-46906
2 GAGE ROSETTE 18	35	-1910	36	-560	-93316	-44248
2 GAGE ROSETTE 19	37	-1842	38	-580	-90389	-44489
2 GAGE ROSETTE 20	39	-1807	40	-183	-84926	-25884
2 GAGE ROSETTE 21	41	-1921	42	-436	-92637	-38621
2 GAGE ROSETTE 22	43	-1300	44	-1433	-73666	-78505
2 GAGE ROSETTE 23	45	-961	46	-1198	-55798	-64423
2 GAGE ROSETTE 24	47	-617	48	-79	-29185	-9609
2 GAGE ROSETTE 25	49	-1672	50	-580	-82587	-42850
2 GAGE ROSETTE 26	51	-1674	52	-580	-82656	-42865
2 GAGE ROSETTE 27	53	-1685	54	-546	-82844	-41404
2 GAGE ROSETTE 28	55	-1650	56	-568	-81437	-42109
2 GAGE ROSETTE 29	57	-853	58	-469	-43776	-29835
2 GAGE ROSETTE 30	59	-989	60	-226	-19209	-9661
2 GAGE ROSETTE 31	61	-1311	62	352	-21802	-980
2 GAGE ROSETTE 32	63	-1393	64	159	-24381	-4948
2 GAGE ROSETTE 33	65	-893	66	-258	-17661	-9711
2 GAGE ROSETTE 34	67	-1319	68	561	-20774	2755
2 GAGE ROSETTE 35	69	-1770	70	446	-29601	-1863
2 GAGE ROSETTE 36	71	-1110	72	530	-17155	3366
2 GAGE ROSETTE 37	73	-1574	74	1629	-19390	20709
2 GAGE ROSETTE 38	75	-1097	76	1599	-10914	22844
2 GAGE ROSETTE 39	77	-1490	78	1932	-16168	26679
2 GAGE ROSETTE 40	79	-1320	80	1705	-14362	23510
2 GAGE ROSETTE 41	81	-1201	82	1626	-12638	22753
2 GAGE ROSETTE 42	83	-1706	84	447	-28434	-1489
2 GAGE ROSETTE 43	85	-1314	86	410	-21543	44
2 GAGE ROSETTE 44	87	-1612	88	385	-27082	-2089
2 GAGE ROSETTE 45	89	-1180	90	500	-18602	2438
2 GAGE ROSETTE 46	91	-1078	92	660	-21281	4228
2 GAGE ROSETTE 47	93	-783	94	679	-10382	7912
2 GAGE ROSETTE 48	95	-1010	96	-97	-18874	-7436
2 GAGE ROSETTE 49	97	-900	98	304	-14617	456
2 GAGE ROSETTE 50	99	-1067	100	-48	-19629	-6866

Table 5. Strains recorded during pressurization of the scale-model housing assembly to 9,500 psi, Sheet 8.

12-17-1992

SCAN NUMBER 47
PRESSURE = 8000.00

	CHANNEL	UE	CHANNEL	UE	STRESS:HOOP	STRESS:LONG
2 GAGE ROSETTE 1	1	-2202	2	-2186	-102492	-101922
2 GAGE ROSETTE 2	3	-1808	4	-1866	-101264	-100257
2 GAGE ROSETTE 3	5	-793	6	-1777	-53680	-89456
2 GAGE ROSETTE 4	7	-2057	8	-391	-98447	-27675
2 GAGE ROSETTE 5	9	-2023	10	-236	-95389	-20412
2 GAGE ROSETTE 6	11	-2146	12	-637	-104926	-50048
2 GAGE ROSETTE 7	13	-2123	14	-576	-103309	-47053
2 GAGE ROSETTE 8	15	-2021	16	-659	-99383	-49867
2 GAGE ROSETTE 9	17	-2194	18	-677	-107529	-52388
2 GAGE ROSETTE 10	19	-2089	20	-663	-102555	-50716
2 GAGE ROSETTE 11	21	-1944	22	-452	-93830	-29593
2 GAGE ROSETTE 12	23	-2057	24	-364	-98184	-36623
2 GAGE ROSETTE 13	25	-1955	26	-371	-93559	-35960
2 GAGE ROSETTE 14	27	-1966	28	-305	-93438	-33047
2 GAGE ROSETTE 15	29	-2168	30	-677	-106355	-52142
2 GAGE ROSETTE 16	31	-2147	32	-648	-105093	-50578
2 GAGE ROSETTE 17	33	-2126	34	-716	-104764	-53509
2 GAGE ROSETTE 18	35	-2205	36	-663	-107914	-51842
2 GAGE ROSETTE 19	37	-2113	38	-671	-103752	-51296
2 GAGE ROSETTE 20	39	-2070	40	-229	-97473	-30531
2 GAGE ROSETTE 21	41	-525	42	-525	-104945	-45137
2 GAGE ROSETTE 22	43	-1559	44	-1633	-87562	-90219
2 GAGE ROSETTE 23	45	-1027	46	-1396	-60704	-73906
2 GAGE ROSETTE 24	47	-732	48	-113	-34776	-12275
2 GAGE ROSETTE 25	49	-1898	50	-671	-93869	-49221
2 GAGE ROSETTE 26	51	-1865	52	-648	-92107	-47851
2 GAGE ROSETTE 27	53	-1899	54	-625	-93438	-47130
2 GAGE ROSETTE 28	55	-1876	56	-625	-92389	-46910
2 GAGE ROSETTE 29	57	-955	58	-536	-49133	-33908
2 GAGE ROSETTE 30	59	-1112	60	-305	-21896	-11792
2 GAGE ROSETTE 31	61	-1537	62	477	-25199	18
2 GAGE ROSETTE 32	63	-1629	64	182	-28534	-5863
2 GAGE ROSETTE 33	65	-1039	66	-258	-20304	-10530
2 GAGE ROSETTE 34	67	-1548	68	691	-24196	3829
2 GAGE ROSETTE 35	69	-2018	70	555	-33501	-1284
2 GAGE ROSETTE 36	71	-1301	72	632	-20052	4144
2 GAGE ROSETTE 37	73	-1823	74	1876	-22523	23777
2 GAGE ROSETTE 38	75	-1224	76	1771	-12240	25242
2 GAGE ROSETTE 39	77	-1711	78	2185	-18760	20016
2 GAGE ROSETTE 40	79	-1492	80	1913	-16314	26523
2 GAGE ROSETTE 41	81	-1379	82	1827	-14742	25395
2 GAGE ROSETTE 42	83	-1952	84	524	-32469	-1466
2 GAGE ROSETTE 43	85	-1481	86	496	-24074	700
2 GAGE ROSETTE 44	87	-1829	88	461	-30583	-1913
2 GAGE ROSETTE 45	89	-1371	90	638	-21284	3856
2 GAGE ROSETTE 46	91	-1607	92	746	-24962	4499
2 GAGE ROSETTE 47	93	-889	94	754	-11886	8682
2 GAGE ROSETTE 48	95	-1157	96	-155	-21870	-5315
2 GAGE ROSETTE 49	97	-1014	98	343	-16458	538
2 GAGE ROSETTE 50	99	-1154	100	0	-20971	-6489

FEATURED RESEARCH

Table 5. Strains recorded during pressurization of the scale-model housing assembly to 9,500 psi, Sheet 9.

12-17-1992

SCAN NUMBER 48
PRESSURE = 9000.00

	CHANNEL	UE	CHANNEL	UE	STRESS (HOOP)	STRESS (LONG)
2 GAGE ROSETTE 1	1	-2483	2	-2473	-138195	-137852
2 GAGE ROSETTE 2	3	-2034	4	-2121	-114132	-117299
2 GAGE ROSETTE 3	5	-938	6	-1977	-62296	-100061
2 GAGE ROSETTE 4	7	-2305	8	-424	-110215	-41821
2 GAGE ROSETTE 5	9	-2283	10	-270	-107678	-34476
2 GAGE ROSETTE 6	11	-2438	12	-715	-119128	-56471
2 GAGE ROSETTE 7	13	-2393	14	-678	-116703	-54341
2 GAGE ROSETTE 8	15	-2308	16	-715	-113138	-55213
2 GAGE ROSETTE 9	17	-2455	18	-766	-120422	-59005
2 GAGE ROSETTE 10	19	-2346	20	-778	-115486	-58463
2 GAGE ROSETTE 11	21	-2200	22	-486	-105983	-43637
2 GAGE ROSETTE 12	23	-2305	24	-409	-110067	-41119
2 GAGE ROSETTE 13	25	-2234	26	-427	-106955	-41245
2 GAGE ROSETTE 14	27	-2200	28	-362	-104782	-37915
2 GAGE ROSETTE 15	29	-2460	30	-722	-120230	-57010
2 GAGE ROSETTE 16	31	-2418	32	-716	-118236	-56338
2 GAGE ROSETTE 17	33	-2421	34	-773	-118917	-58982
2 GAGE ROSETTE 18	35	-2478	36	-743	-121245	-58163
2 GAGE ROSETTE 19	37	-2384	38	-762	-117115	-58104
2 GAGE ROSETTE 20	39	-2333	40	-297	-110241	-36231
2 GAGE ROSETTE 21	41	-2441	42	-581	-117968	-50330
2 GAGE ROSETTE 22	43	-1706	44	-1777	-95720	-98284
2 GAGE ROSETTE 23	45	-1126	46	-1559	-66917	-82669
2 GAGE ROSETTE 24	47	-812	48	-124	-38570	-13569
2 GAGE ROSETTE 25	49	-2124	50	-762	-105151	-55591
2 GAGE ROSETTE 26	51	-2112	52	-739	-104363	-54425
2 GAGE ROSETTE 27	53	-2123	54	-727	-104770	-54011
2 GAGE ROSETTE 28	55	-2113	56	-705	-104081	-52866
2 GAGE ROSETTE 29	57	-1046	58	-558	-53534	-35816
2 GAGE ROSETTE 30	59	-1236	60	-339	-24329	-13102
2 GAGE ROSETTE 31	61	-1695	62	546	-27686	365
2 GAGE ROSETTE 32	63	-1854	64	284	-32035	-5270
2 GAGE ROSETTE 33	65	-1175	66	-268	-22824	-11468
2 GAGE ROSETTE 34	67	-1769	68	771	-27733	4046
2 GAGE ROSETTE 35	69	-2286	70	614	-38026	-1712
2 GAGE ROSETTE 36	71	-1473	72	715	-22706	4693
2 GAGE ROSETTE 37	73	-2072	74	2169	-25390	27704
2 GAGE ROSETTE 38	75	-1359	76	1970	-13583	28105
2 GAGE ROSETTE 39	77	-1904	78	2486	-20555	34396
2 GAGE ROSETTE 40	79	-1684	80	2179	-18294	30059
2 GAGE ROSETTE 41	81	-1538	82	2095	-16129	29358
2 GAGE ROSETTE 42	83	-2277	84	573	-38098	-2415
2 GAGE ROSETTE 43	85	-1677	86	527	-27469	128
2 GAGE ROSETTE 44	87	-2074	88	509	-34814	-2594
2 GAGE ROSETTE 45	89	-1571	90	657	-24801	3090
2 GAGE ROSETTE 46	91	-1856	92	871	-28775	5356
2 GAGE ROSETTE 47	93	-1005	94	820	-13619	9227
2 GAGE ROSETTE 48	95	-1305	96	-126	-24376	-9617
2 GAGE ROSETTE 49	97	-1137	98	412	-18306	1081
2 GAGE ROSETTE 50	99	-1317	100	-57	-24218	-8444

Table 5. Strains recorded during pressurization of the scale-model housing assembly to 9,500 psi, Sheet 10.

12-17-1992

SCAN NUMBER 49

PRESSURE = 9500.00

	CHANNEL	UE	CHANNEL	UE	STRESS(HOOP)	STRESS(LONG)
2 GAGE ROSETTE 1	1	-2618	2	-2628	-145895	-146271
2 GAGE ROSETTE 2	3	-2147	4	-2221	-120300	-122992
2 GAGE ROSETTE 3	5	-1005	6	-2110	-66669	-106843
2 GAGE ROSETTE 4	7	-2441	8	-436	-116565	-43646
2 GAGE ROSETTE 5	9	-2418	10	-303	-114246	-37338
2 GAGE ROSETTE 6	11	-2584	12	-771	-126390	-60453
2 GAGE ROSETTE 7	13	-2517	14	-746	-123047	-58656
2 GAGE ROSETTE 8	15	-2451	16	-771	-120285	-59171
2 GAGE ROSETTE 9	17	-2592	18	-777	-126808	-60835
2 GAGE ROSETTE 10	19	-2469	20	-812	-121473	-61230
2 GAGE ROSETTE 11	21	-2323	22	-509	-111857	-45865
2 GAGE ROSETTE 12	23	-2430	24	-443	-116119	-43890
2 GAGE ROSETTE 13	25	-2334	26	-449	-111800	-43251
2 GAGE ROSETTE 14	27	-2334	28	-350	-110842	-38691
2 GAGE ROSETTE 15	29	-2595	30	-766	-126865	-60358
2 GAGE ROSETTE 16	31	-2554	32	-807	-125356	-61835
2 GAGE ROSETTE 17	33	-2523	34	-807	-123955	-61541
2 GAGE ROSETTE 18	35	-2603	36	-789	-127443	-61477
2 GAGE ROSETTE 19	37	-2520	38	-807	-123796	-61507
2 GAGE ROSETTE 20	39	-2458	40	-274	-115810	-36394
2 GAGE ROSETTE 21	41	-2588	42	-570	-124622	-51236
2 GAGE ROSETTE 22	43	-1808	44	-1888	-101474	-104379
2 GAGE ROSETTE 23	45	-1204	46	-1627	-71131	-86537
2 GAGE ROSETTE 24	47	-846	48	-147	-40367	-14941
2 GAGE ROSETTE 25	49	-2215	50	-796	-109642	-58035
2 GAGE ROSETTE 26	51	-2224	52	-762	-109754	-56558
2 GAGE ROSETTE 27	53	-2247	54	-750	-110678	-56252
2 GAGE ROSETTE 28	55	-2249	56	-739	-110653	-55746
2 GAGE ROSETTE 29	57	-1091	58	-581	-55843	-37283
2 GAGE ROSETTE 30	59	-1314	60	-373	-25946	-14159
2 GAGE ROSETTE 31	61	-1842	62	637	-29840	1189
2 GAGE ROSETTE 32	63	-1977	64	239	-34533	-6790
2 GAGE ROSETTE 33	65	-1243	66	-297	-24219	-12371
2 GAGE ROSETTE 34	67	-1877	68	801	-29558	3973
2 GAGE ROSETTE 35	69	-2392	70	694	-39490	-866
2 GAGE ROSETTE 36	71	-1569	72	799	-23971	5672
2 GAGE ROSETTE 37	73	-2261	74	2311	-28024	29217
2 GAGE ROSETTE 38	75	-1418	76	2123	-13783	30540
2 GAGE ROSETTE 39	77	-2000	78	2661	-21316	37027
2 GAGE ROSETTE 40	79	-1760	80	2311	-18936	32034
2 GAGE ROSETTE 41	81	-1595	82	2191	-16612	30777
2 GAGE ROSETTE 42	83	-2356	84	631	-39202	-1801
2 GAGE ROSETTE 43	85	-1844	86	566	-30275	-102
2 GAGE ROSETTE 44	87	-2177	88	558	-36371	-2130
2 GAGE ROSETTE 45	89	-1647	90	726	-25796	3907
2 GAGE ROSETTE 46	91	-1913	92	937	-29440	6248
2 GAGE ROSETTE 47	93	-1053	94	858	-14283	9640
2 GAGE ROSETTE 48	95	-1383	96	-48	-25365	-8656
2 GAGE ROSETTE 49	97	-1175	98	432	-18884	1224
2 GAGE ROSETTE 50	99	-1375	100	-48	-25211	-8596

FEATURED RESEARCH

Table 5. Strains recorded during pressurization of the scale-model housing assembly to 9,500 psi, Sheet 11.

12-17-1982

SCAN NUMBER 50
PRESSURE = 0.000

	CHANNEL	UE	CHANNEL	UE	STRESS(HOOP)	STRESS(LONG)
2 GAGE ROSETTE 1	1	0	2	0	0	0
2 GAGE ROSETTE 2	3	0	4	0	0	0
2 GAGE ROSETTE 3	5	0	6	0	0	0
2 GAGE ROSETTE 4	7	3	8	22	355	1063
2 GAGE ROSETTE 5	9	22	10	33	1329	1728
2 GAGE ROSETTE 6	11	11	12	0	505	106
2 GAGE ROSETTE 7	13	33	14	-22	1297	-688
2 GAGE ROSETTE 8	15	45	16	33	2387	1951
2 GAGE ROSETTE 9	17	33	18	11	1606	823
2 GAGE ROSETTE 10	19	23	20	33	1361	1743
2 GAGE ROSETTE 11	21	11	22	0	514	108
2 GAGE ROSETTE 12	23	0	24	34	326	1551
2 GAGE ROSETTE 13	25	0	26	56	540	2571
2 GAGE ROSETTE 14	27	22	28	34	1340	1756
2 GAGE ROSETTE 15	29	11	30	11	615	615
2 GAGE ROSETTE 16	31	33	32	11	1633	834
2 GAGE ROSETTE 17	33	-11	34	33	-189	1426
2 GAGE ROSETTE 18	35	34	36	0	1542	324
2 GAGE ROSETTE 19	37	45	38	33	2391	1968
2 GAGE ROSETTE 20	39	34	40	54	2082	2812
2 GAGE ROSETTE 21	41	-22	42	-22	-1212	-1221
2 GAGE ROSETTE 22	43	12	44	11	635	614
2 GAGE ROSETTE 23	45	45	46	0	2057	432
2 GAGE ROSETTE 24	47	0	48	0	0	0
2 GAGE ROSETTE 25	49	-22	50	-22	-1228	-1247
2 GAGE ROSETTE 26	51	-44	52	11	-1937	82
2 GAGE ROSETTE 27	53	0	54	-11	-106	-503
2 GAGE ROSETTE 28	55	0	56	-11	-107	-511
2 GAGE ROSETTE 29	57	-11	58	-23	-727	-1147
2 GAGE ROSETTE 30	59	0	60	0	0	0
2 GAGE ROSETTE 31	61	0	62	0	0	0
2 GAGE ROSETTE 32	63	22	64	0	413	132
2 GAGE ROSETTE 33	65	0	66	0	0	0
2 GAGE ROSETTE 34	67	0	68	0	0	0
2 GAGE ROSETTE 35	69	18	70	9	395	281
2 GAGE ROSETTE 36	71	0	72	-19	-112	-350
2 GAGE ROSETTE 37	73	36	74	9	722	384
2 GAGE ROSETTE 38	75	-18	76	-9	-383	-275
2 GAGE ROSETTE 39	77	36	78	48	944	1087
2 GAGE ROSETTE 40	79	27	80	10	561	337
2 GAGE ROSETTE 41	81	56	82	-19	920	-12
2 GAGE ROSETTE 42	83	-56	84	65	-640	873
2 GAGE ROSETTE 43	85	10	86	28	338	564
2 GAGE ROSETTE 44	87	-9	88	10	-114	121
2 GAGE ROSETTE 45	89	-9	90	0	-171	-55
2 GAGE ROSETTE 46	91	0	92	-19	-109	-342
2 GAGE ROSETTE 47	93	28	94	-9	467	-7
2 GAGE ROSETTE 48	95	0	96	-29	-169	-528
2 GAGE ROSETTE 49	97	0	98	-84	-494	-1544
2 GAGE ROSETTE 50	99	19	100	-9	296	-56

Table 6. Comparison of FEA calculations to test results on model housing components, Sheet 1.

Gauge Location	Hoop Stress (Tested, kpsi)	Hoop Stress (FEA, kpsi)	Axial Stress (Tested, kpsi)	Axial Stress (FEA, kpsi)
1	-138	-145	-138	-145
2	-114	-99	-117	-99
3	-62		-100	
4	-110	-123	-42	-50
5	-108		-34	
6	-119		-56	
7	-116		-54	
8	-113	-130	-55	-64
9	-120		-59	
10	-115		-58	
11	-106	-113	-44	-57
12	-110		-41	
13	-107	-113	-41	-50
14	-105		-38	
15	-120		-57	
16	-118	-130	-56	-64
17	-119		-59	
18	-121		-58	
19	-117		-58	
20	-110	-123	-36	-57
21	-118		-50	
22	-96		-98	
23	-67	-116	-83	-116
24	-39	-18	-14	-18
25	-105	-116	-56	-64
26	-104		-54	
27	-105	-116	-54	-64
28	-104		-53	
29	-56	-50	-36	-50

Table 6. Comparison of FEA calculations to test results on model housing components, Sheet 2.

Gauge Location	Titanium Components			
	Hoop Stress (Tested, kpsi)	Axial Stress (Tested, kpsi)	von Mises Stress (Tested, kpsi)	von Mises Stress (FEA, kpsi)
30	-24	-13	21	40
31	-28	0	28	36
32	-32	-5	30	32
33	-23	-11	20	40
34	-28	4	30	36
35	-38	-2	37	32
36	-23	5	26	27
37	-25	28	46	51
38	-14	28	37	
39	-21	35	49	
40	-18	30	42	
41	-16	29	40	
42	-38	-2	37	36
43	-27	0	27	27
44	-35	-3	34	36
45	-25	3	27	36
46	-29	5	32	36
47	-14	9	22	24
48	24	-10	15	27
49	-18	1	15	24
50	-24	-8	16	27

**APPENDIX A: ENGINEERING FIGURES
OF SCALE-MODEL CERAMIC
PRESSURE HOUSING**

FEATURED RESEARCH

FIGURES

- A-1. Model housing assembly, Sheet 1.
- A-1. Model housing assembly, Sheet 2.
- A-2. Model housing ceramic cylinder.
- A-3. Scale-model housing of Type 1 ceramic hemisphere.
- A-4. Scale-model housing of Type 2 ceramic hemisphere.
- A-5. Scale-model housing gasket.
- A-6. Scale-model housing central stiffener.
- A-7. Scale-model housing cylinder end cap.
- A-8. Scale-model housing hemisphere end cap.
- A-9. Electrical feedthrough penetration.
- A-10. Scale-model penetration pads.
- A-11. Scale-model housing cylinder seal.
- A-12. Scale-model housing hemisphere seal.
- A-13. Scale-model housing cylinder jacket.
- A-14. Scale-model housing hemisphere jacket.
- A-15. Scale-model housing O-ring.
- A-16. Scale-model housing gasket assembly fixture.
- A-17. Scale-model housing belly band.
- A-18. Ceramic housing end bell.
- A-19. Scale-model housing spacer.
- A-20. Scale-model housing hemisphere clamp.
- A-21. Electrical feedthrough.
- A-22. Pressure vessel end closure feedthrough.
- A-23. End bell feedthrough.
- A-24. Penetration plug electrical feedthrough.

APPENDIX A: ENGINEERING FIGURES OF SCALE-MODEL CERAMIC PRESSURE HOUSING

The assembly figure for the scale-model housing is shown in figure A-1. The assembly consists of two ceramic cylinders (figure A-2) capped at the aft end with a Type 1 tapered ceramic hemisphere (figure A-3) and capped at the forward end with a Type 2 ceramic hemisphere with a single polar penetration (figure A-4). Each of these ceramic components has a GFR PEEK composite gasket (figure A-5) epoxy bonded to its bearing surface or surfaces. The two ceramic cylinders are joined with a central stiffener (figure A-6), and their remaining ends are encapsulated with cylinder end caps (figure A-7). Similarly, both ceramic hemispheres have hemisphere end caps (figure A-8) epoxy bonded to their bearing surfaces. The penetrator used for passing wire to the internal strain gages during pressure testing is the same design as used for

the 26-inch housing as shown in figure A-9, but uses the composite bearing pads shown in figure A-10.

The seals used for protecting the cylinder and hemisphere end cap epoxy bonds against water infiltration are shown in figures A-11 and A-12. The polyurethane jackets used to protect the scale-model housing ceramic components during handling and testing are shown in figures A-13 and A-14. The O-ring used to seal the interface of each hemisphere/cylinder joint is shown in figure A-15. Figure A-16 shows the fixture used to assemble the GFR PEEK composite gasket to the ends of the ceramic hemispheres and cylinders. Belly bands (figure A-17) were used to handle the scale-model assembly during pressure testing. The titanium end bell, aluminum spacer ring, and clamp band used to individually pressure test each of the ceramic hemispheres are shown in figures A-18, A-19, and A-20. Feedthroughs and plugs used during pressure tests are shown in figures A-21, A-22, A-23, and A-24.

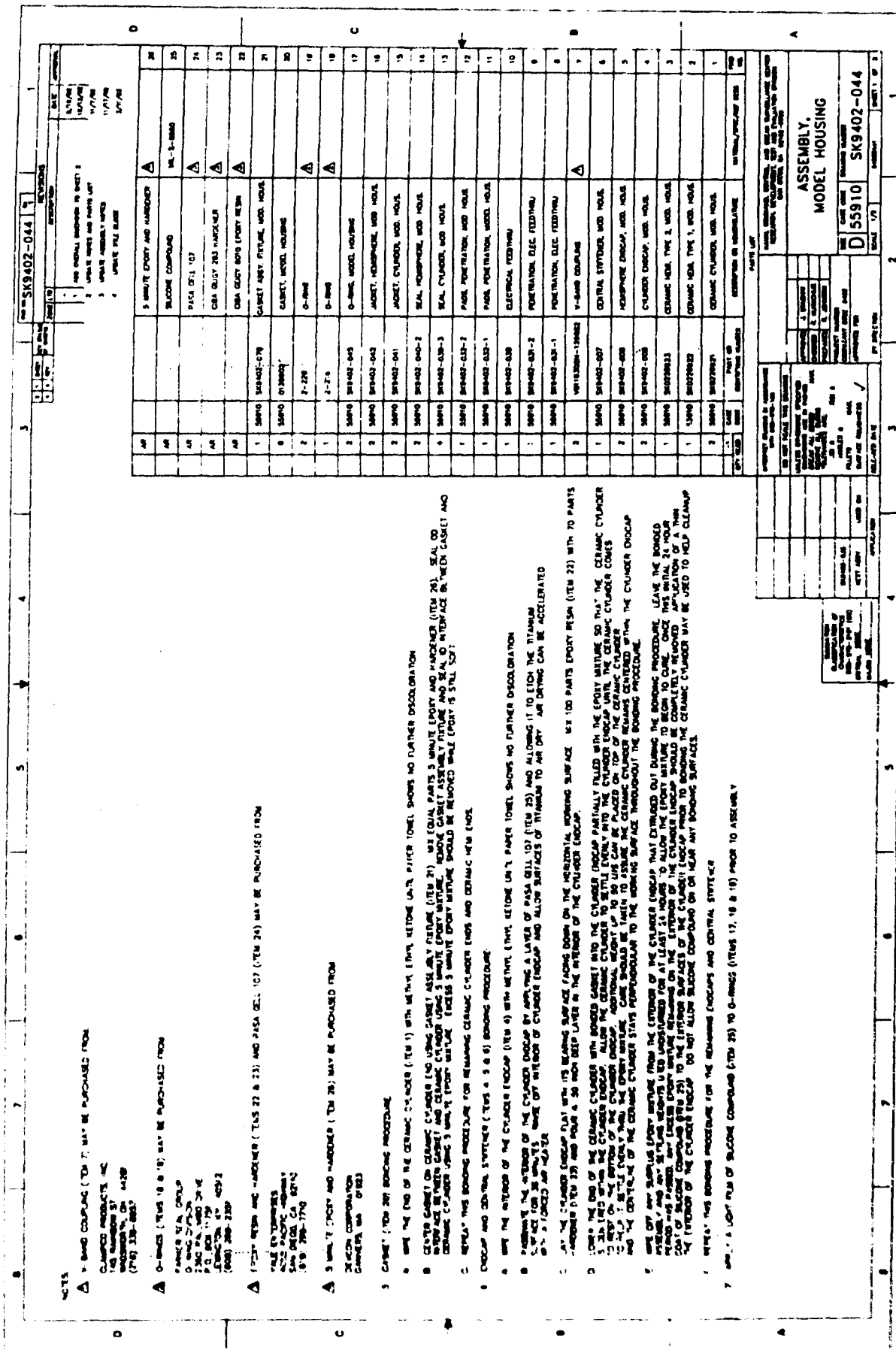


Figure A-1. Model housing assembly, Sheet 1.

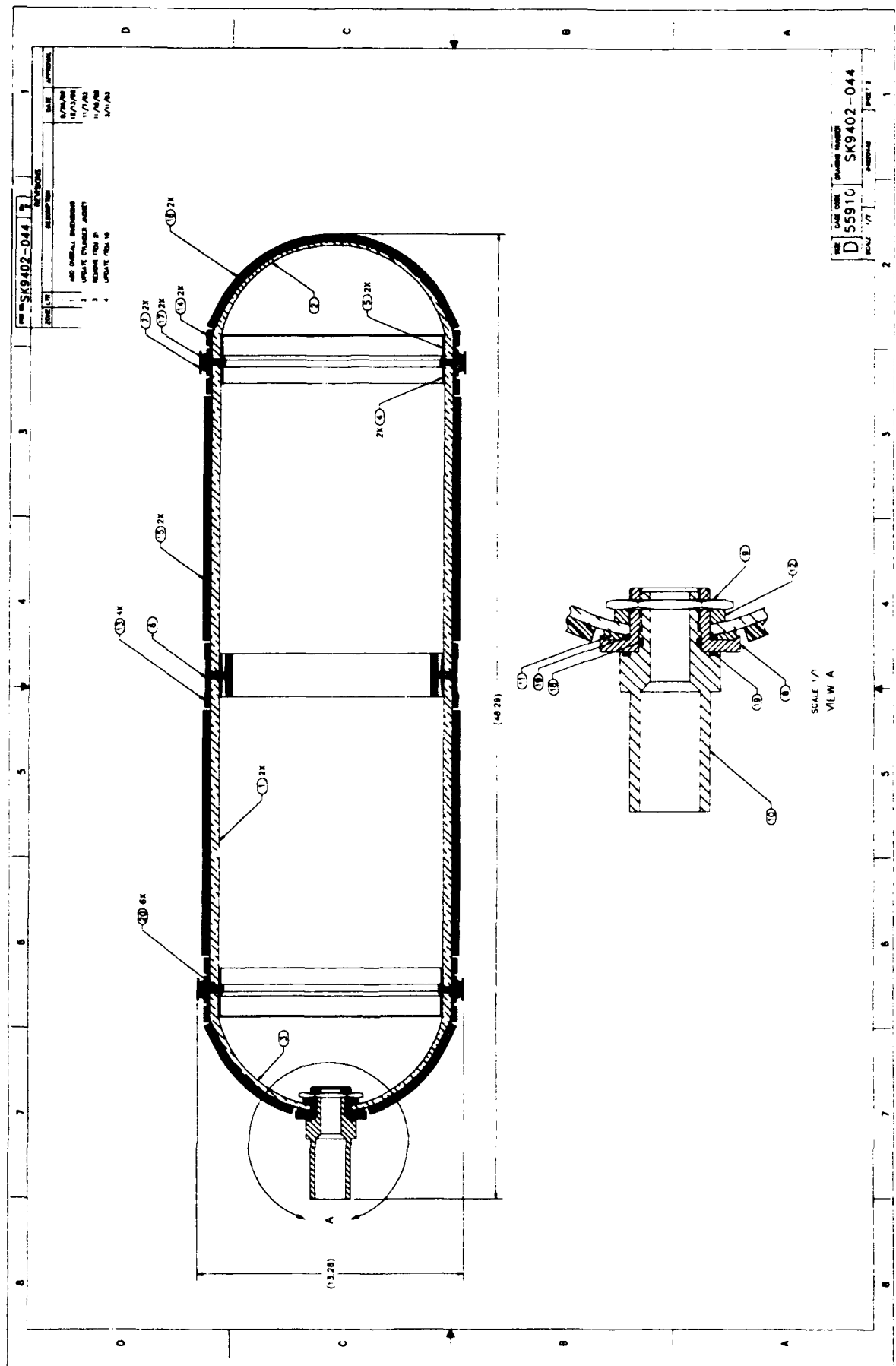


Figure A-1. Model housing assembly, Sheet 2.

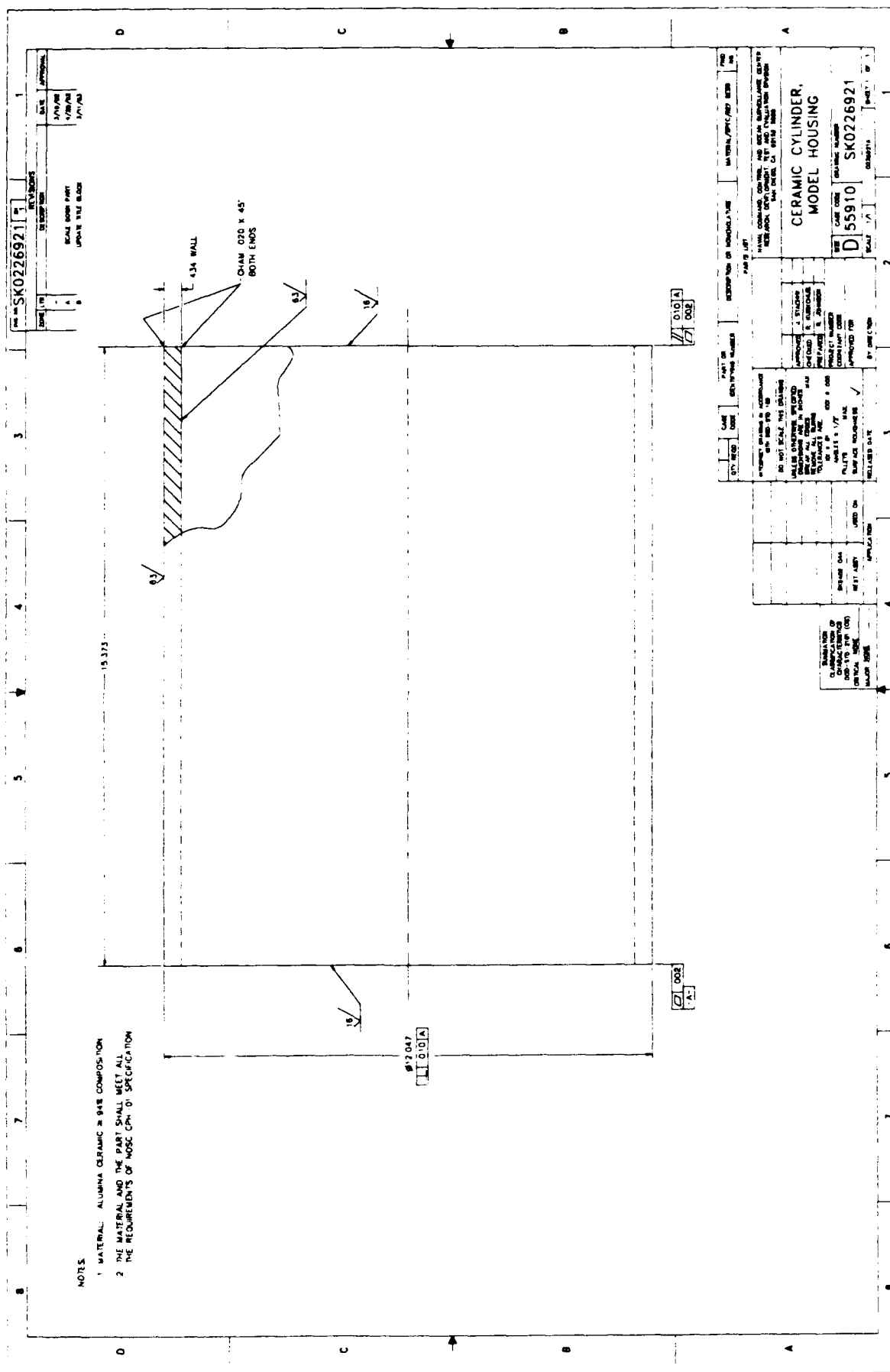


Figure A-2. Model housing ceramic cylinder.

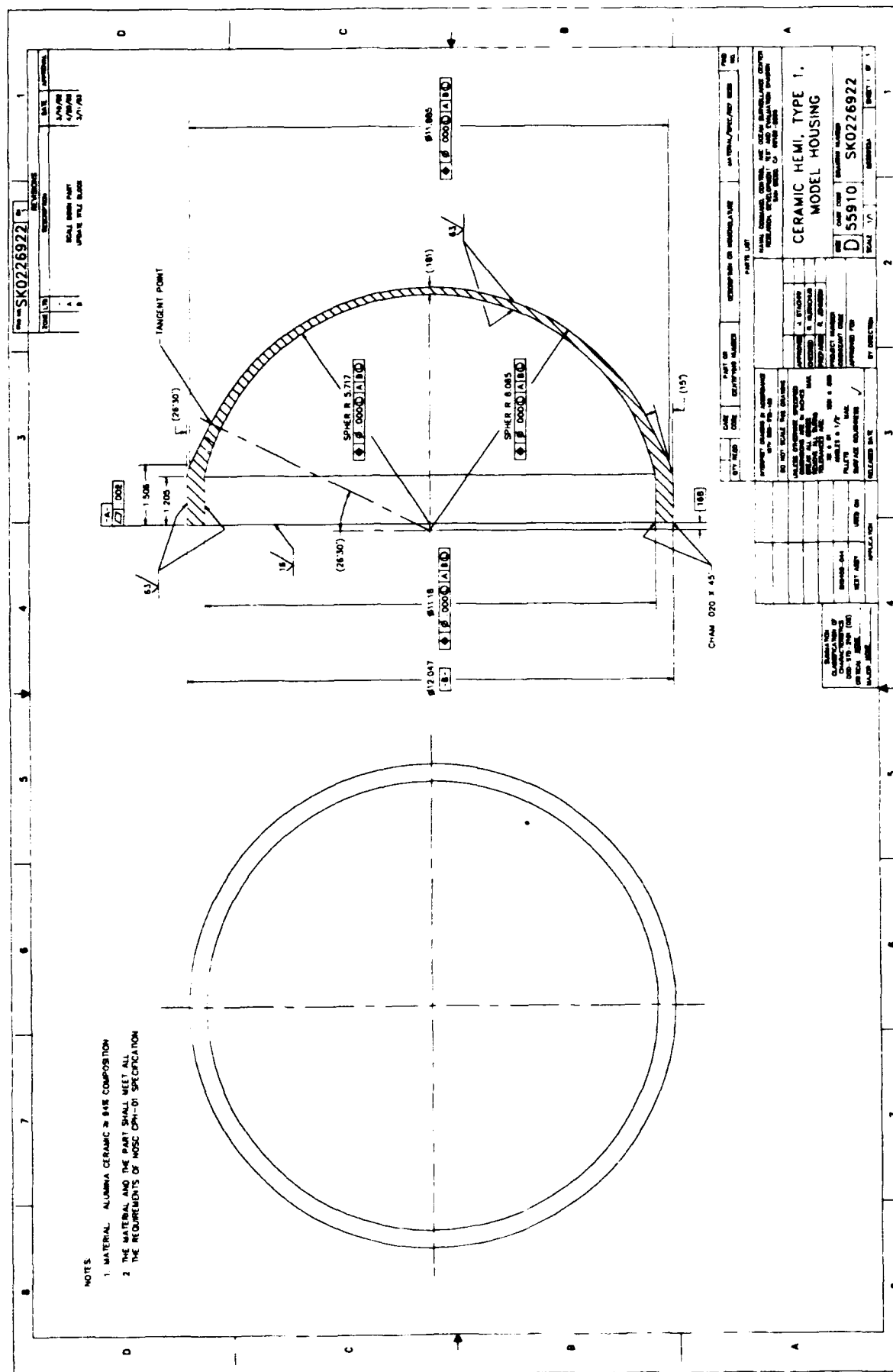


Figure A-3. Scale-model housing of Type 1 ceramic hemisphere.

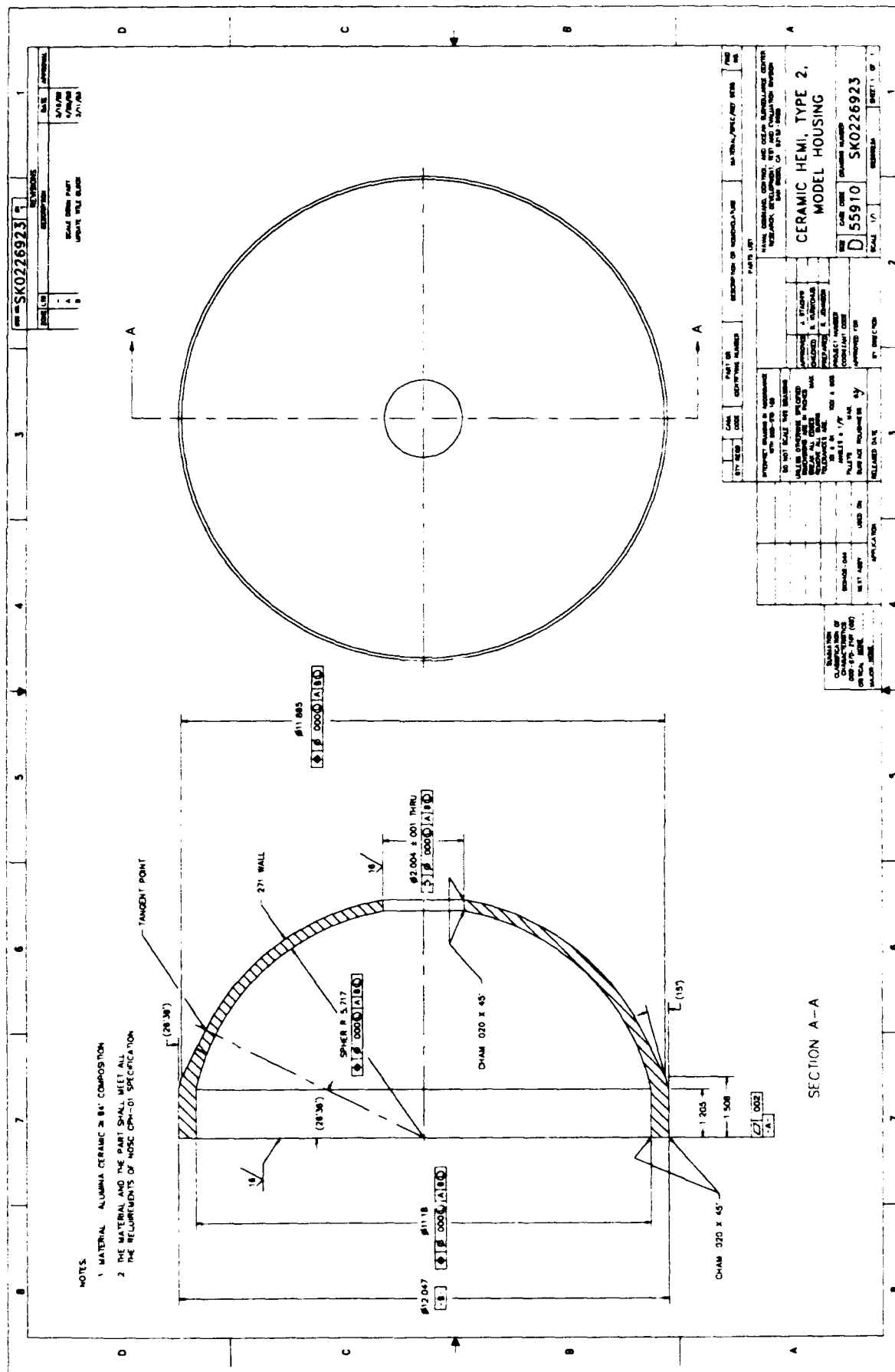


Figure A-4. Scale-model housing of Type 2 ceramic hemisphere.

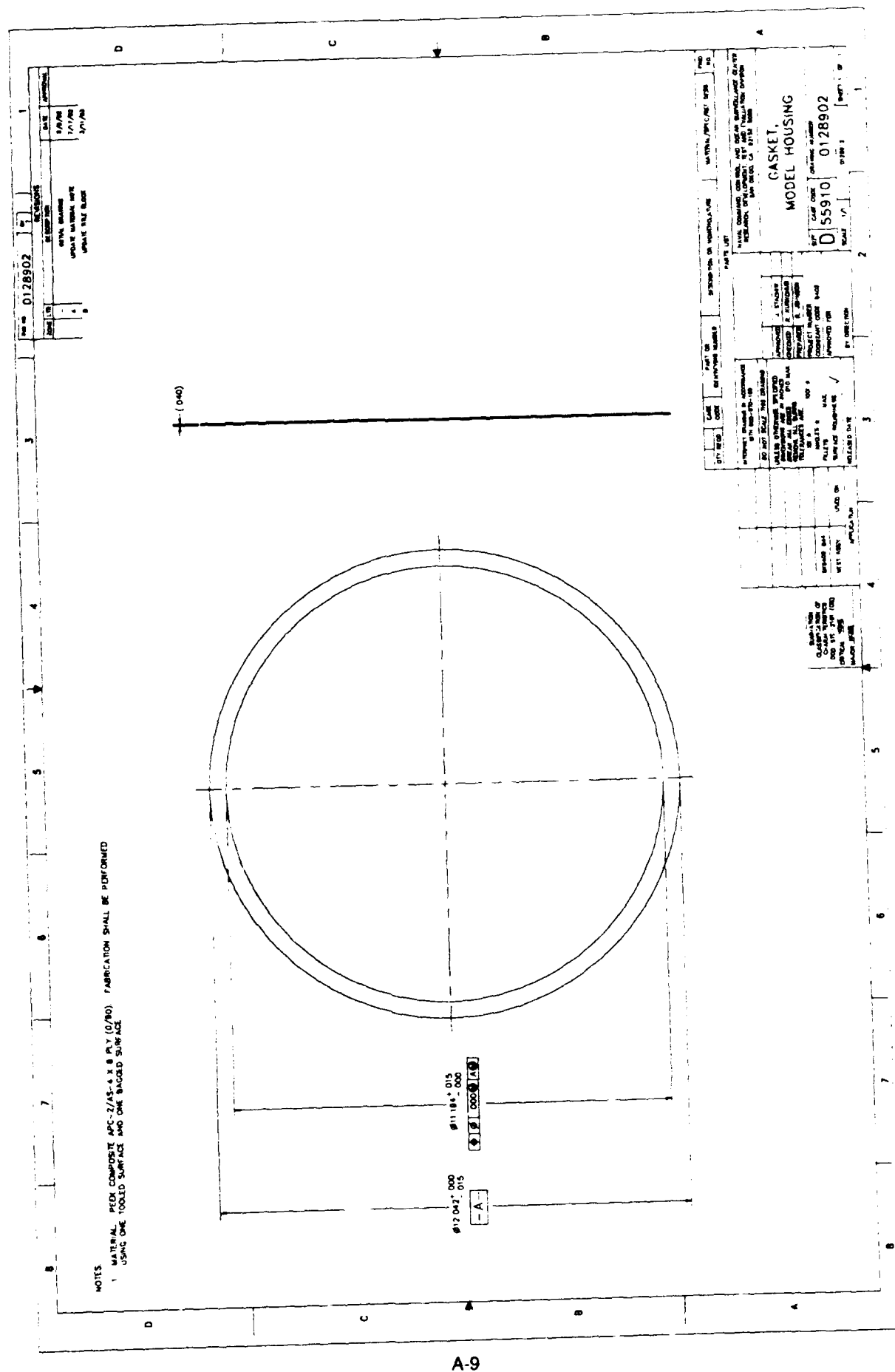
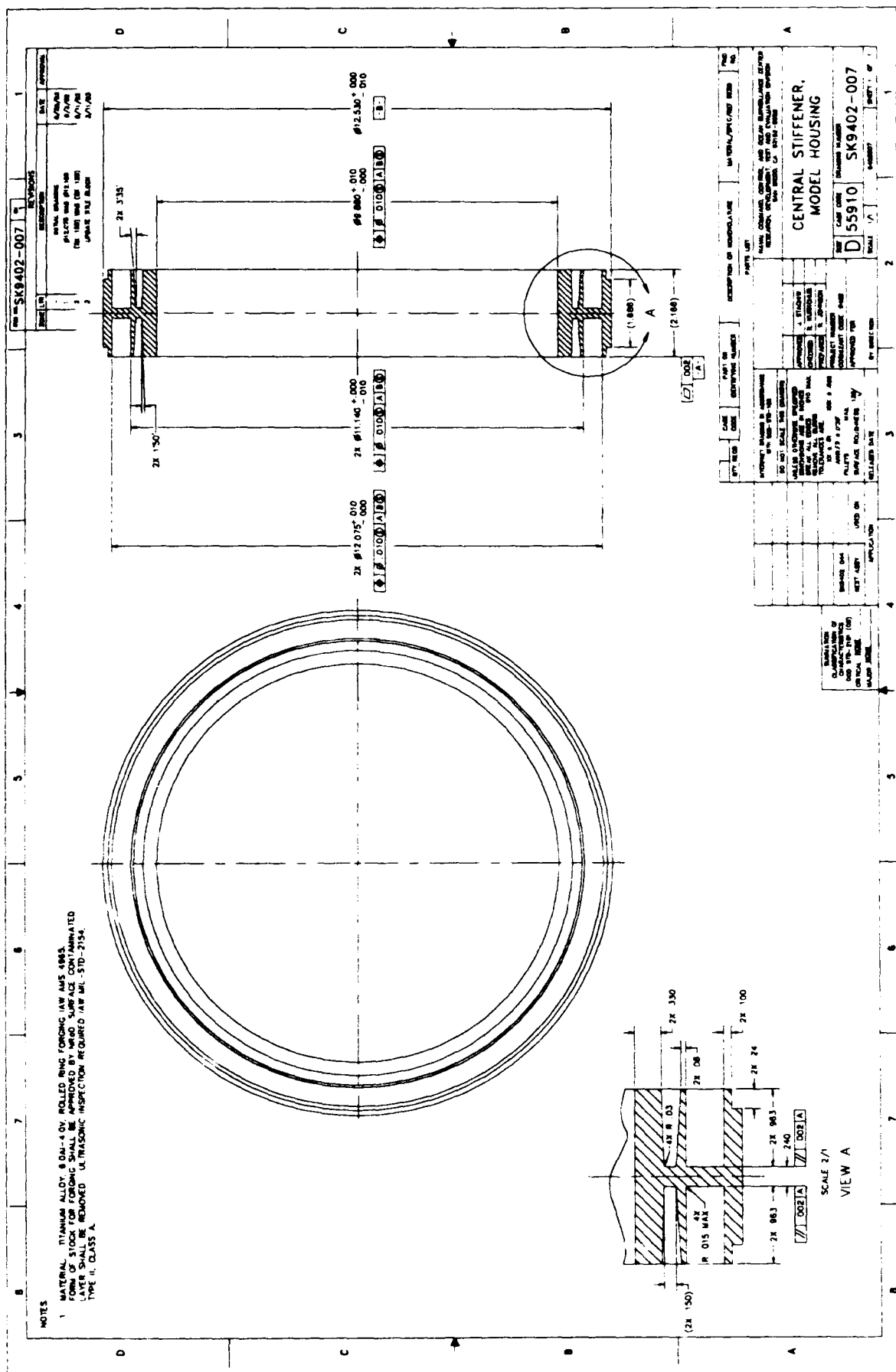


Figure A-5. Scale-model housing gasket.



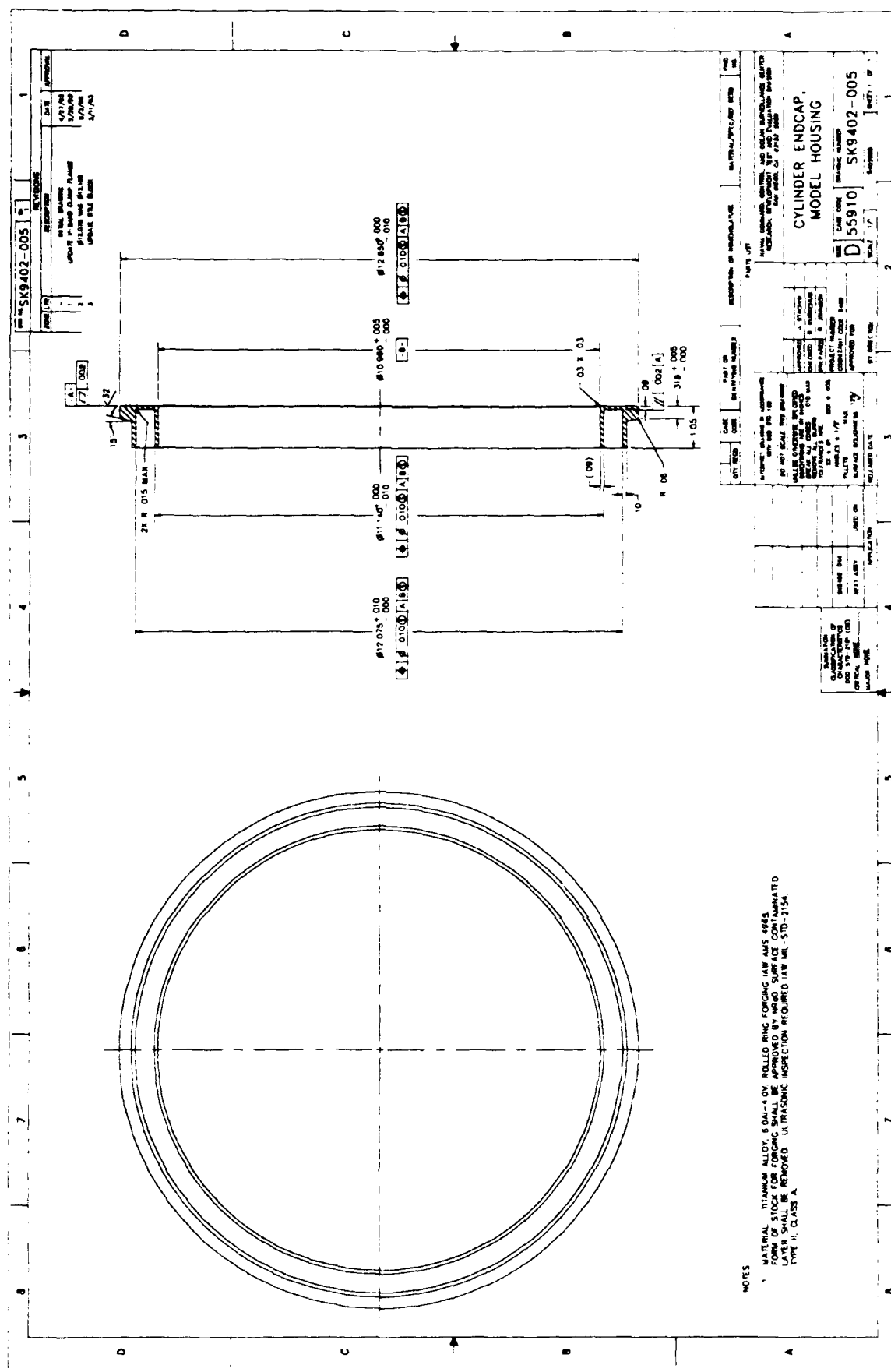
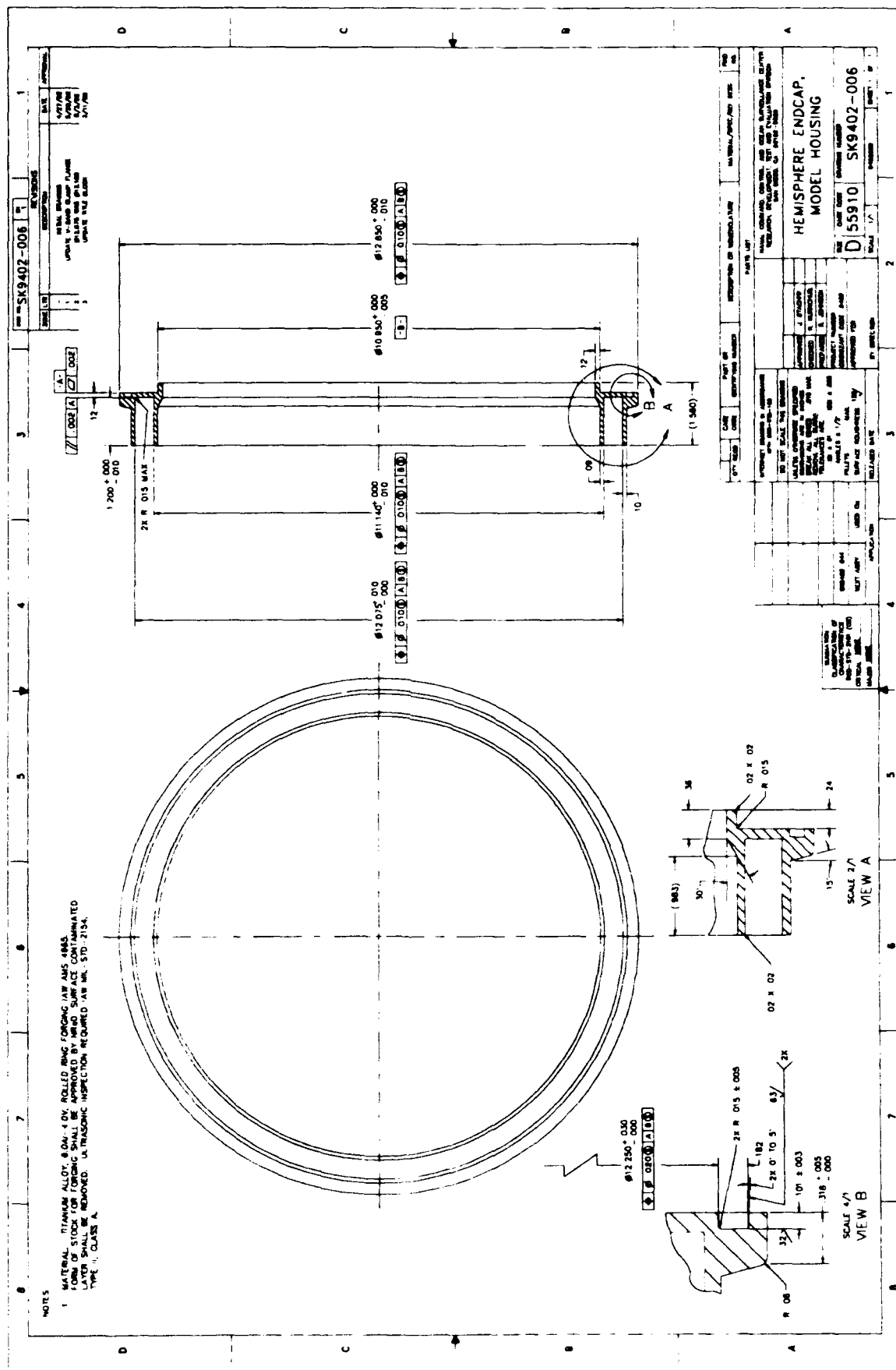


Figure A-7 Scale-model housing cylinder end cap.



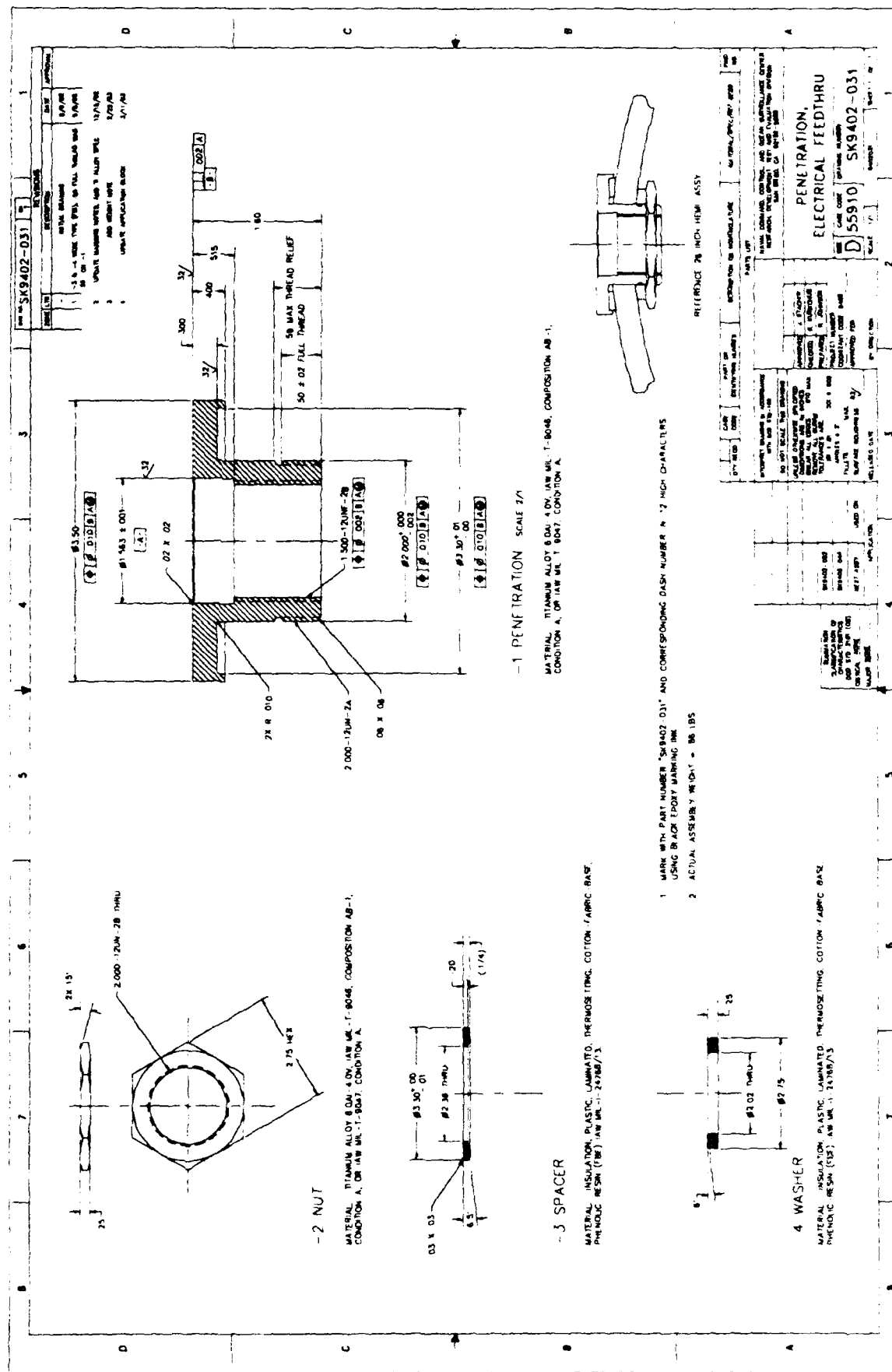


Figure A-9. Electrical feedthrough penetration.

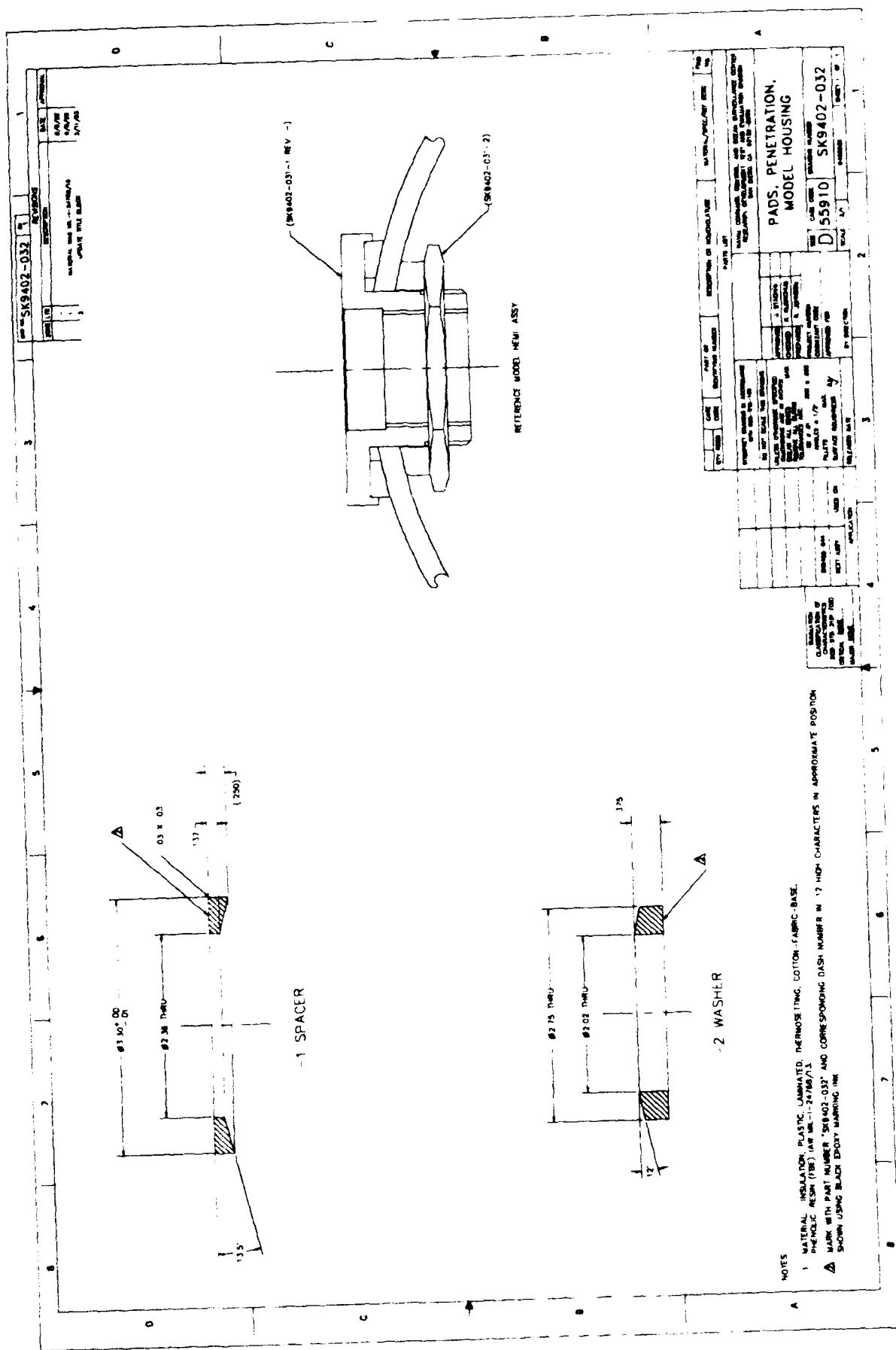
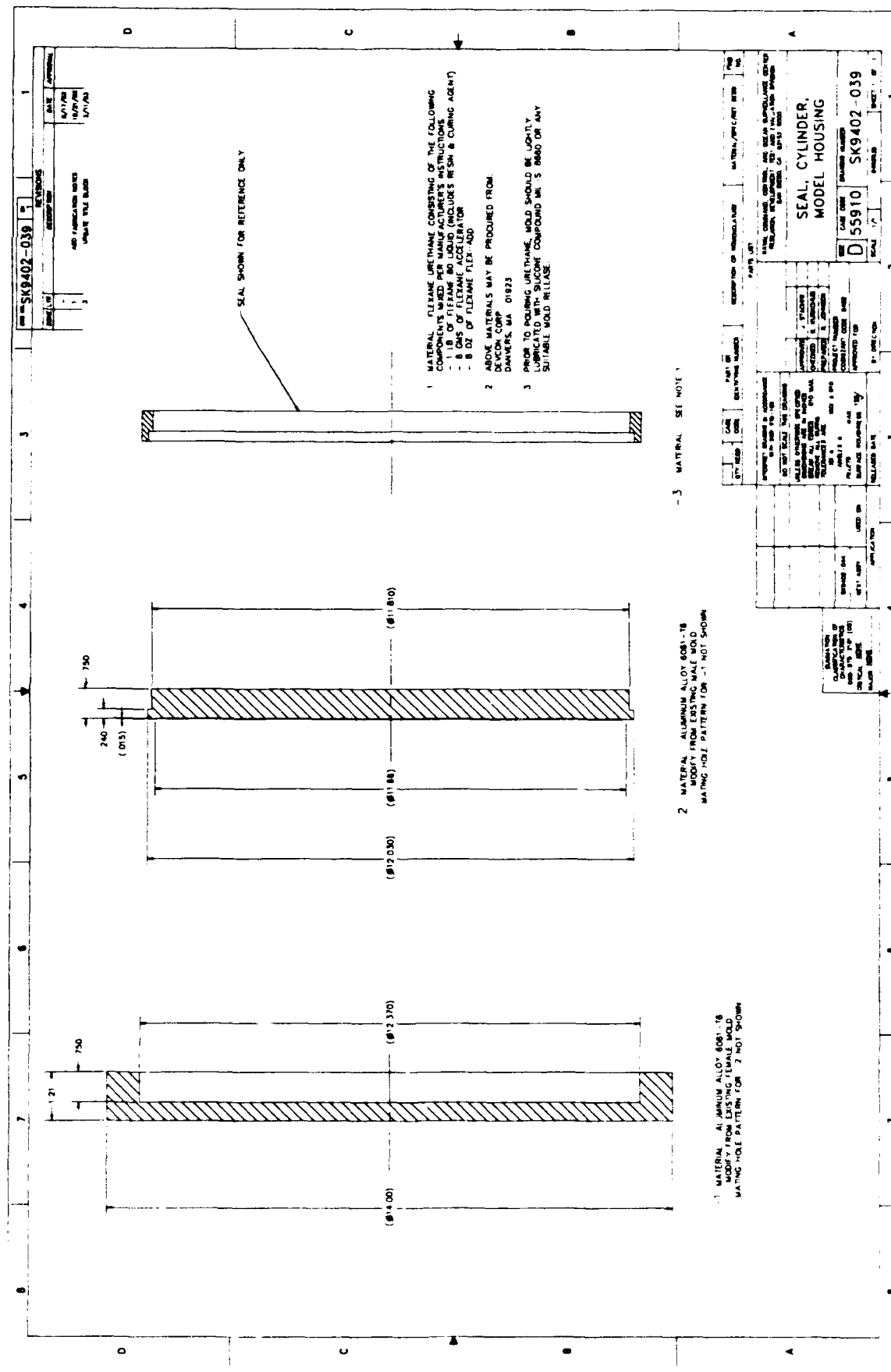


Figure A-10. Scale-model penetration pads.



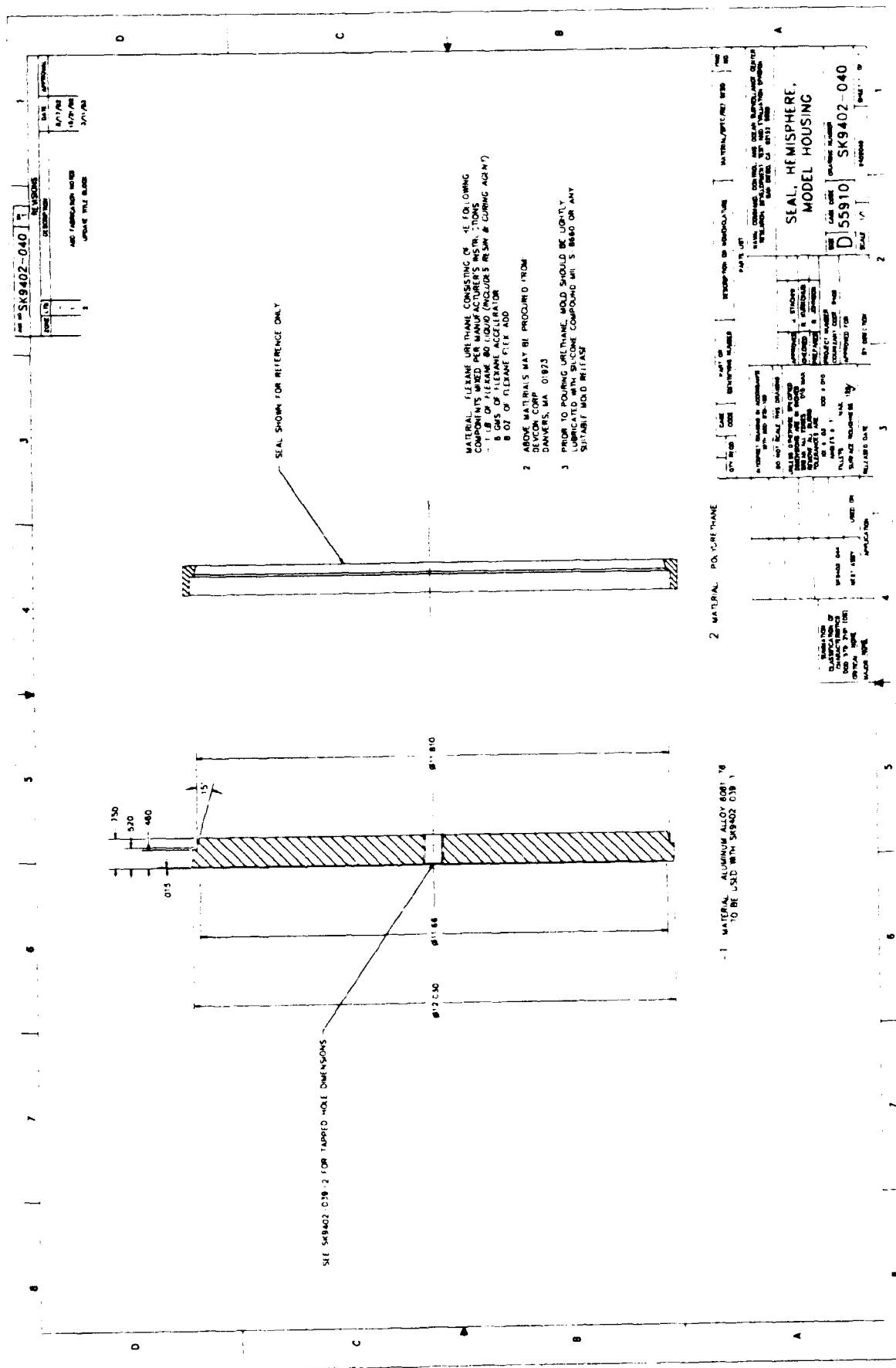




Figure 13. Scale-model housing cylinder jacket.

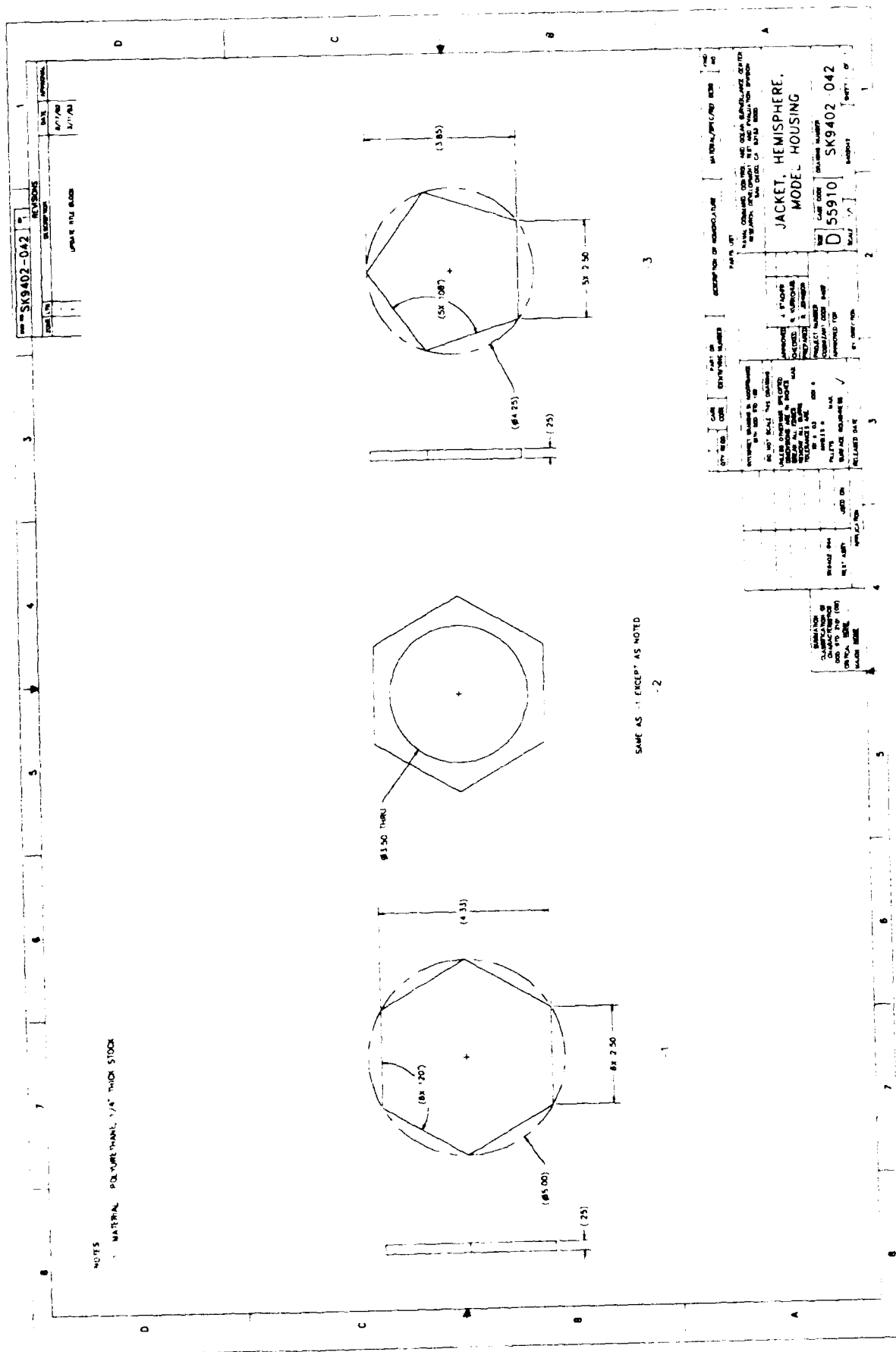


Figure A-14. Scale-model housing hemisphere jacket.

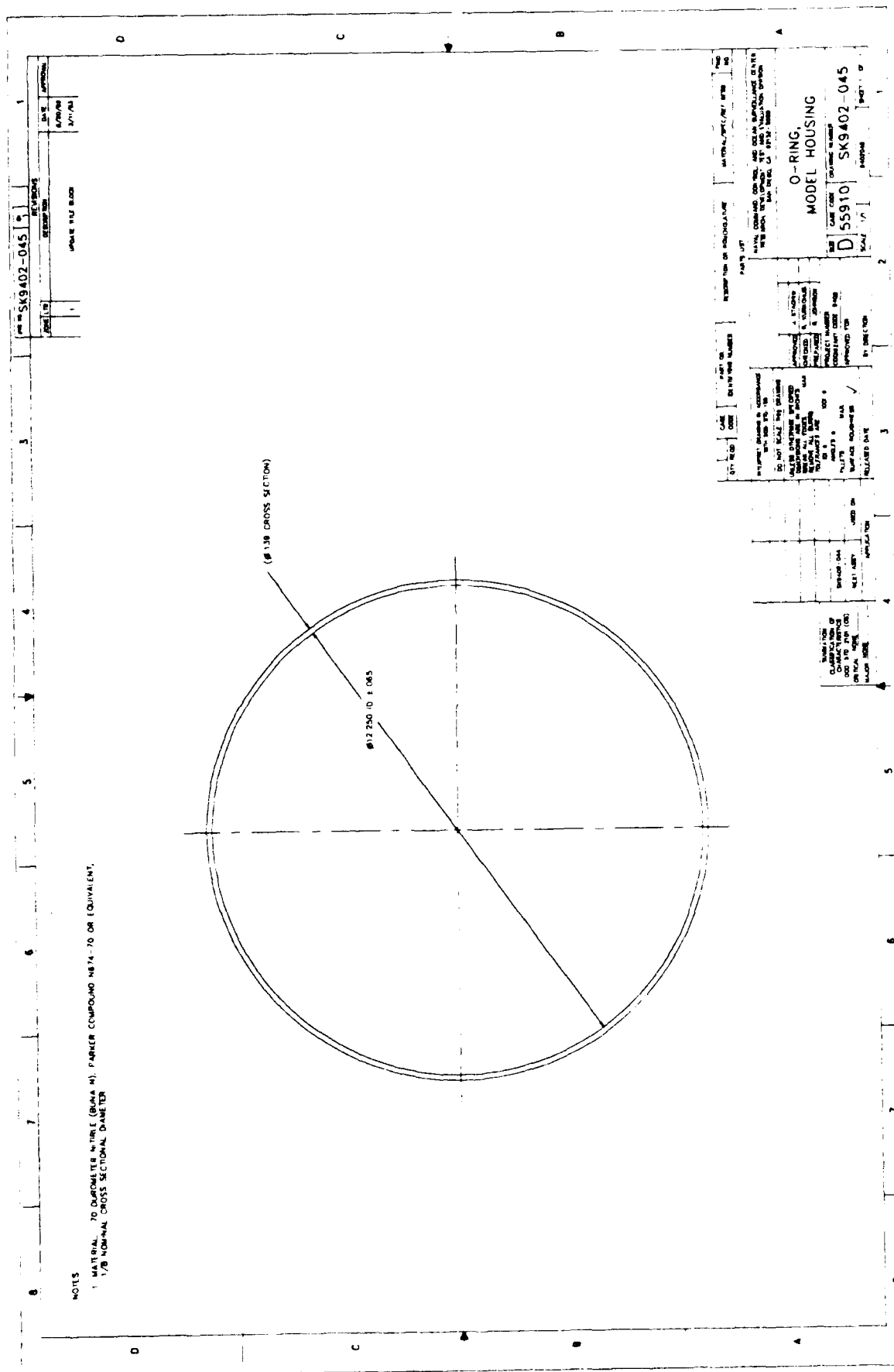


Figure A-15. Scale-model housing O-ring.

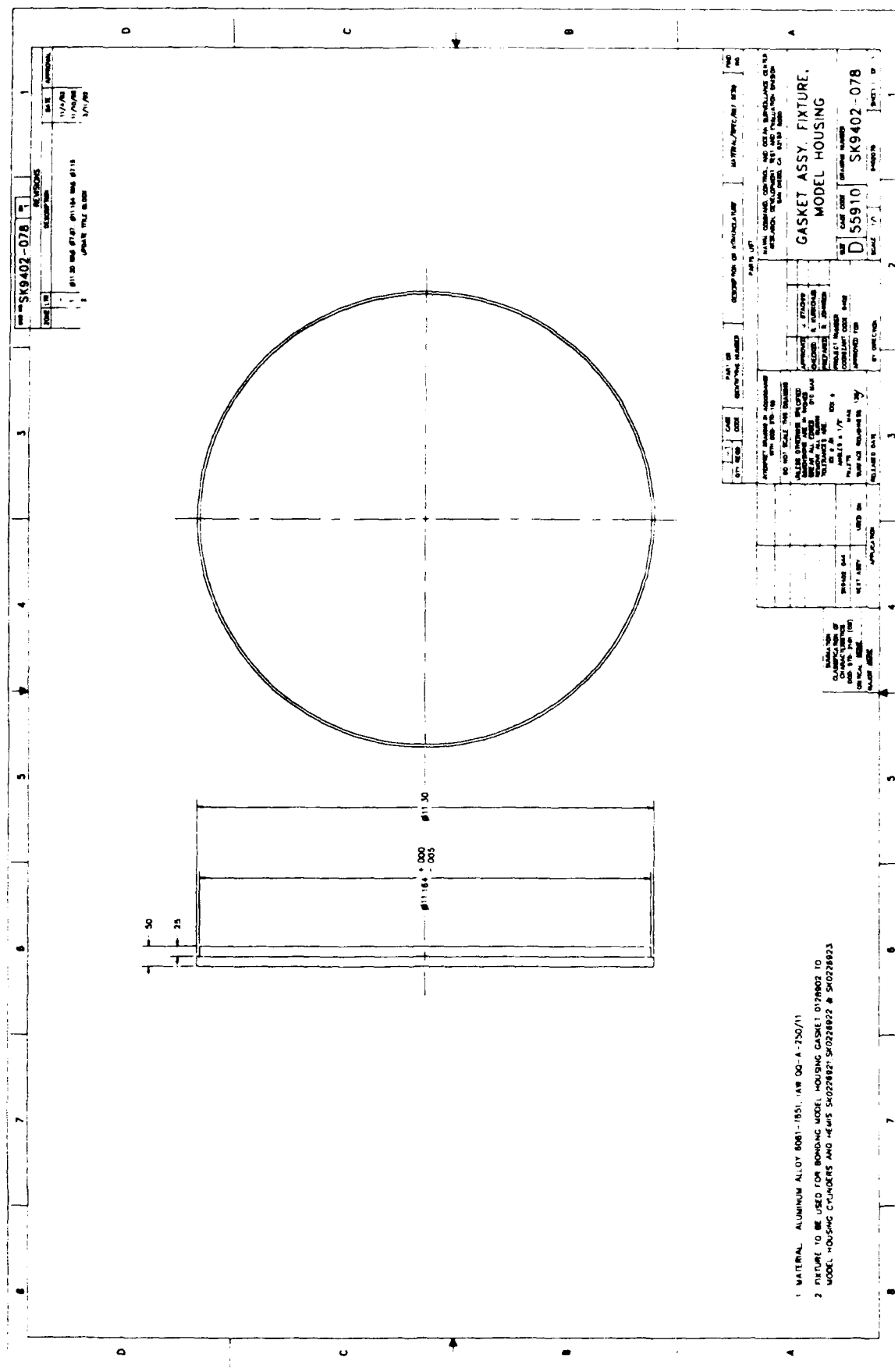
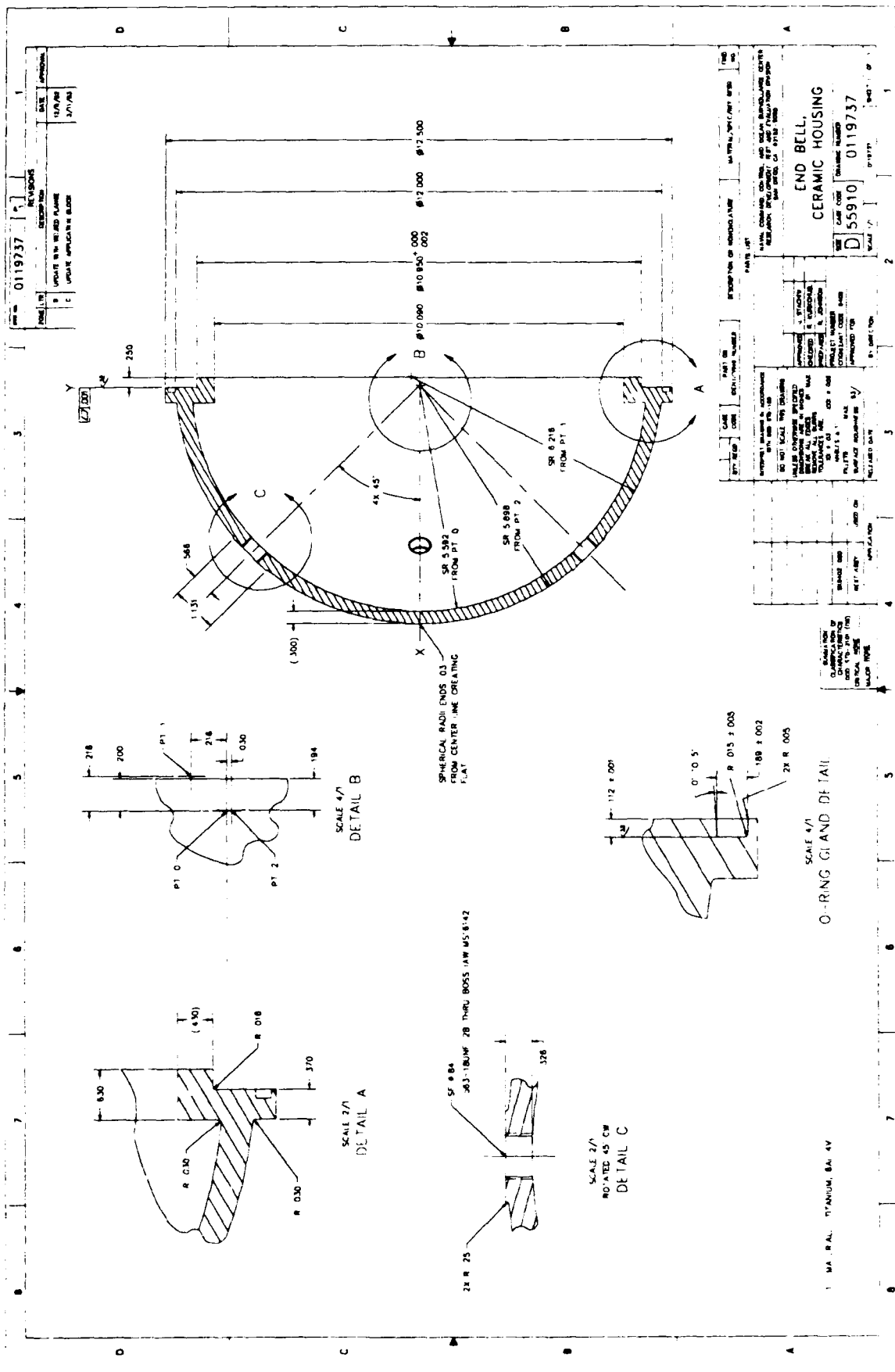
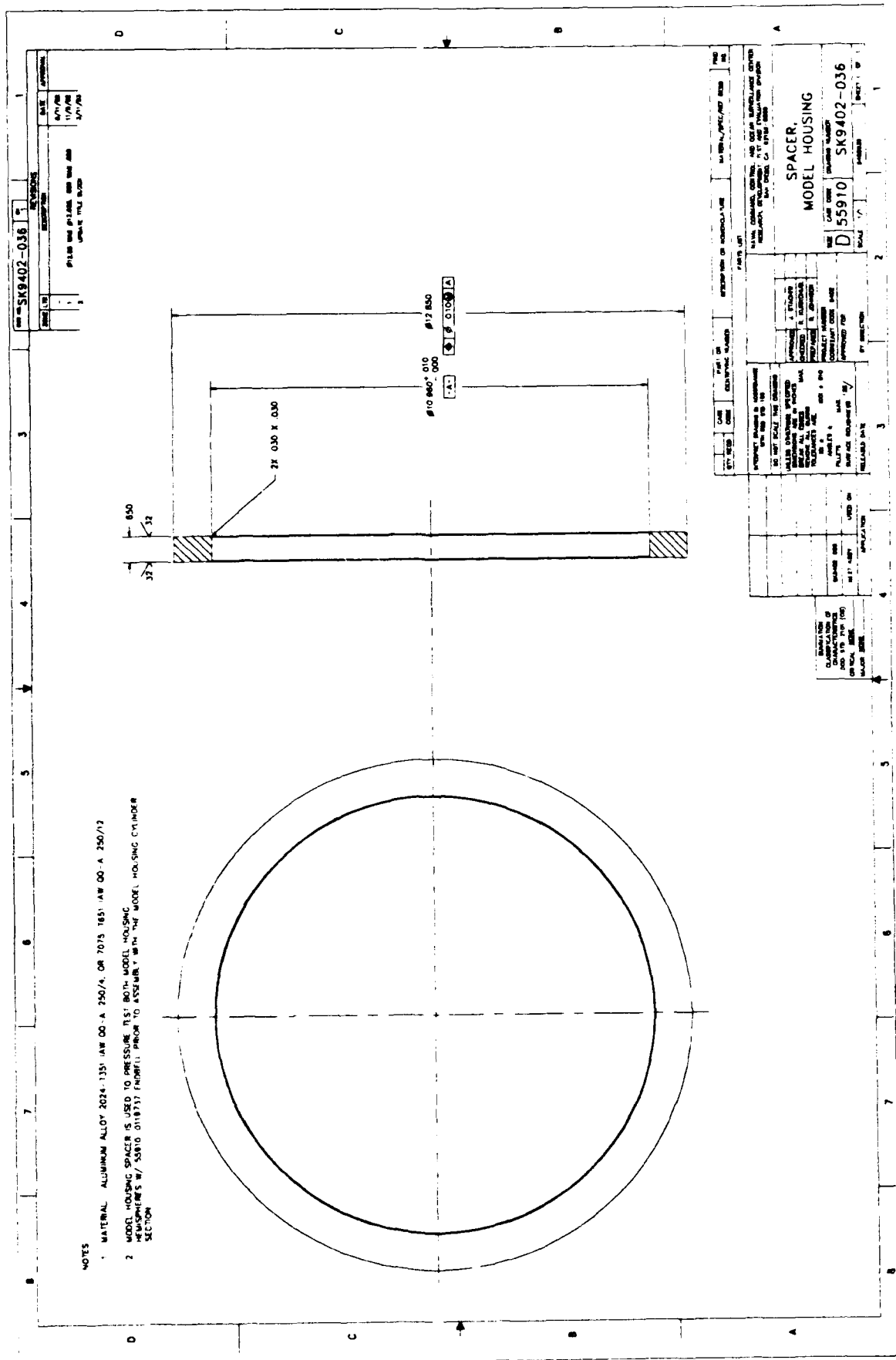


Figure A-16. Scale-model housing gasket assembly fixture.





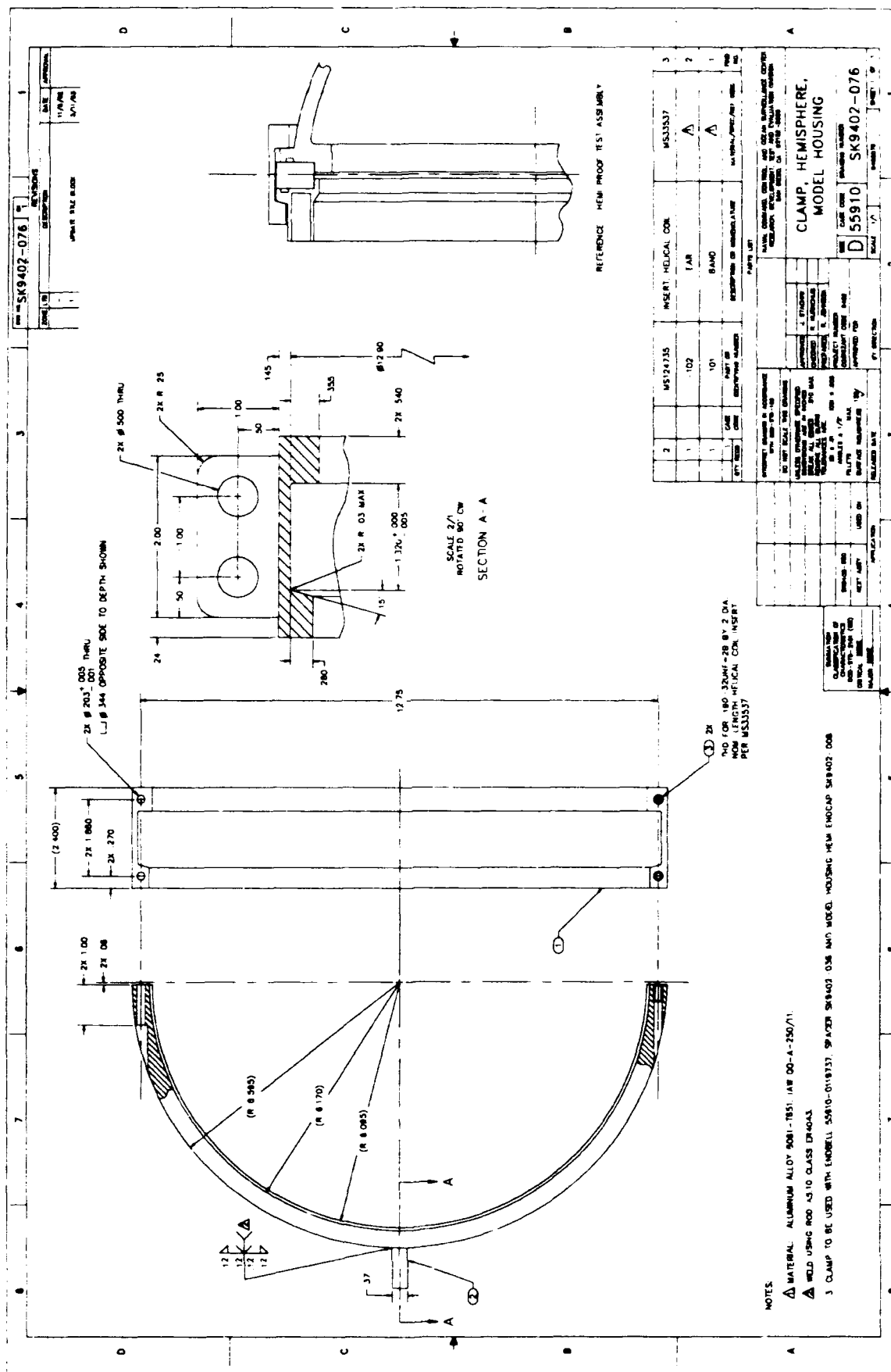


Figure A-20. Scale-model housing hemisphere clamp.

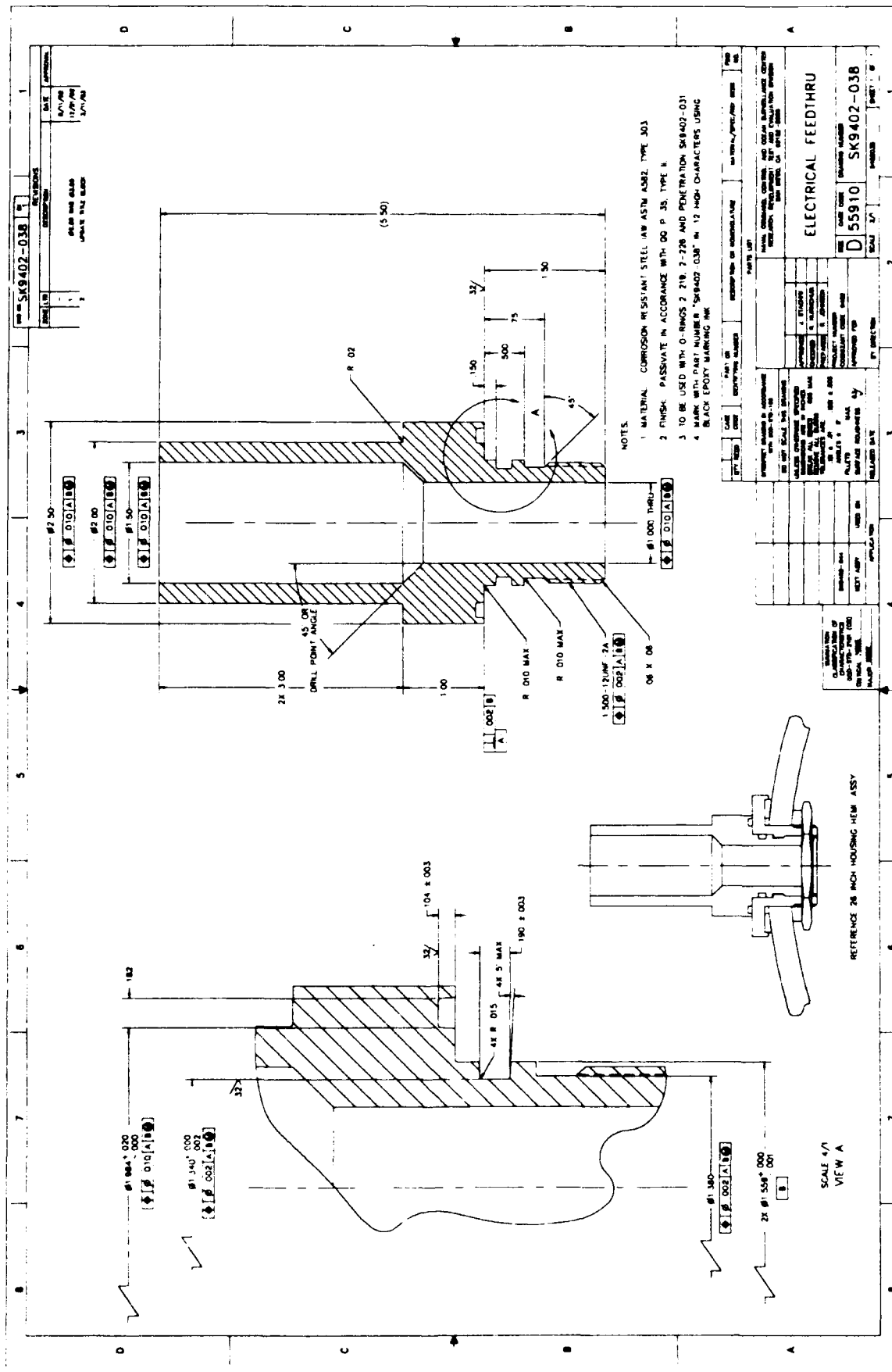


Figure A-21. Electrical feedthrough.

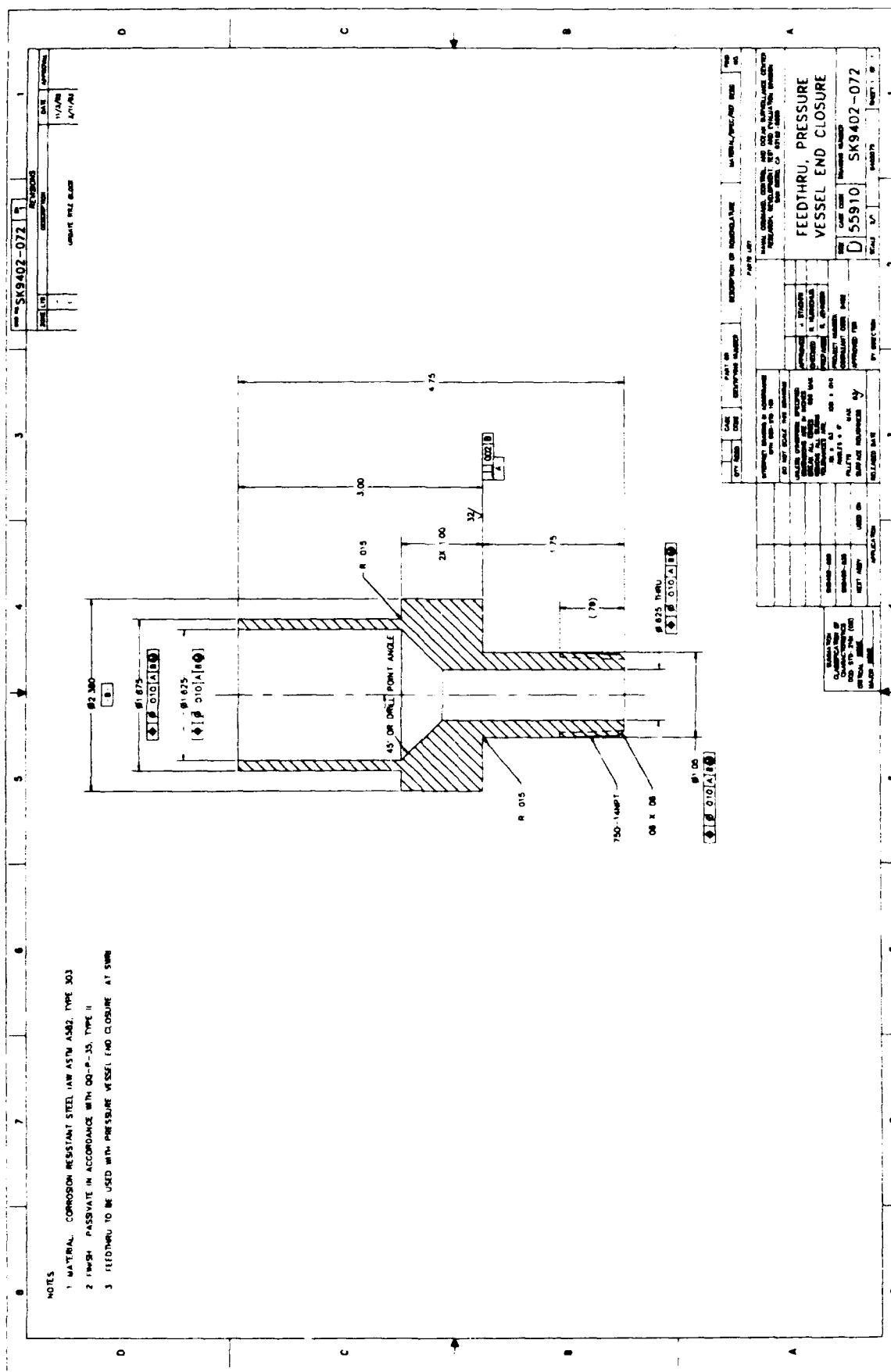
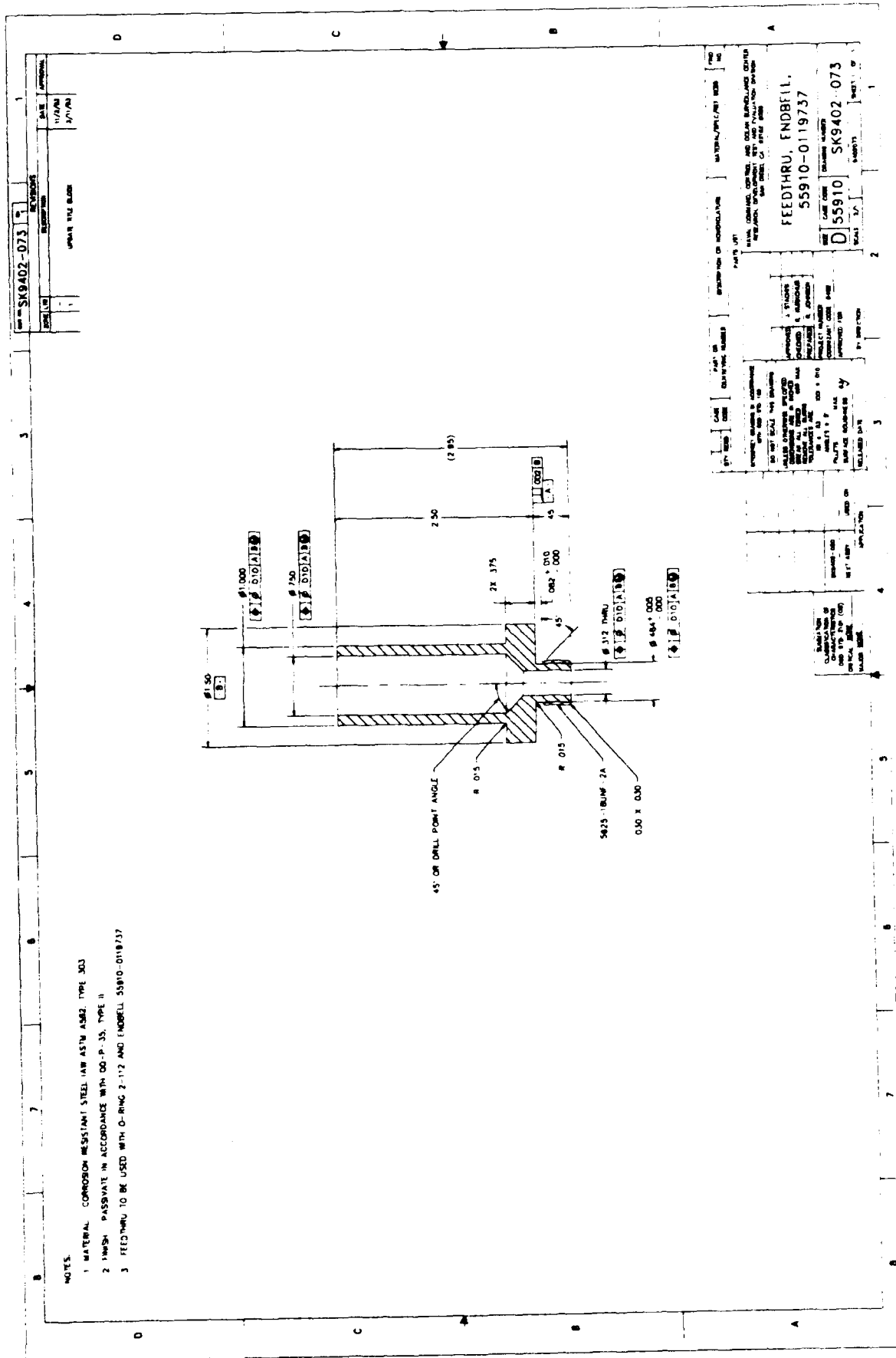


Figure A-22. Pressure vessel end closure feedthrough.



**APPENDIX B: STRESS AND STABILITY
ANALYSIS OF SCALE-MODEL
CERAMIC PRESSURE HOUSING**

FIGURES

- B-1. Radial stress plot for scale-model housing Type 1 hemisphere.
- B-2. Circumferential stress plot for scale-model housing Type 1 hemisphere.
- B-3. Minimum principal stress plot for scale-model housing Type 1 hemisphere.
- B-4. Maximum principal stress plot for scale-model housing Type 1 hemisphere.
- B-5. Minimum principal stress plot for scale-model housing Type 2 hemisphere.
- B-6. Radial stress plot for scale-model housing cylinder.
- B-7. Circumferential stress plot for scale-model housing cylinder.
- B-8. Axial stress plot for scale-model housing cylinder.
- B-9. Minimum principal stress plot for scale-model housing cylinder.
- B-10. Maximum principal stress plot for scale-model housing cylinder.
- B-11. The von Mises stress plot for scale-model housing central stiffener.
- B-12. The von Mises stress plot for scale-model housing hemisphere and cylinder end caps.
- B-13. N=2 buckled configuration of scale-model housing.

APPENDIX B: STRESS AND STABILITY ANALYSIS OF SCALE-MODEL CERAMIC PRESSURE HOUSING

Structural analysis was performed on the scale-model housing for external hydrostatic pressure loading for two primary reasons. The first was to validate the computer-aided analysis tools used to design the 26-inch housing. Stresses calculated through finite-element analysis (FEA) were to be compared to strain gage readouts taken during pressure tests of the scale-model housing. Prediction of collapse pressure due to buckling was to be compared to the actual tested pressure required to implode the scale-model housing. The second reason was to verify that scaling down the dimensions of the 26-inch housing was performed correctly to obtain equivalent stress static and buckling resistance in the scale-model housing under depth loading. This would ensure that the test results for the model housing would be indicative of the structural performance of the 26-inch housing.

All structural analysis was based on the following linear elastic isotropic material properties:

94-percent alumina-ceramic:	Elastic Modulus = 4436 psi Poisson's Ratio = 0.21
Ti-6Al-4V titanium alloy:	Elastic Modulus = 16.4e6 psi Poisson's Ratio = 0.31

The finite element model (FEM) of the scale-model housing was created using the pre/post processing code PATRAN (version 2.5) and then run using the analysis software ABAQUS (version 4.9). The FEM consisted of a 2-D axisymmetric mesh of the model housing meridian using both linear 4-noded (CAX4R) and quadratic 8-nodes (CAX8R) reduced integration solid element. To model the lap joint between the cylinder end cap and the hemisphere end cap, gap interface (INTER3A) elements were used. These elements transmit pressure and shear stress between the contact surfaces, but allow normal separation and relative transverse displacements. The boundary nodes were shared between the element mesh in their titanium end caps in the FEM presented here. This rigid linking of the ceramic components directly to the titanium components neglects the effects of the epoxy layer and

the composite gasket on the stress state in the immediate joint region. This was deemed acceptable since verification of the stress state in these localized regions was not achievable using strain gages during the pressure tests. This simplified joint model does not affect the stress values calculated away from the joint region where strain gages could be physically located.

As expected the predicted stress state in the scale-model housing closely paralleled the stress state in the 26-inch housing (reference 5) under the modeled external pressure loading of 10,000 psi. Additionally, strain gage data recorded during pressure testing of the scale-model housing compared well to the results of the FEA analysis. Radial stress and circumferential stress plots of the Type 1 tapered hemisphere are shown in figures B-1 and B-2, and the corresponding minimum and maximum principal stress plots are shown in figures B-3 and B-4. Figure B-5 shows the minimum stress plot for the Type 2 hemisphere and the stress concentration effects of the single polar penetration.

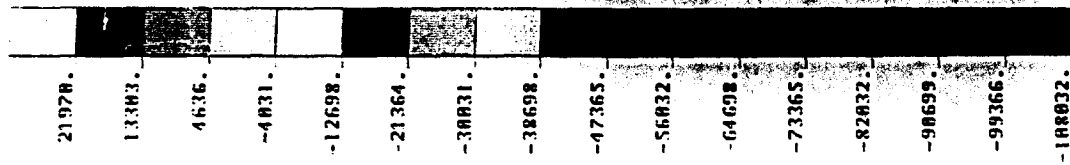
Similarly, figures B-6 through B-10 show radial, circumferential, axial, minimum principal, and maximum principal stress plots for the scale-model ceramic cylinders. Finally, figures B-11 and B-12 represent von Mises stress plots for the major titanium components used in the scale-model housing assembly. Half symmetry of the central stiffener is shown in figure B-11, and both the cylinder and hemisphere end cap are shown together in figure B-12. Commentary on the design criteria and philosophy used in evaluating acceptable stress levels for each of these components is referred to in reference 5.

Stability analysis of the scale-model housing was performed using BOSOR4, a structural analysis program that can be used to make buckling predictions of complex shells of revolution. BOSOR4 was developed by David Bushnell at Lockheed Missiles and Space Company, Inc. The meridian of the shell of revolution is modeled using a number of segments with material, geometric, and boundary condition properties representative of the real structure.

The scale-model housing stability results presented here were based on a 15-segment model constructed using BOSOR4. Earlier BOSOR4 models used more segments to incorporate the effects of the cylinder and hemisphere end caps, but they were eventually removed since the presence of the relatively thin-walled end caps had little effect on the overall general instability of the scale-model housing. The BOSOR4 model of the scale-model housing allowed for meridional rotations at the joints between the cylinder ends and the hemisphere ends. Detailed modeling of the central stiffener using seven discrete branched shell segments was incorporated.

The BOSOR4 model predicted collapse of the scale-model housing to occur at 12,208 psi external pressure due to a general instability, with two circumferential lobes ($N=2$) forming. BOSOR4 graphics output of this failure mode is shown in figure B-13. Local instabilities in the central stiffener, and cylinder and hemisphere end caps were checked, but were not found to be a factor at the operating depths for which the scale-model housing was intended. The predicted collapse pressure fell within 2 percent of the actual tested value of 11,933 psi.

The intent of the scale-model housing was to validate the 26-inch housing design, yet the scale-model housing represents a documented and tested design that could also be deployed for service to depth loads of 10,000 psi, like the full-size housing. Increased depth capacity could also be obtained by utilizing a single scale-model housing ceramic cylinder capped with scale-model housing hemispheres. The BOSOR4 calculated collapse pressure for this single cylinder assembly is predicted to be 16,823 psi. Similarly, a housing incorporating both ceramic cylinders and both ceramic hemispheres, but with a redesigned central stiffener, could be designed for increased depth capacity. Decreasing the inner diameter of the central stiffener from 9.88 inches to about 8.75 inches by lengthening the inner web, and holding the inner flange thickness and width dimensions constant also increases the predicted external pressure required for implosion to 16,800 psi. Drawbacks for increasing the depth of the central stiffener are the increased possibility for local web buckling and decreased packaging volume available inside the pressure housing. Modification of the scale-model housing for higher pressures would, of course, require recalculating the stress analysis to prevent the chance of material failure in any of the housing components.



MAX



Figure B-1. Radial stress plot for scale-model housing Type 1 hemisphere.

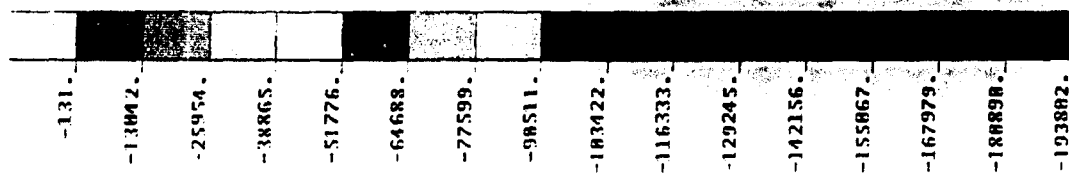


Figure B-2. Circumferential stress plot for scale-model housing Type 1 hemisphere.

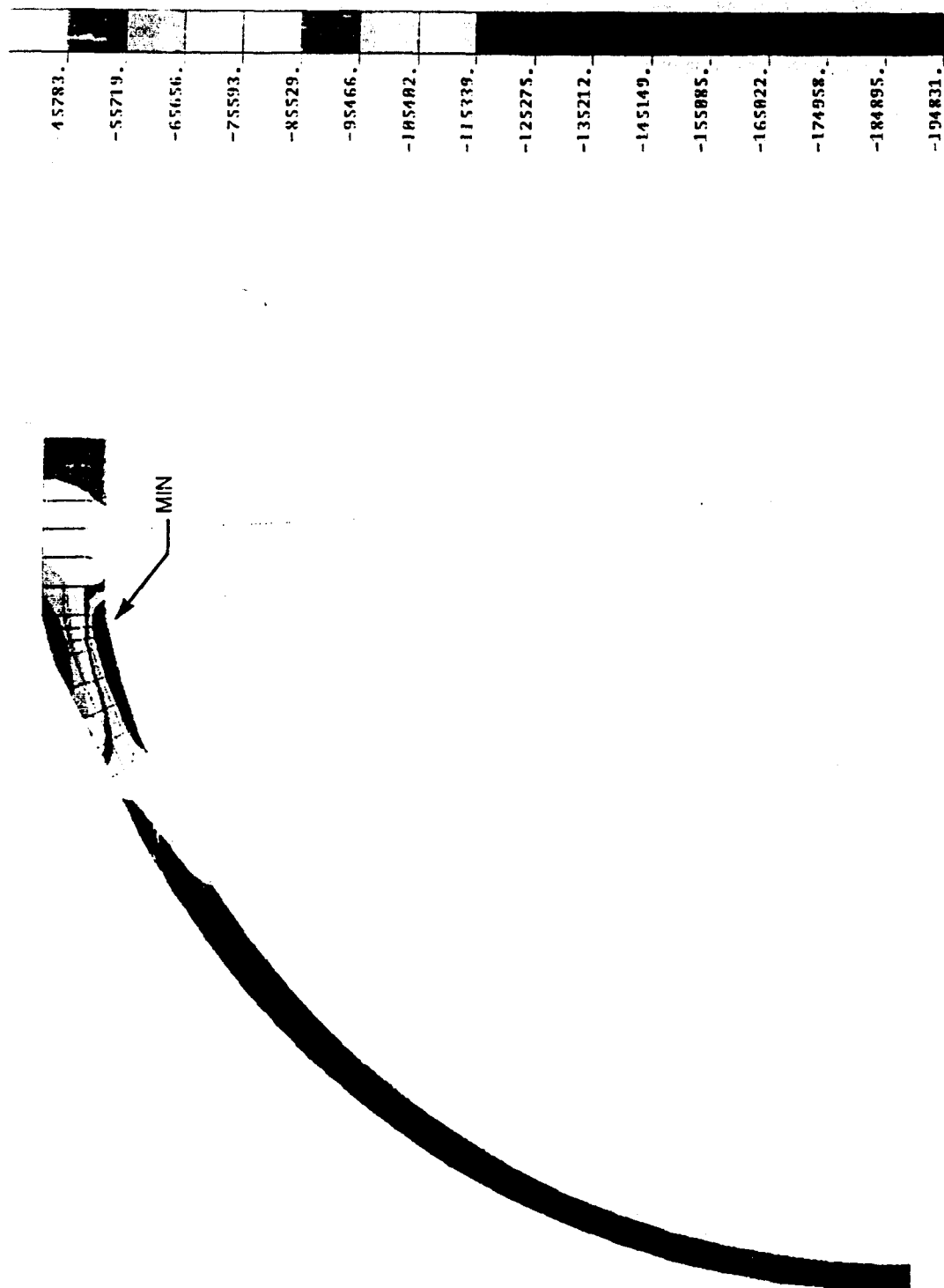


Figure B-3. Minimum principal stress plot for scale-model housing Type 1 hemisphere.

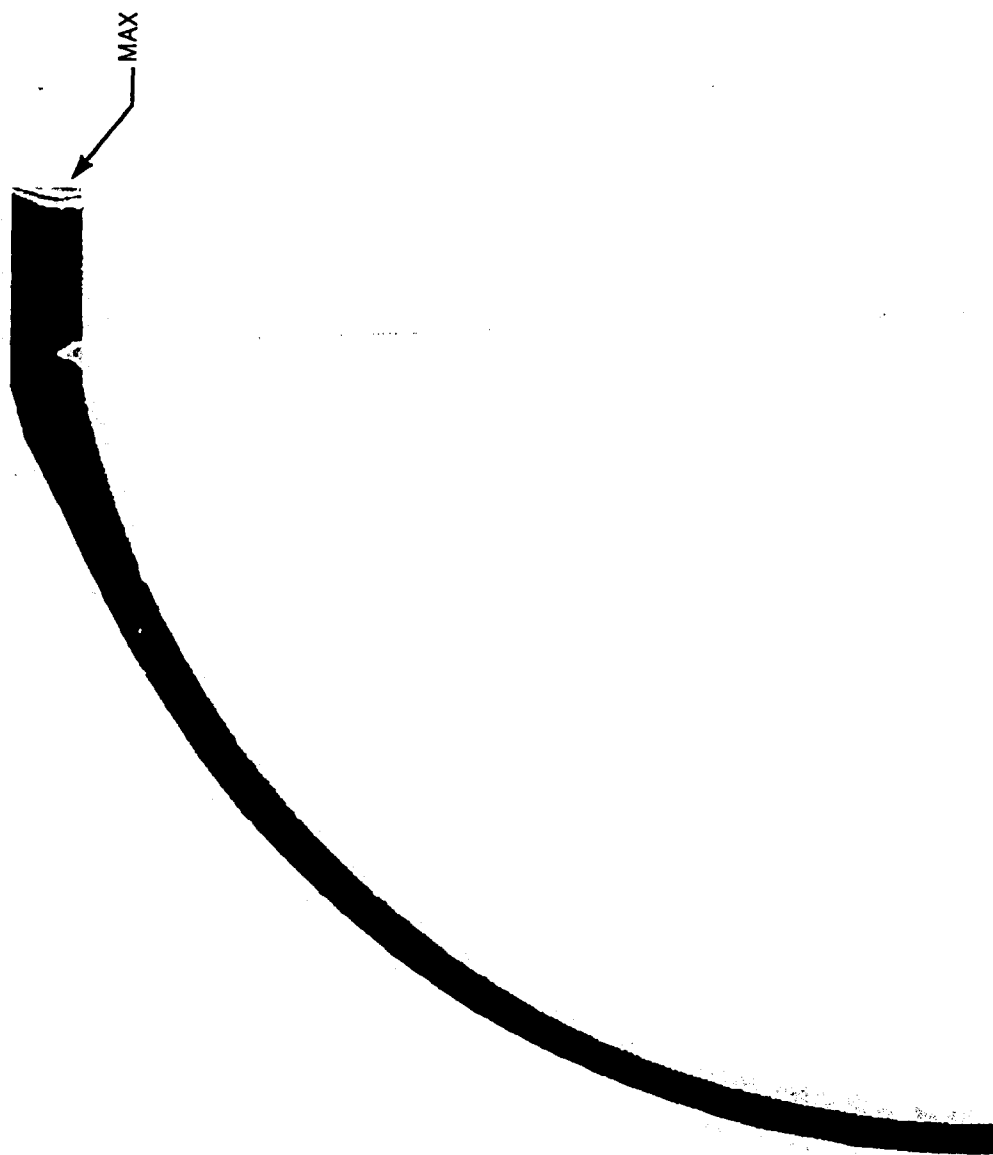
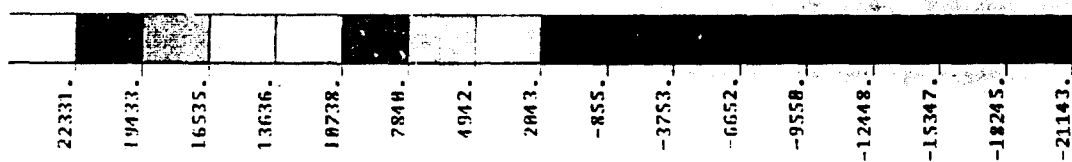


Figure B-4. Maximum principal stress plot for scale-model housing Type 1 hemisphere.

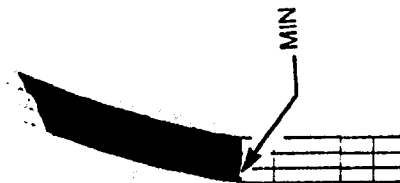
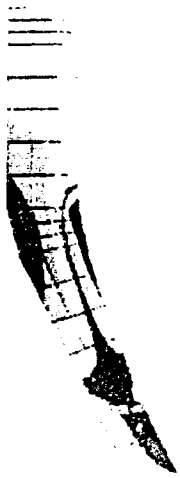
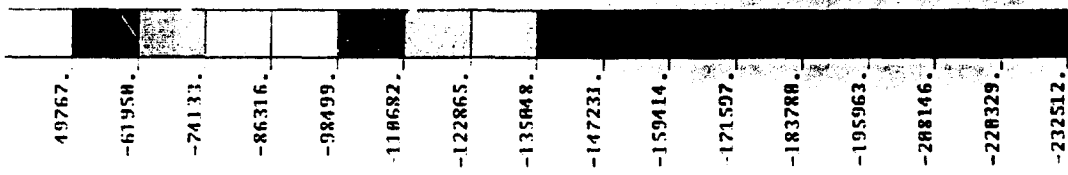


Figure B-5. Minimum principal stress plot for scale-model housing Type 2 hemisphere.

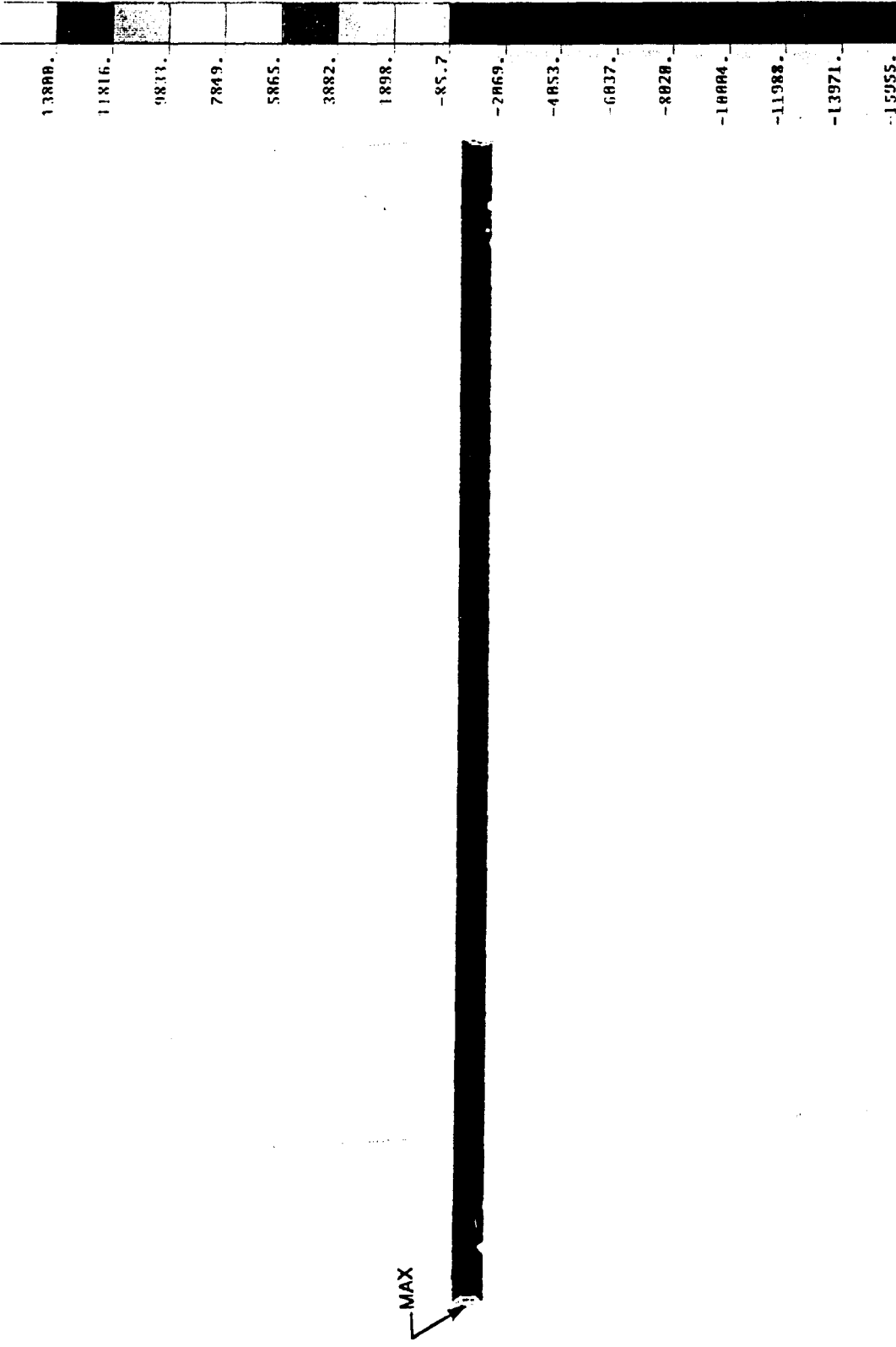


Figure B-6. Radial stress plot for scale-model housing cylinder.

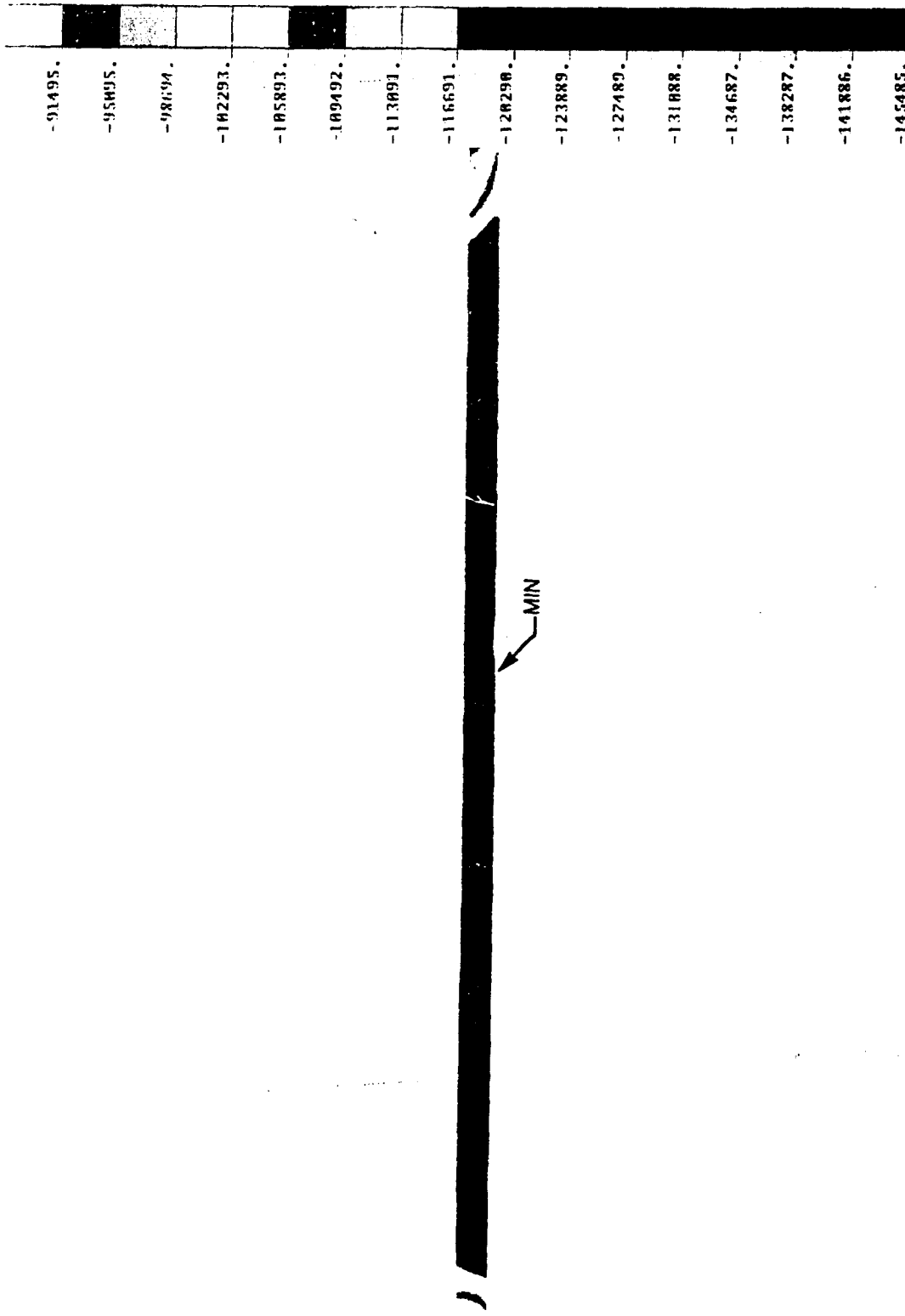


Figure B-7. Circumferential stress plot for scale-model housing cylinder.

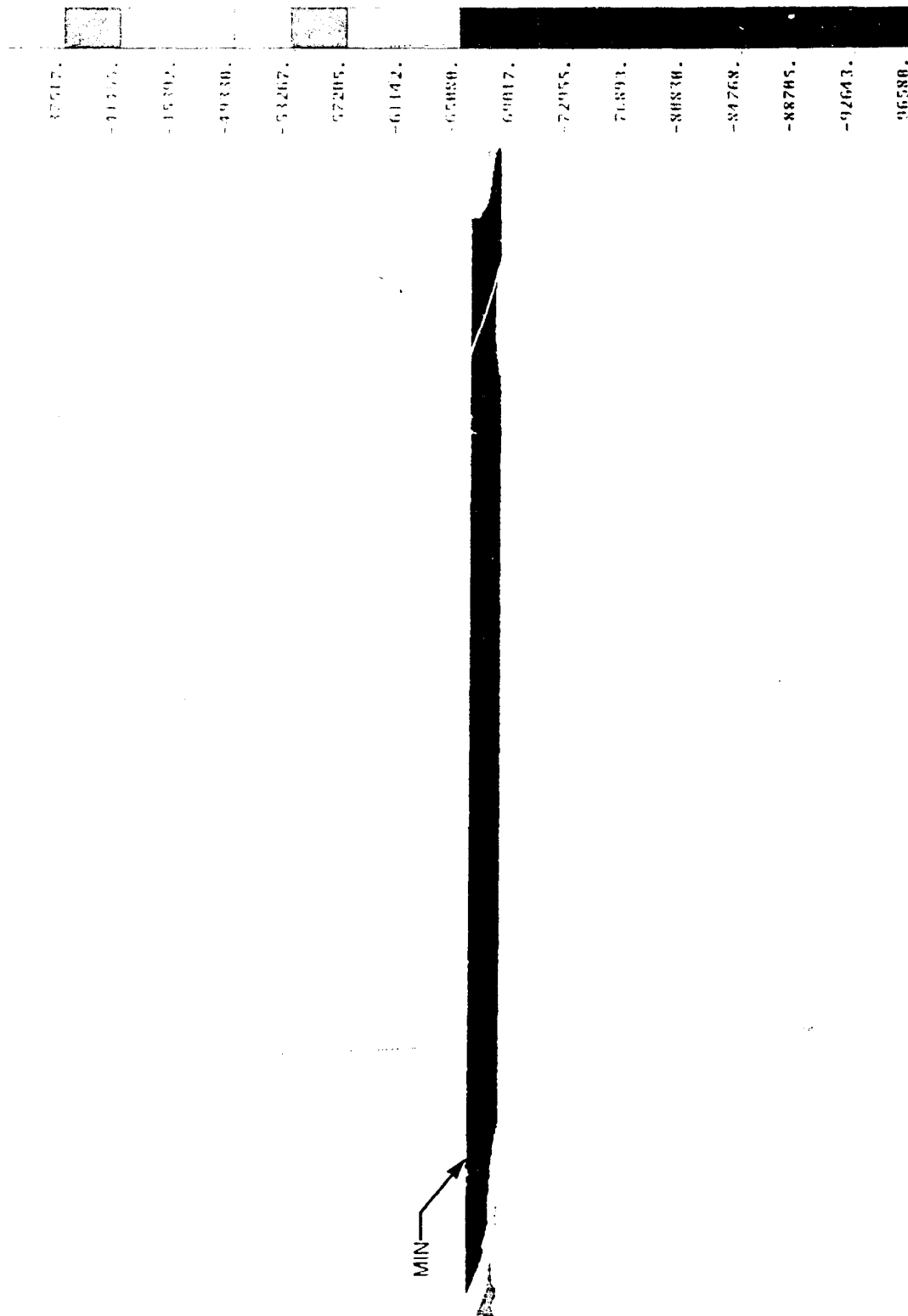


Figure B-8. Axial stress plot for scale-model housing cylinder.

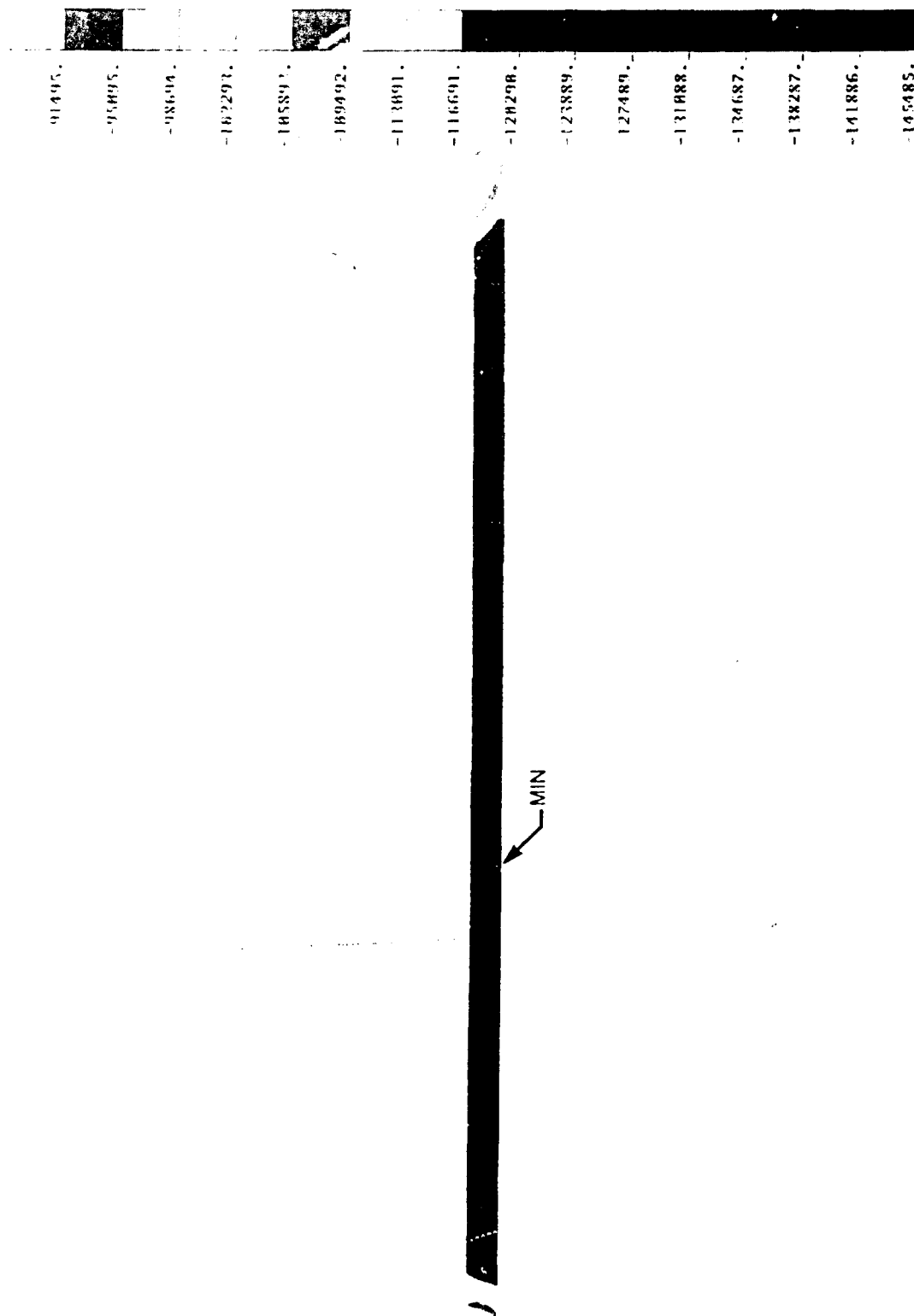


Figure B-9. Minimum principal stress plot for scale-model housing cylinder.

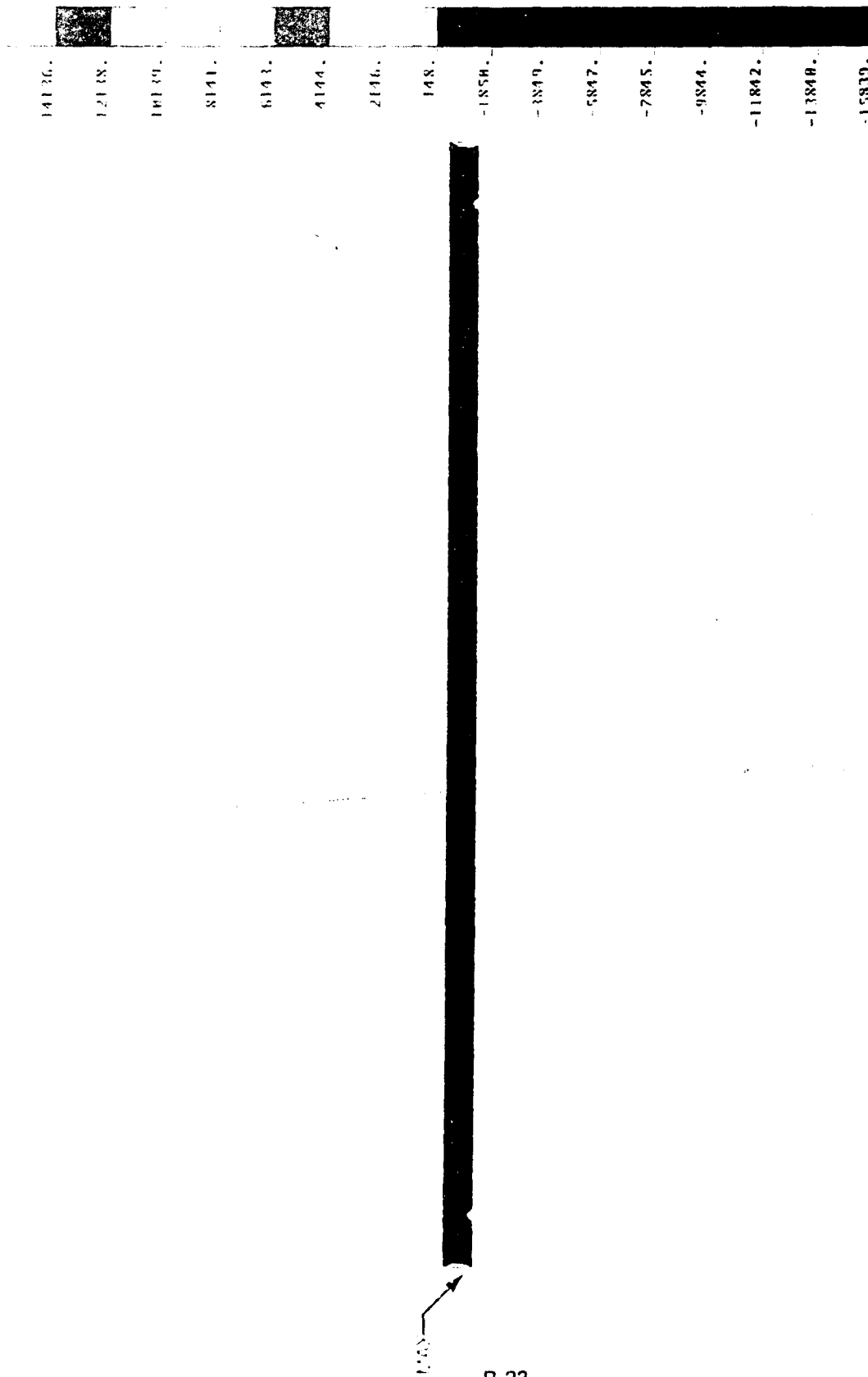


Figure B-10. Maximum principal stress plot for scale-model housing cylinder.

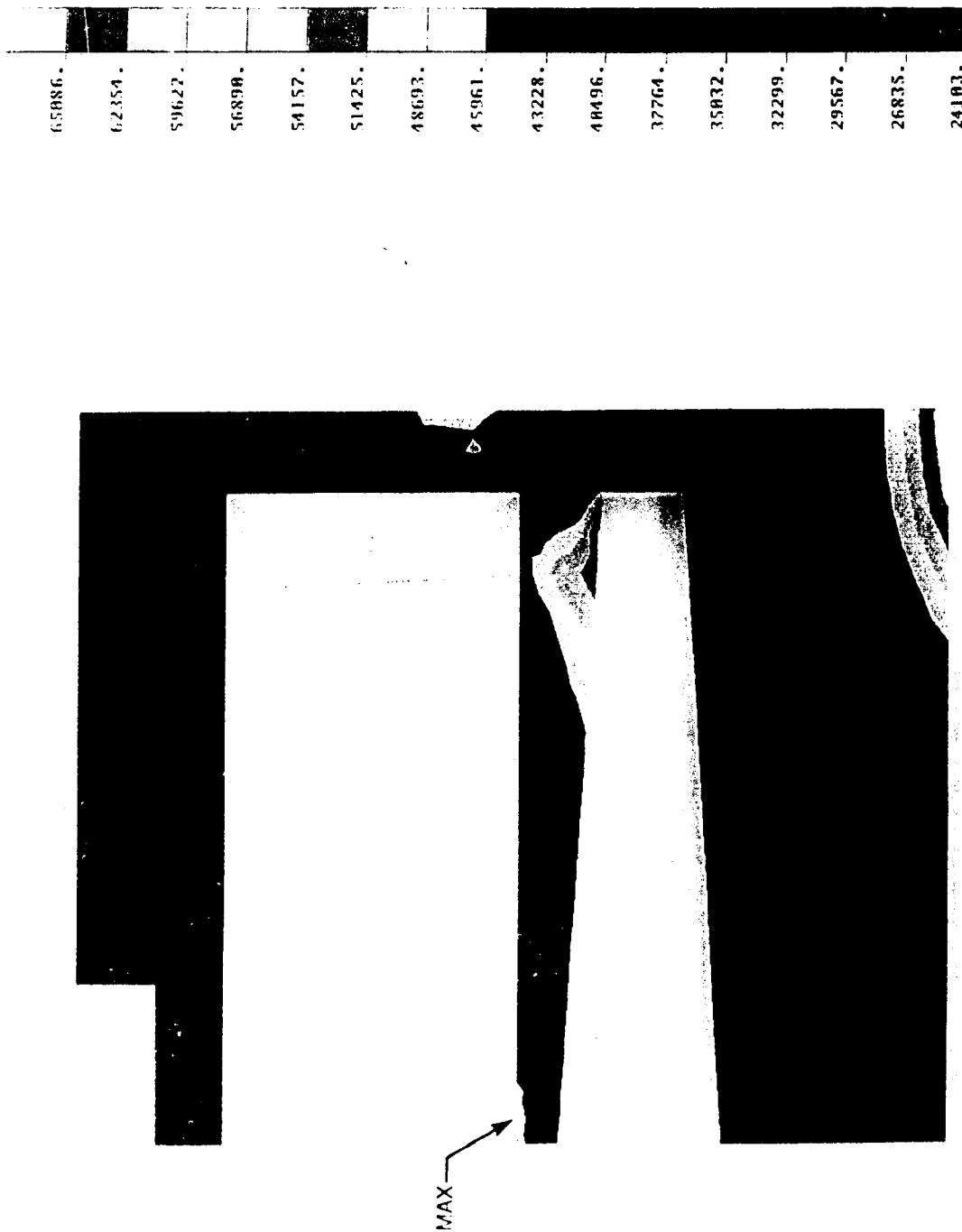


Figure B-11. The von Mises stress plot for scale-model housing central stiffener.

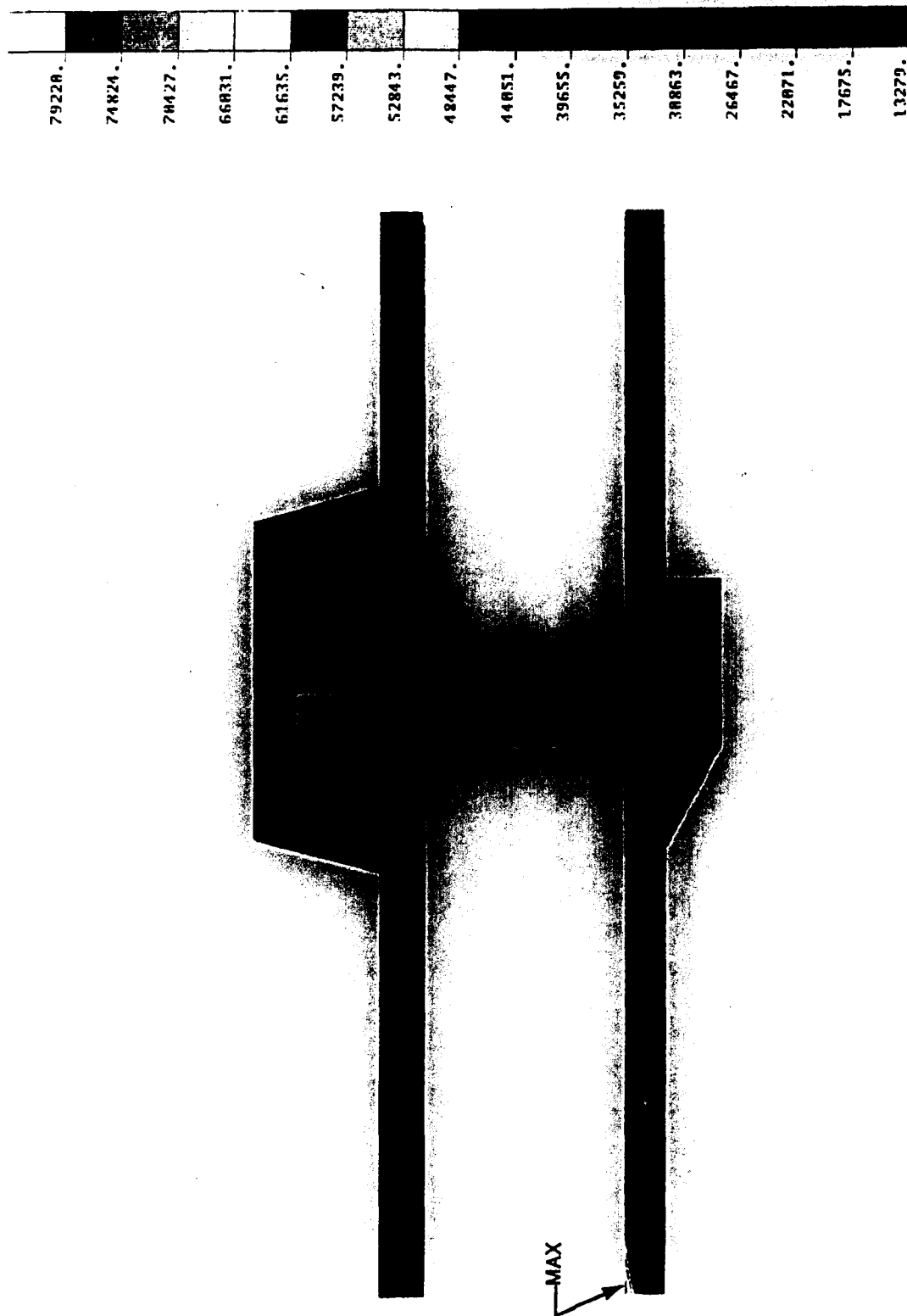
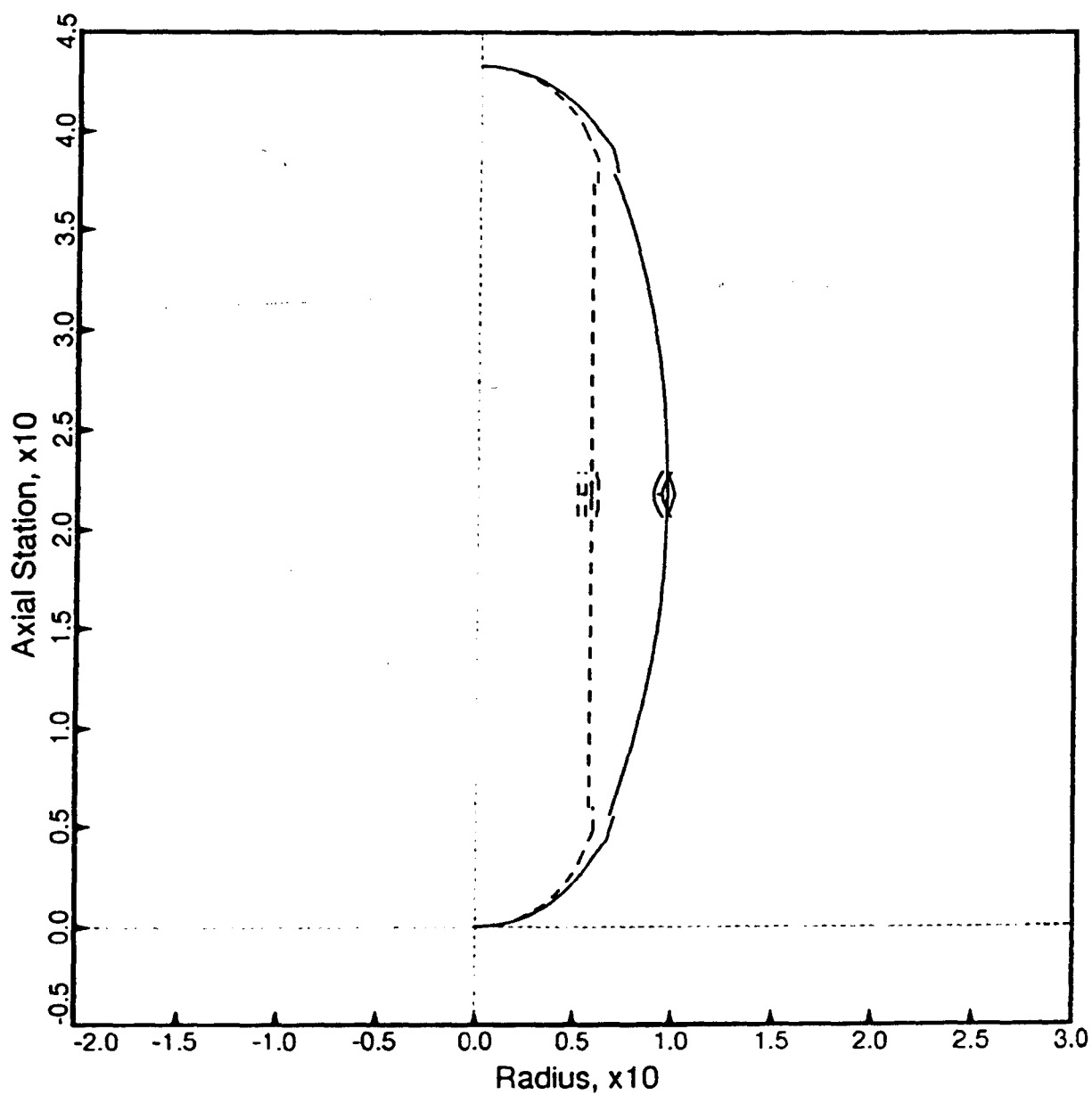


Figure B-12. The von Mises stress plot for scale-model housing hemisphere and cylinder end caps.



SCALE MODEL HOUSING $P_c = 12,208$ psi

Figure B-x13. N=2 buckled configuration of scale-model housing.

**APPENDIX C: FORMATION OF
FATIGUE CRACKS IN PLANE-
BEARING SURFACES OF CYLINDERS
AND HEMISPHERES**

FIGURES

- C-1. Maximum principal stress versus flange length.
- C-2. Maximum principal stress versus flange thickness.
- C-3. Maximum principal stress versus radial gap width.
- C-4. Maximum principal stress versus gasket thickness.
- C-5. Maximum principal stress versus ring thickness.
- C-6. Test arrangement for pressure cycling of cylinders.
- C-7. Dimensions of cylindrical ceramic test specimens.
- C-8. End cap for Type A cylindrical test specimens.
- C-9. End cap for Type B cylindrical test specimens.
- C-10. Bulkheads serving as spacers in the test rack for cylindrical test specimens.
- C-11. Bulkheads serving as end caps in the test rack for cylindrical test specimens.
- C-12. Components of the test rack for cylindrical test specimens.
- C-13. Test rack assembly of cylindrical test specimens.
- C-14. Jig for removal of bonded end caps from ceramic cylinders that were pressure cycled.
- C-15. Fatigue cracks on the surface of ceramic cylinders after 310 pressure cycles generating 64,000 psi bearing stress on the 0.2-inch-thick steel gasket.

TABLES

- C-1. Test results of NRaD gasket material study.

APPENDIX C: FORMATION OF FATIGUE CRACKS IN PLANE-BEARING SURFACES OF CYLINDERS AND HEMISPHERES

INTRODUCTION

The only factor limiting extensive application of ceramics to construction of external pressure housings is the short, cyclic fatigue life of plane-bearing surfaces on cylinders and hemispheres in contact with metallic rings joining these ceramic components into a housing. This is in sharp contrast with the long, cyclic fatigue life of ceramic inside the bodies of ceramic cylinders, or hemispheres at locations distant from the joints.

At locations distant from the plane-bearing surfaces, the cyclic fatigue life of alumina in a stress field defined by $-150,000$ psi hoop and $-75,000$ psi axial stresses in cylinders, and $-150,000$ psi hoop and $-150,000$ psi meridional stresses in hemispheres approaching infinity. Even if the stresses are increased to $-200,000$ psi, the cyclic fatigue life is still in excess of several thousand cycles.

On the plane ceramic bearing surfaces in contact with plane metallic surfaces, however, the cyclic fatigue life, as defined by appearance of spalling, usually is measured in hundreds, instead of thousands of cycles. Previous studies with glass and ceramic housing components have shown that the fatigue life of ceramic and glass components resting directly on metal surfaces rarely exceeds 1 cycle under bearing stresses equal to 50 percent, or 100 cycles equal to 25 percent of material strength in compression (references C-1, C-2, C-3, and C-4). At lower bearing stresses, the fatigue life becomes longer, but at the expense of added weight to the ceramic component. Clearly, some solution to the problem had to be found.

There are only two approaches to this problem. Either increase the tensile strength of the brittle material, decrease the radial tensile stress component on the bearing surface of the brittle material, or both. The first approach has been successfully applied only to glass, where, by chemical treatment, the surface of glass has been put into com-

pression. The $-30,000$ to $-90,000$ psi compression stresses generated on glass surfaces by chemical treatment prevent formation of microcracks, as the radial tensile stress component generated on the bearing surfaces by hydrostatic loading of the cylinder, or hemisphere rarely exceeds $+20,000$ psi. Glass components of pressure housings the surface of which have been placed chemically into compression have demonstrated infinite cyclic fatigue life (reference C-5).

REVIEW OF PAST STUDIES

Currently, a chemical process has not yet been developed that could place alumina-ceramic surfaces into compression. For this reason, the efforts of investigators have been directed, instead, toward reducing maximum principal stresses on the ceramic bearing surface in contact with the metallic joint. The techniques utilized for reduction of the tensile stress on the ceramic bearing surface are (1) insertion of a gasket between the mating surfaces and (2) confinement of the ceramic cylinders, or hemisphere edges, between metallic flanges on the joint ring (references C-1, C-2, C-3, C-6, and C-7). Both techniques have been found effective in extending the fatigue life of ceramic bearing surfaces by more than a factor of ten.

The confinement of glass or ceramic cylinder and hemisphere edges between metallic flanges on joint rings has been found quite effective in extending the fatigue life of ceramic housing components by significantly reducing the spalling of ceramic components at their edges. Raising the height of the metallic flanges from $0.5t$ to $3t$ (t = ceramic shell thickness) raises the cyclic fatigue life of alumina ceramic by approximately a factor of 10 (references C-7 and C-8). The increase in cyclic fatigue life of ceramic cylinders with edges that are seated in Mod 1 end caps with extended double flanges is due to the fact that lengthened flanges reduce the magnitude of maximum principal stress on the ceramic plane bearing surface (reference C-9). Flanges with lengths of about $2.5t$ appear to provide the lowest maximum principal stress on ceramic surfaces, while at the same time minimizing the weight of the flanges (figure C-1). Keeping the thickness of the flanges to ≤ 0.1 inch and the radial gap between ceramic shell and the

FEATURED RESEARCH

flanges to ≥ 0.02 inches also reduces the magnitude of maximum principal stress (figures C-2, C-3, C-4, and C-5). Also, joint rings fabricated from materials with high modulus of elasticity (i.e., steel) were found to be more effective in extending the fatigue life of glass or ceramic surfaces (reference C-1) than identical joint rings made from materials with low modulus of elasticity (i.e., aluminum). All NRaD studies, however, utilized either titanium, or high strength aluminum, because of housing weight considerations, even though it was known that the application of these materials would not maximize the cyclic fatigue of ceramic bearing surfaces.

Since the type of material in the gasket can make a significant difference in the cyclic fatigue life of glass or ceramic bearing surfaces extensive investigations have been conducted at many institutions to determine which gasket material is most effective in extending the cyclic fatigue life of ceramic housings (references C-8 and C-9). Evaluation of materials for their suitability to serve as bearing gaskets was usually performed in three stages.

In the screening stage the testing was conducted with solid ceramic specimens placed between titanium anvils covered with appropriate gasket material. Titanium was chosen for the anvils because the joint rings between ceramic components of the housing are also made from this material. Testing was conducted by repeated application of 70-kpsi axial loading to the test specimen. Testing was terminated when either spalling was observed on the edges of the cylindrical test specimen, or some small number of cycles were completed without visible spalling. Gaskets that failed, or caused the ceramic specimen to spall were dropped from further consideration.

The cyclic evaluation stage usually followed the screening stage. In this testing program, gasket materials that successfully passed the screening stage tests were subjected to a series of tests in which they were repeatedly subjected to axial compression between a ceramic block and a titanium anvil of the same dimensions as in the screening stage. The testing took place sequentially at -70 kpsi, -80 kpsi, and -90 kpsi bearing stress

levels in series, with 300 to 500 cycles being applied at each stress level.

The operational stage consisted of testing the gasket materials under simulated operational conditions (reference C-11). Circular gaskets were inserted into the annular cavity of titanium end caps that subsequently were bonded to the ends of alumina ceramic cylinders. The cylindrical test assembly was mounted between spherical metallic bulkheads and repeatedly pressurized externally until the desired stress level was generated on the bearing surfaces of ceramic cylinder. Pressure cycling was generally terminated when either spalling was observed on external surfaces of the ceramic component, or at least 300 cycles were completed without appearance of spalls on ceramic surfaces at the joint.

Thin gaskets of soft metals (lead, copper, aluminum) or soft plastics (polyethylene, polyvinyl, Teflon, Nylon, or discontinuous carbon fiber-reinforced fluorocarbon) did not provide any benefits; they generally caused the ceramic to fail in one to two cycles under 70-kpsi bearing stress. Thin gaskets of high-strength steel raised the load-carrying capacity of the ceramic bearing surfaces significantly over that of soft gaskets under single, but not multiple, load applications (references C-1 and C-9).

The material which was found to provide not only high load-bearing capacity (75 to 90 kpsi), but also cyclic fatigue life in excess of 500 cycles for both the gasket and the ceramic surfaces, is 0/90 GFR PEEK plastic composite. These gaskets are fabricated by laminating 8 plies of 0/90 graphite fiber tape with PEEK resin to form an approximately 0.04-inch-thick sheet suitable for cutting into diverse shapes with these properties:

PEEK-graphite

$$\begin{aligned}E_{\text{in-plane}} &= 7.4\text{E}6 \text{ psi} \\E_{\text{out-of-plane}} &= 1.4\text{E}6 \text{ psi} \\v_{\text{in-plane}} &= 0.33 \\v_{\text{out-of-plane}} &= 0.06 \\\alpha &= 0.3\text{E}-6 \text{ in/in/}^{\circ}\text{F} \\p &= 0.070 \text{ lbs/in}^3\end{aligned}$$

Composite gaskets fabricated from glass or graphite fiber-reinforced epoxy initiated spalling in

ceramic surfaces at less than 500 cycles in the 70-kpsi range of bearing pressures, and exhibited extensive wear on their surfaces. Gaskets fabricated from Spectra fiber-reinforced epoxy composite failed after only a few load cycles to 90-kpsi bearing pressure (reference C-9). Because of the rapid deterioration of epoxy matrix in gaskets fabricated from fiber-reinforced epoxy composites, such materials are not recommended for applications where they must serve as bearing gaskets under compressive loading in excess of 40 kpsi.

It was also found that a thin ≤ 0.01 in layer of epoxy trapped between the mating plane ceramic and titanium bearing surfaces inside a metallic end cap with high flanges serves as a competent gasket material for bearing stresses up to 100,000 kpsi. Ceramic surfaces resting on thin epoxy layers inside deep end caps did not exhibit any visible spalling, even after 500 loadings at 65-kpsi bearing stress level. For this reason, thin (i.e., ≤ 0.01 inch) epoxy layers can be substituted in many applications for the more cyclic fatigue-resistant, but also more-expensive, GFR PEEK gaskets. Although titanium appears to be the ideal material for construction of joint rings because of its resistance to corrosion and high-compressive strength-to-weight ratio, high-strength aluminum has been found to be a structurally acceptable substitute in applications where the ceramic housings is not exposed to seawater for long periods of time. The substitution of aluminum for titanium in end caps or couplings did not change the fatigue life of ceramic bearing surfaces resting on 0.01-inch-thick epoxy layer.

INVESTIGATION INTO REDUCTION OF SPALLING ON CERAMIC COMPONENTS

To explore additional materials for service as potential gaskets/cushioning materials between the ceramic and titanium bearing surfaces at joints between ceramic components of the pressure housing, a brief study was conducted with 8-inch OD 96-percent alumina-ceramic cylinders with ends that were encapsulated with epoxy adhesive in aluminum end caps (table C-1). Each cylinder utilized a different gasketing/cushioning material

between the ends of the ceramic cylinders and the aluminum end caps.

After closing off the ends of the cylinders with flat metallic bulkheads (figures C-6 through C-14), they were repeatedly externally pressurized to 13,000 psi. The resulting bearing loading on the gasket/cushion material varied from 63 to 68 kpsi depending on the wall thickness of the cylinder. Pressure cycling of the test cylinders continued, until either 310 cycles were accumulated, or spalling took place first.

Of the ten cylinders that were pressure tested, only four successfully withstood the 310 pressure cycles (table C-1). All cylinders supported by thick (0.25-inch) plastic gaskets, or a bed of alumina powder failed after one or two cycles. This was the case even with a glass-cloth-reinforced epoxy gasket. Those that survived the cycling regime without spalling utilized the following interface cushioning materials/bearing gaskets.

- Cylinder 5A GFR PEEK gasket, 0.040-inch thick, resting directly against the ceramic bearing surface, and bonded with <0.01 -inch-thick epoxy layer to the metal seat. The finish on ceramic bearing surface is 16 rms.
- Cylinder 6A Steel gasket, 0.02-inch thick, resting directly against the ceramic bearing surface and bonded with <0.01 -inch-thick epoxy layer to the metal seat. The finish on ceramic bearing surface is 2 rms.
- Cylinder 3A Epoxy layer, <0.01 -inch-thick, adhering to both the ceramic and metallic surfaces. The finish on ceramic bearing surface is 16 rms.
- Cylinder 4A Epoxy layer, 0.010-inch-thick, adhering to both the ceramic and metallic bearing surfaces. The finish on ceramic bearing surface is 2 rms.

Since it is not possible to inspect the condition of ceramic bearing surfaces through the metallic end caps, they had to be removed prior to inspection. This was accomplished with a special fixture that applied axial force to the end caps while one of them was heated with an electric plate (figure

C-15). After removal of the end cap, the ceramic bearing surface was cleaned with MEK, treated with dye penetrant, and visually inspected.

The first inspection took place after 100 cycles; the second after 310 cycles to 13,000 psi pressure loading. The 100-cycle inspection discovered fatigue cracking only on cylinder 6A, supported by thin steel gaskets on a 0.01-inch-thick epoxy layer (figure C-10). The 310 cycle inspection did not discover fatigue cracks on the bearing surfaces of cylinders 4A and 5A.

Cylinder 4A – ceramic surfaces ground to 2-rms finish, supported by a 0.01-inch-thick epoxy layer.

Cylinder 5A – ceramic surfaces ground to 16-rms finish, supported by a 0.04-inch-thick GFR PEEK composite gasket resting on a 0.01-inch-thick epoxy layer.

It would appear that crack-free 300-cycle fatigue life at –65,000 psi bearing loading can be achieved either by the insertion of an 0.04-inch-thick GFR PEEK gasket, or a 0.01-inch-thick epoxy layer, provided that the ceramic surface has been ground to 2-rms finish.

CONCLUSIONS

1. Experimental data generated by investigations at NRaD and other activities clearly demonstrates that
 - a. Metallic end caps with double flanges for seating and potting in the ends of ceramic cylinders and hemispheres with epoxy adhesive provide significantly longer fatigue life for ceramic bearing surfaces than end caps with only a single flange, or no flange at all.
 - b. The height of double flanges on metallic end caps influences the fatigue life of the ceramic bearing surfaces potted with

epoxy adhesive inside the annular space between the flanges with epoxy adhesives. Higher flanges result in longer fatigue life. The optimum height of flanges is approximately two-and-a-half times the thickness of the ceramic component potted in the end cap. At this flange height, the maximum principal stress on the plane ceramic bearing surface has been reduced to its lowest value, minimizing the potential for initiation of axial fatigue cracks. Further increase in height is only beneficial in suppressing the appearance of spalling on the ceramic surfaces above end cap flanges and the associated leakage, thus effectively extending the useful fatigue life of the ceramic component (i.e., absence of visible spalling). The NRaD Mod 1 design of end cap specifies flanges with height $\geq 3t$ to delay further the appearance of spalling and associated leakage into the housing interior.

2. The fatigue life of a ceramic component potted inside a Mod 1 double-flanged end cap is defined by three criteria:

Crack-free fatigue life—number of cycles required to generate first axial crack on ceramic bearing surface.

Spall-free fatigue life—number of cycles required to generate the first visible spall above the end cap flange. The number of cycles required to generate the first visible spall is considered, for all practical purposes, to be the end of a ceramic component's life; in this report, it is defined to be the fatigue life.

Implosion-free fatigue life—number of cycles required to catastrophically implode the ceramic specimen.

The three stages of cyclic fatigue life generally progress at this ratio to implosion:

X 0.2 - 0.3 TL X cracks appear on ceramic bearing surfaces.

X 0.5 - 0.8 Total Life X spalling appears above flanges.

X Total Life X implosion.

3. Placement of an interlayer between the mating bearing surfaces of the ceramic housing components and the metallic end caps, or coupling, has a significant effect on the fatigue life of the ceramic component. A layer, or gasket, of inappropriate material or thickness can reduce the fatigue life to 1 cycle, while the appropriate interlayer can extend it beyond 500 cycles.
4. Bearing surfaces on alumina-ceramic components of external pressure housings contacting GFR PEEK gaskets will survive a minimum of 500 pressure cycles without spalling provided that (1) the bearing loading at design pressure does not exceed -65,000 psi, (2) the edges of ceramic components are potted with epoxy inside Mod 1 end caps with double flanges of optimum length, and (3) the thickness of the gasket does not exceed 0.04 inch.
5. Bearing surfaces on alumina-ceramic components separated by a ≤ 0.01 -inch-thick layer of epoxy adhesive from the bearing surface of metallic joint rings will survive without spalling at least 500 cycles, and with some spalling at least 750 cycles, provided that (1) the bearing loading does not exceed -65,000 pounds, (2) the edges of ceramic components are potted inside Mod 1 end caps with double flanges of optimum length, and (3) the ceramic surfaces are ground to 2-rms finish.
6. Axial fatigue cracks may appear on ceramic plane-bearing surfaces after approximately 400 cycles at -65,000 psi bearing loading if supported by 0.01-inch-thick epoxy layer, and 300 cycles if resting on a 0.04-inch-thick GFR PEEK composite gasket.
7. It has not been conclusively shown that
 - a. Bonding of the GFR PEEK composite gasket to a ceramic plane-bearing surface with epoxy results in lower fatigue life than if the gasket was not bonded to the ceramic surface.
 - b. The cyclic fatigue life of bearing surfaces with 2-rms finish is significantly longer than of surfaces with 16-rms finish.

RECOMMENDATIONS

To maximize cyclic fatigue life of the ceramic components in pressure housing the following steps must be taken:

- a. The ends of ceramic components must be inserted into metallic seats with double flanges of $\geq 2.5t$ height (where t denotes ceramic shell thickness) and the gaps between the ceramic shell and flanges filled with epoxy adhesive.
- b. The ends of the ceramic components must rest either on a 0.04-inch-thick GFR PEEK gasket bonded to metallic seat, or an epoxy resin layer of 0.005- to 0.010-inch thickness adhering to the mating plane ceramic and metallic surfaces.
- c. The external edges of the metallic flanges must be sealed to the ceramic surfaces with a silicon, polyurethane, or polysulfide coating. An external elastomer boot may serve the same purpose.

REFERENCES

- C-1. Kvitka, A. L., and Diachkov. 1983. "Stress Composition and Strength of Containers From Brittle Non-Metallic Materials," Ukrainian SSR Academy of Sciences, Kiev.
- C-2. Pysarenko, G. S. 1989. "Strong Envelopes From Silicate Materials," Ukrainian SSR Academy of Sciences, Kiev.
- C-3. Collected articles. 1983. "Strength of Structural Elements From Glass and Glass Ceramics," Ukrainian SSR Academy of Sciences, Kiev.
- C-4. Stachiw, J. D., and K. O. Gray. 1970. "Glass Housing For Hydro-Space Lights and Instruments," American Society of Mechanical Engineers, Transactions ASME/Journal of Engineering for Industry, vol. 92, no. 1 (Feb).
- C-5. Stachiw, J. D. 1974. "Glass or Ceramic Spherical Shell Window Assembly for 20,000 psi Operational Pressure," NUC TR 393 (May). Naval Undersea Center, San Diego, CA.
- C-6. Stachiw, J. D., and J. L. Held. 1987. "Exploratory Evaluation of Alumina Ceramic Housings for Deep Submergence Service—The Second Generation NOSC Ceramic Housings," NOSC TR 1176 (Sep), Naval Ocean Systems Center, San Diego, CA.
- C-7. Stachiw, J. D. 1989. "Exploratory Evaluation of Alumina Ceramic Housings For Deep Submergence Service—Third Generation Housings," NOSC TR 1314 (Sep), Naval Ocean Systems Center, San Diego, CA.
- C-8. Stachiw, J. D. 1992. "Adhesive Bonded Mod 1 Joint with Improved Cyclic Fatigue Life For Ceramic External Pressure Housings—Fourth Generation Housings," NRaD TR 1587. NCCOSC RDT&E Division, San Diego, CA.
- C-9. Shields, W. 1992. "Ceramic/Metal Joint Design Report," Westinghouse Electric Corporation, Oceanic Division, Ocean Engineering Report 92-10 (Jul).
- C-10. Burke, M. A. 1991. "The Selection and Testing of a Gasket Material To Interface Between Ceramic and Metallic Pressure Vessel Components," Westinghouse Science and Technology Center, Document No. 91-8Tc3-GORDN-R1 (Aug).
- C-11. Farnworth, S. K. 1992. "Ceramic-Metal Joint Screening Test Report," Westinghouse Electric Corporation, Oceanic Division, Ocean Engineering Report 92 (Apr).

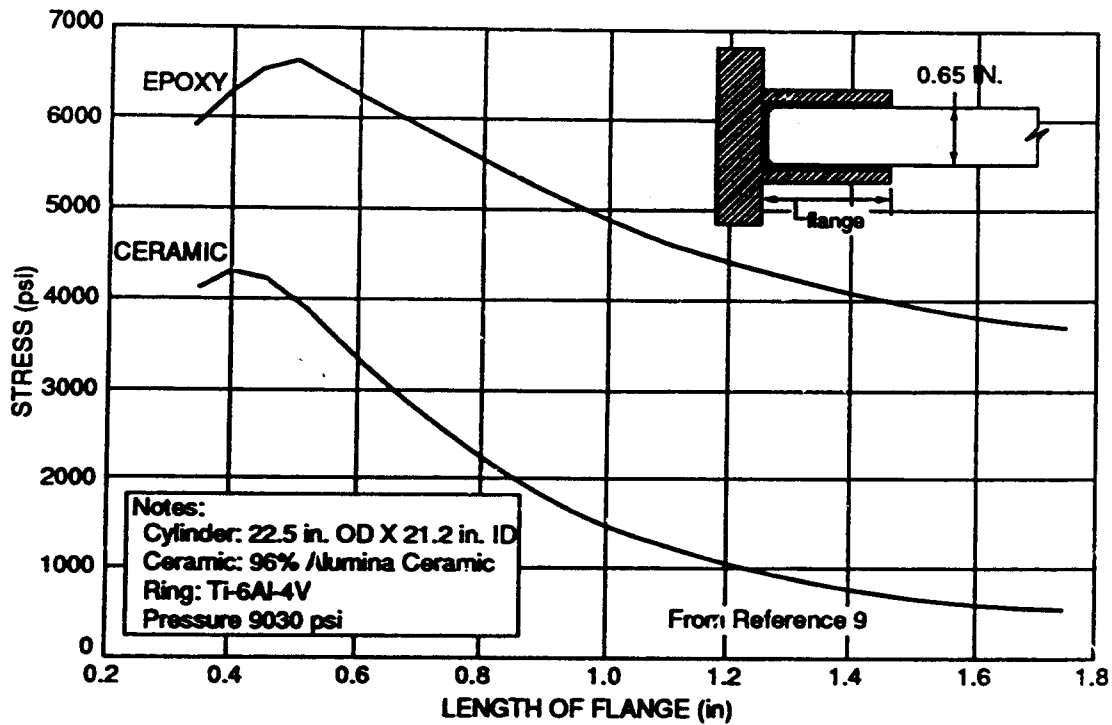


Figure C-1. Maximum principal stress versus flange length.

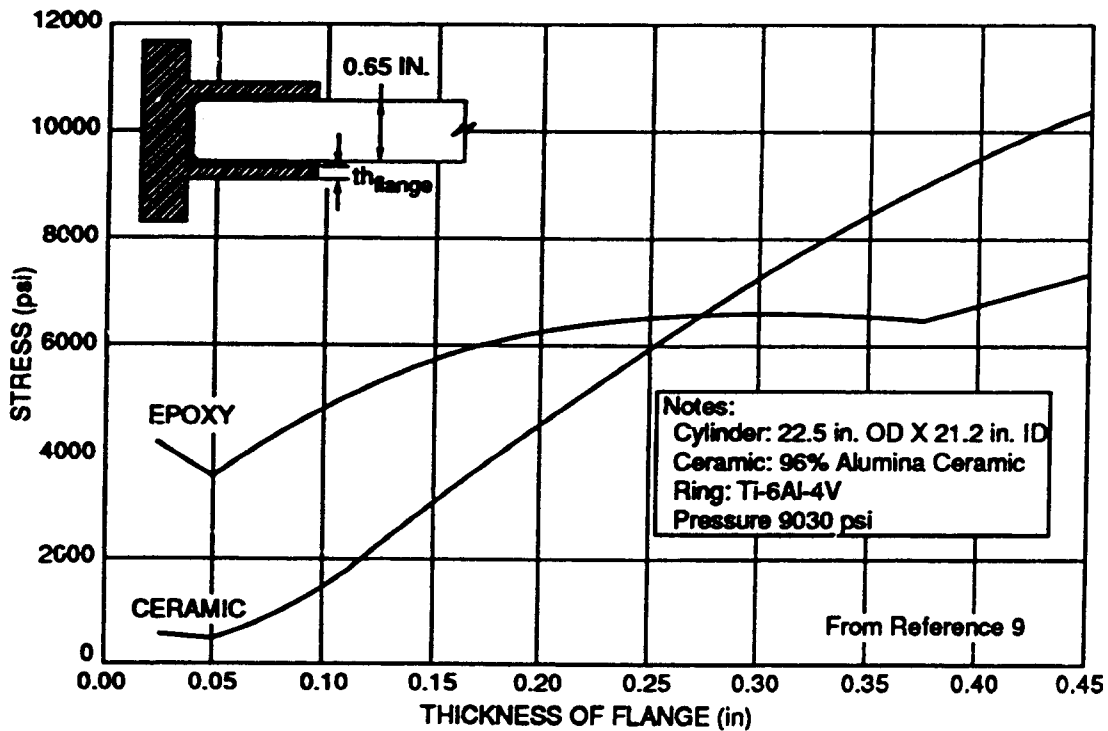


Figure C-2. Maximum principal stress versus flange thickness.

FEATURED RESEARCH

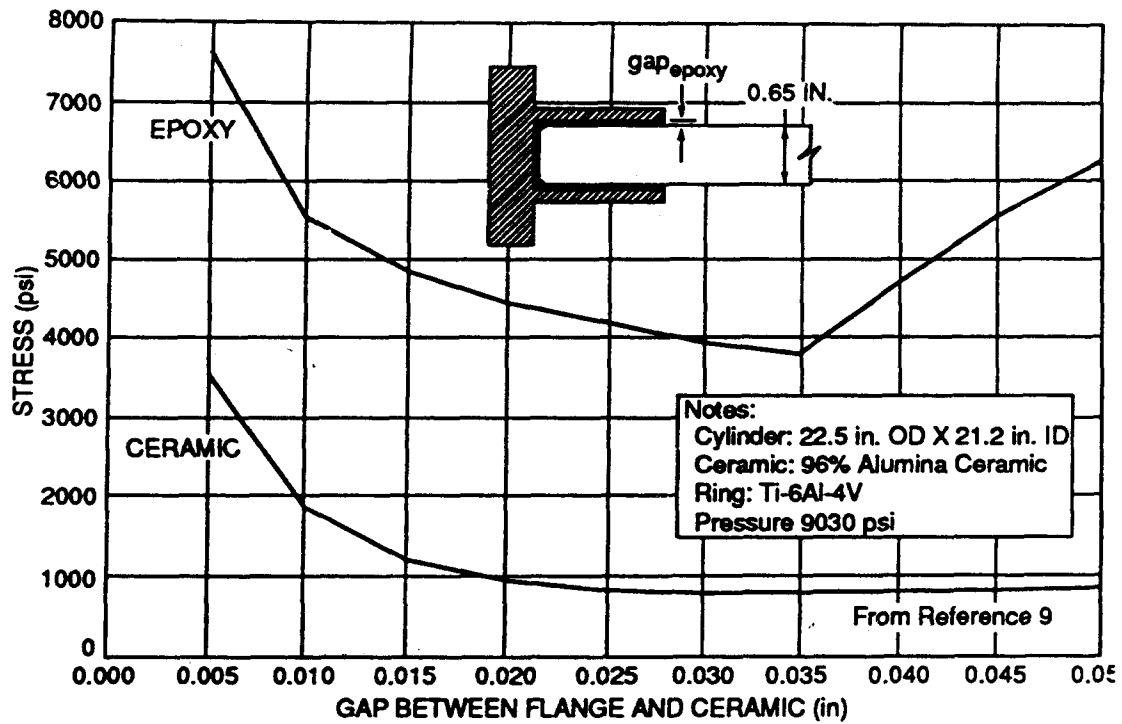


Figure C-3. Maximum principal stress versus radial gap width.

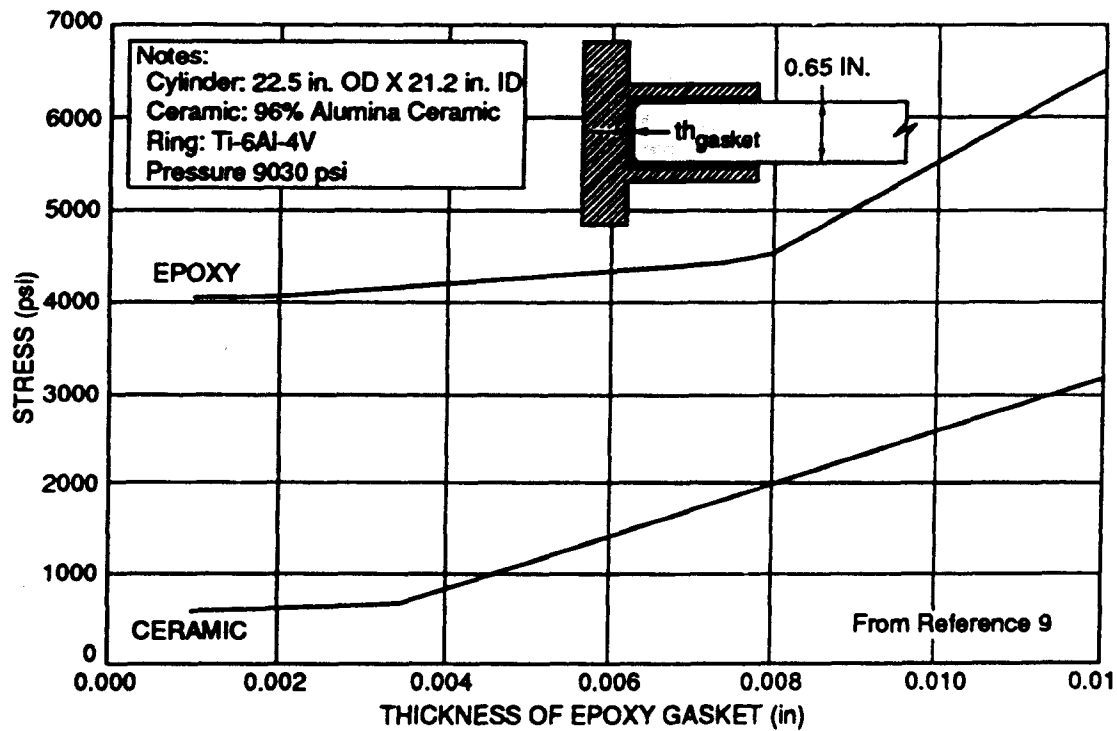


Figure C-4. Maximum principal stress versus gasket thickness.

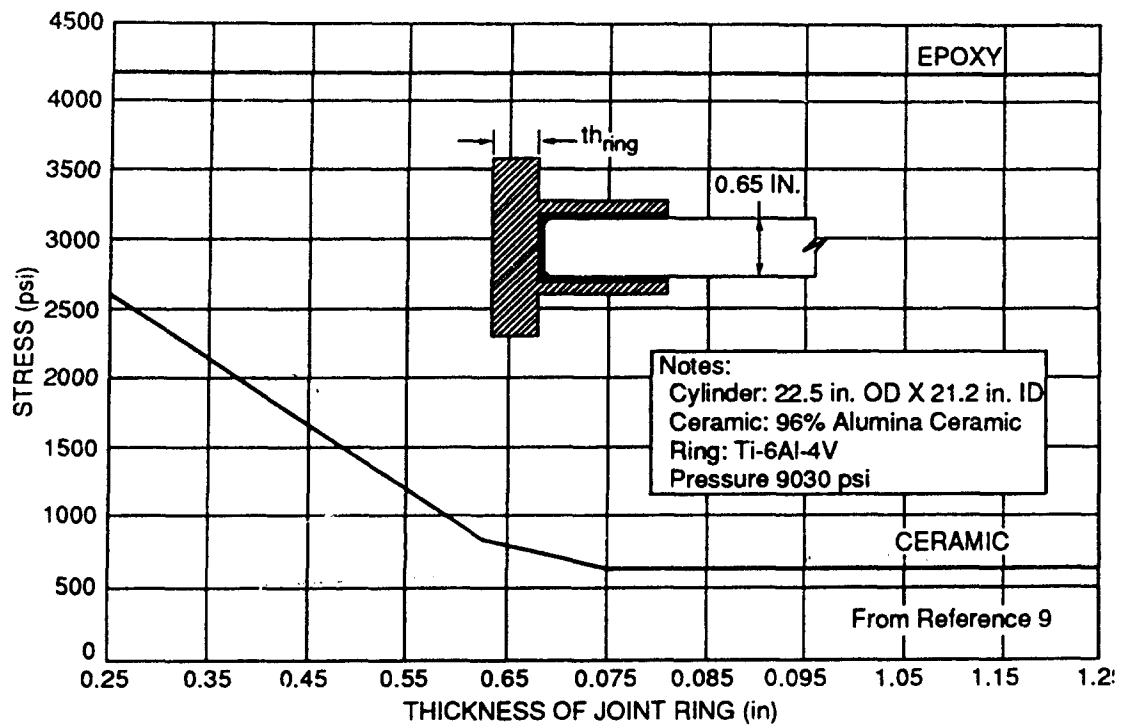


Figure C-5. Maximum principal stress versus ring thickness.

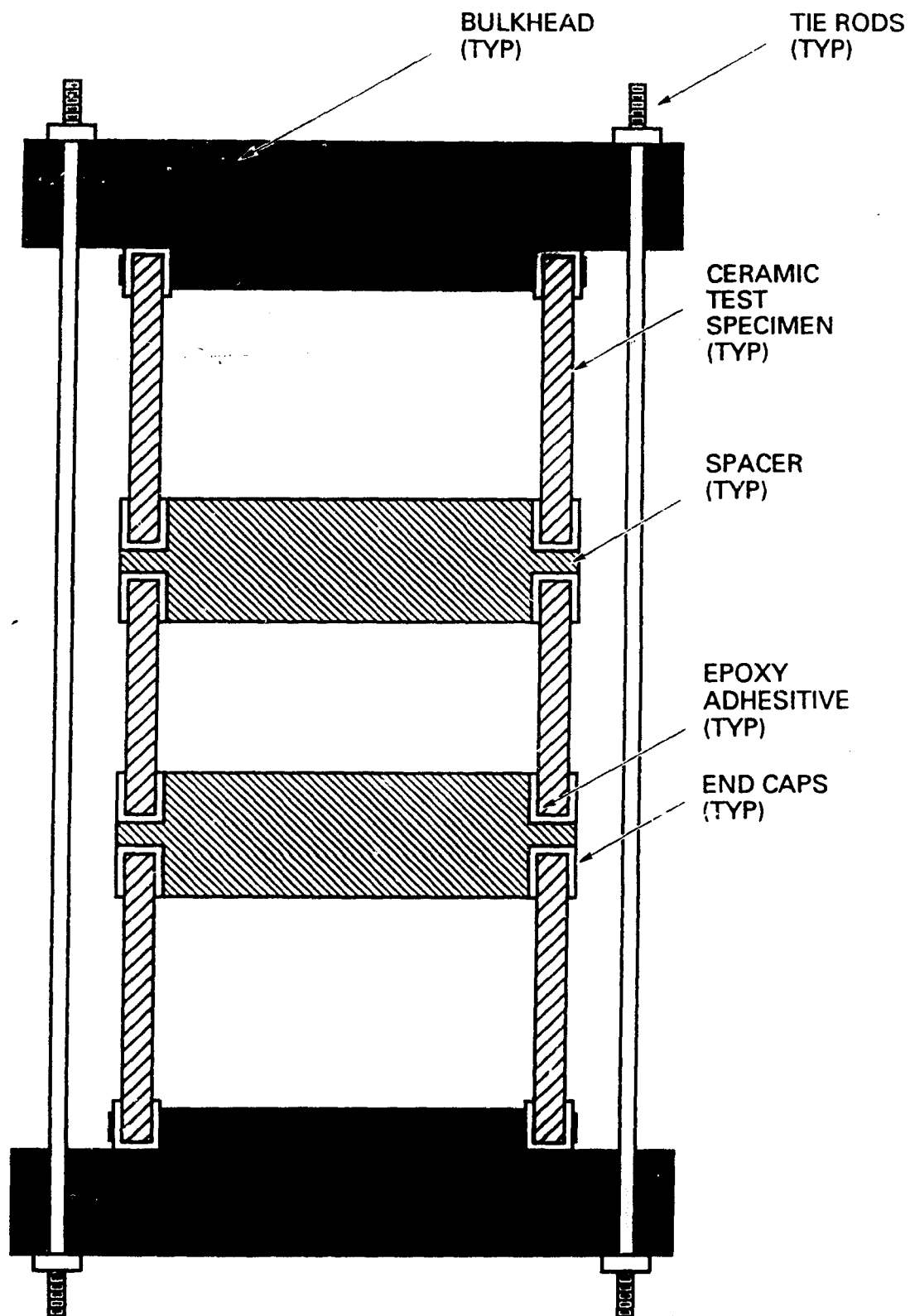
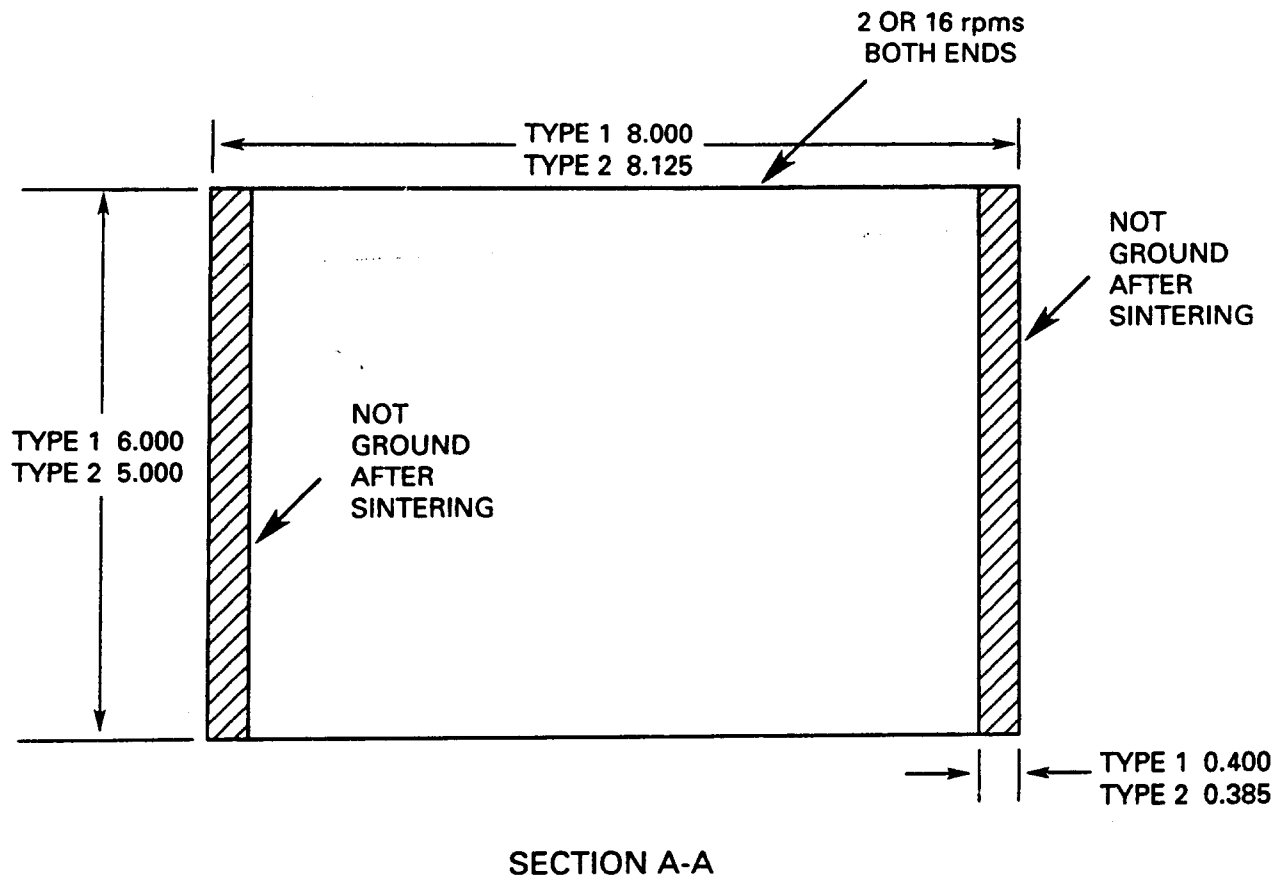


Figure C-6. Test arrangement for pressure cycling of cylinders.



MATERIAL: **96%** ALUMINA CERAMIC

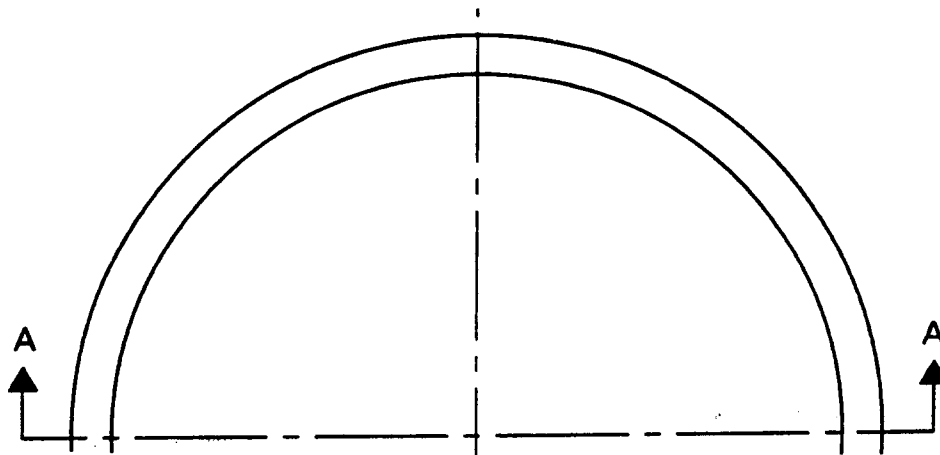
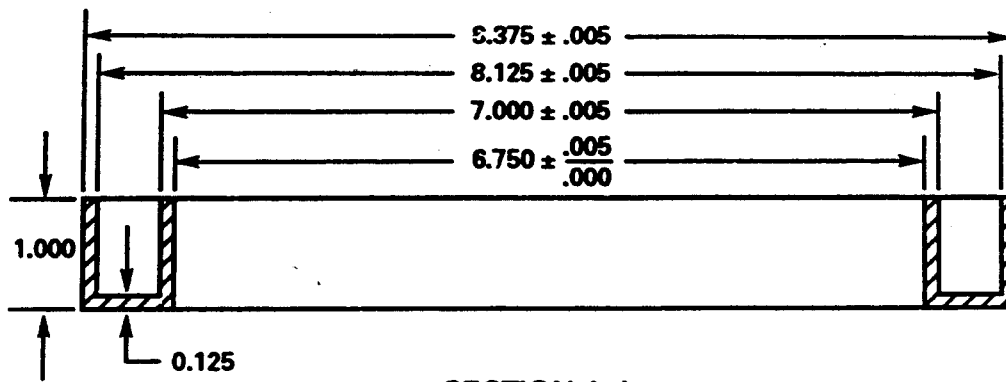
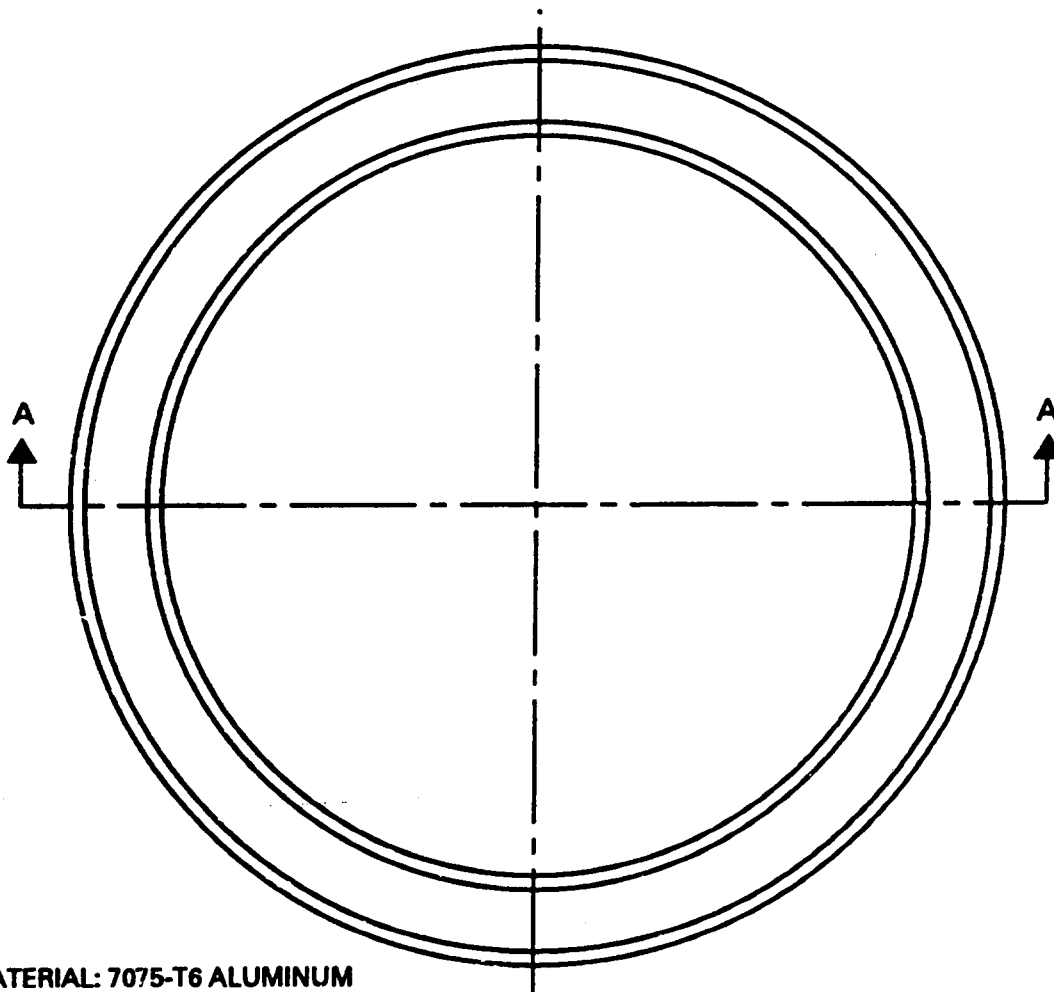


Figure C-7. Dimensions of cylindrical ceramic test specimens.

END CAP TYPE 1



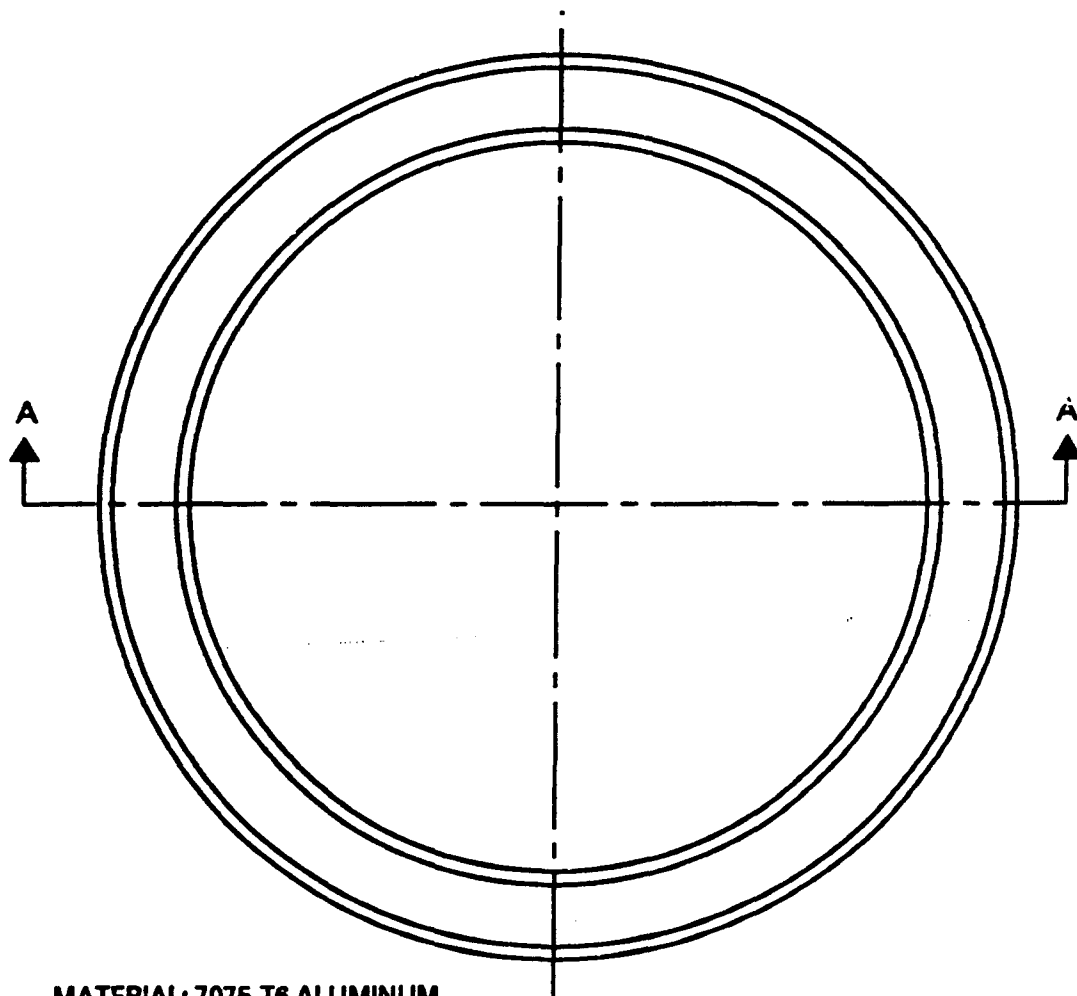
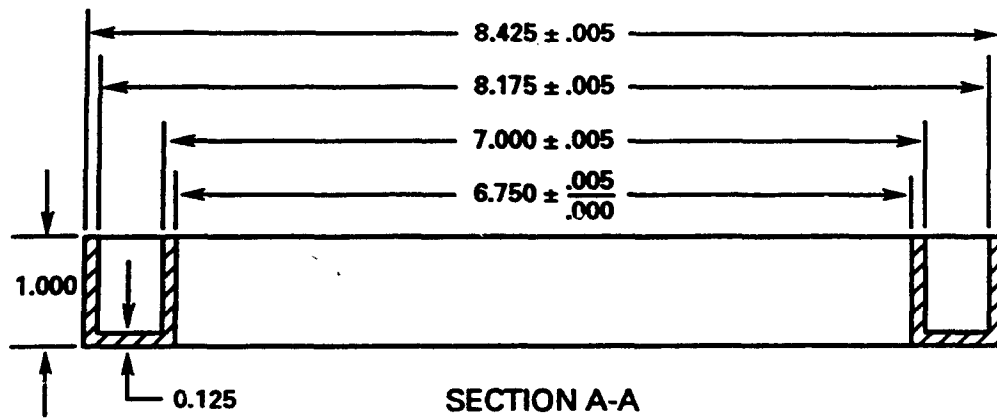
SECTION A-A



MATERIAL: 7075-T6 ALUMINUM

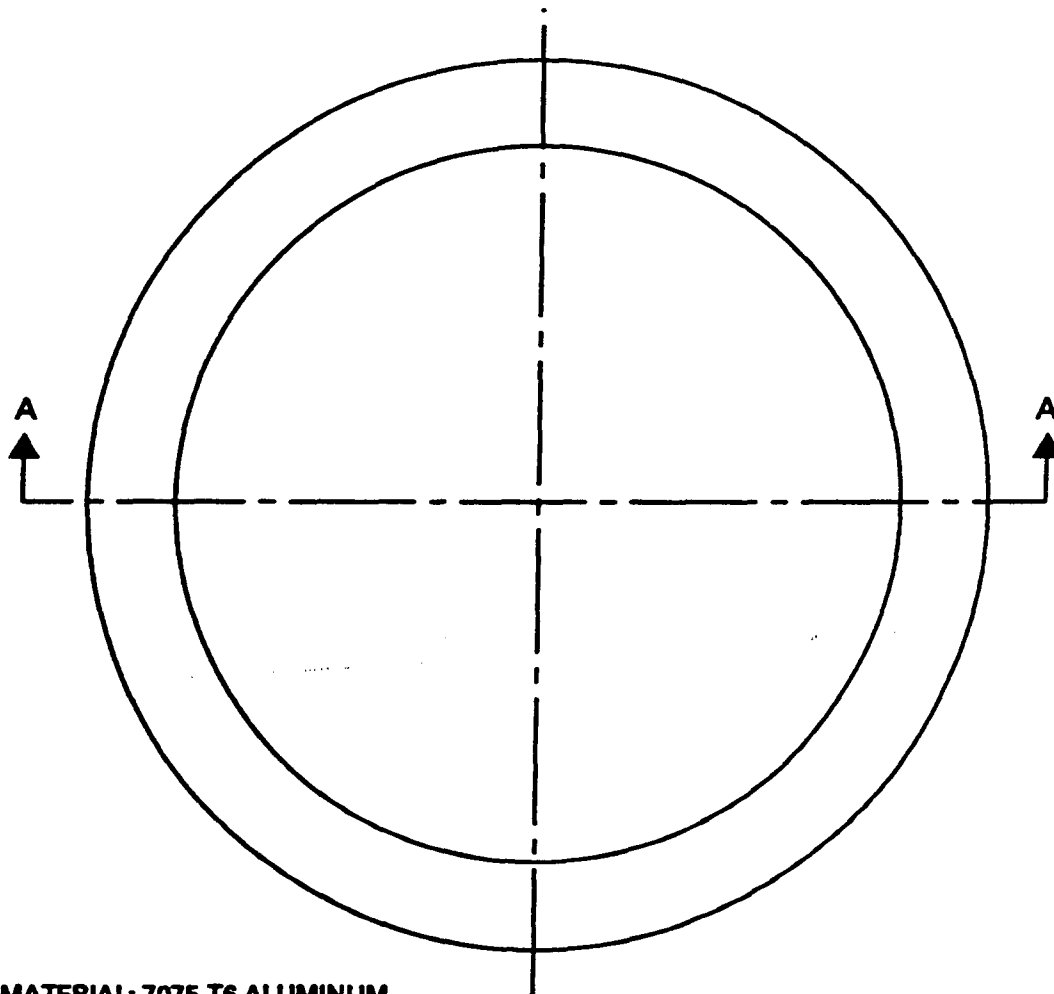
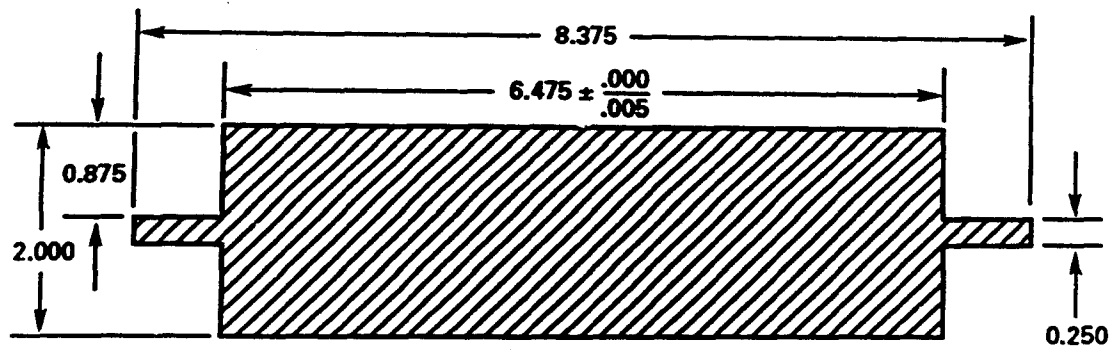
Figure C-8. End cap for Type A cylindrical test specimens.

END CAP TYPE 2



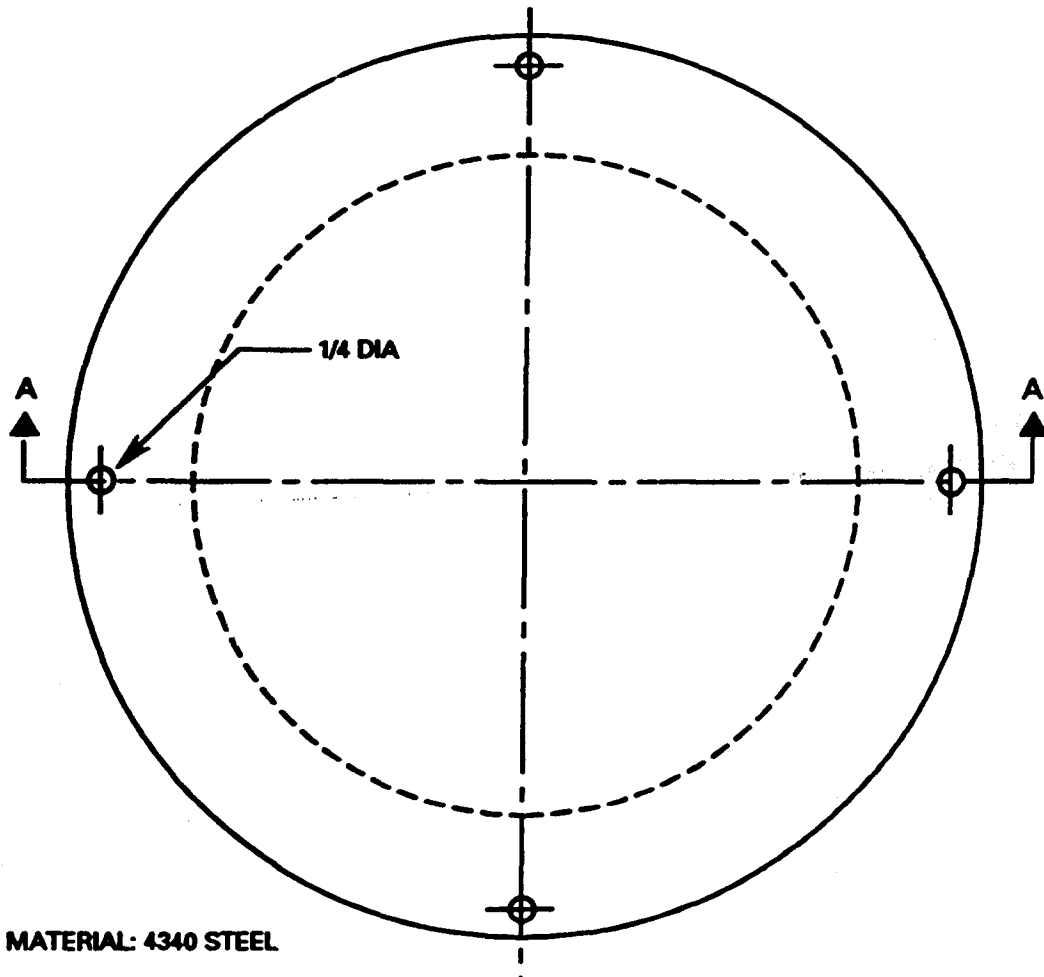
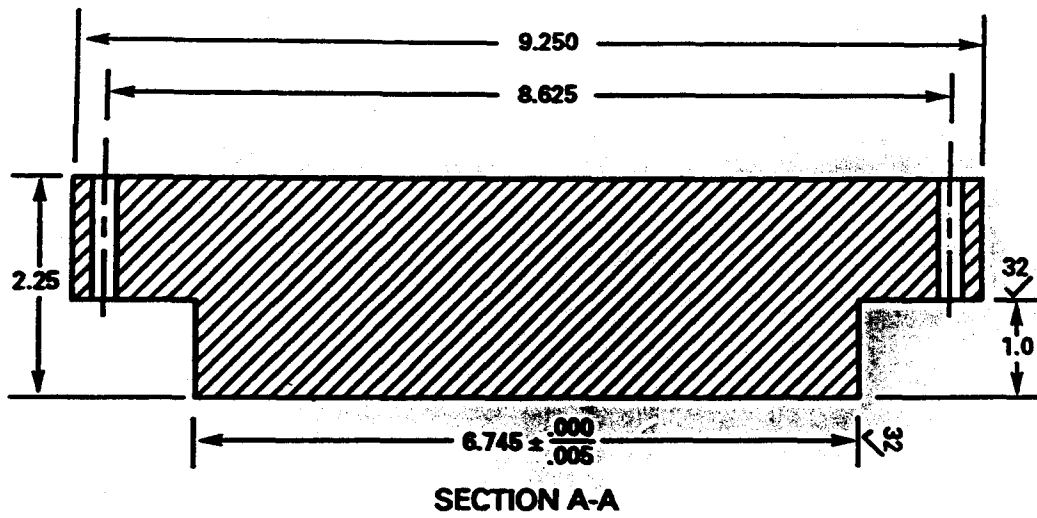
MATERIAL: 7075-T6 ALUMINUM

Figure C-9. End cap for Type B cylindrical test specimens.



MATERIAL: 7075-T6 ALUMINUM

Figure C-10. Bulkheads serving as spacers in the test rack for cylindrical test specimens.



MATERIAL: 4340 STEEL

Figure C-11. Bulkheads serving as end caps in the test rack for cylindrical test specimens.

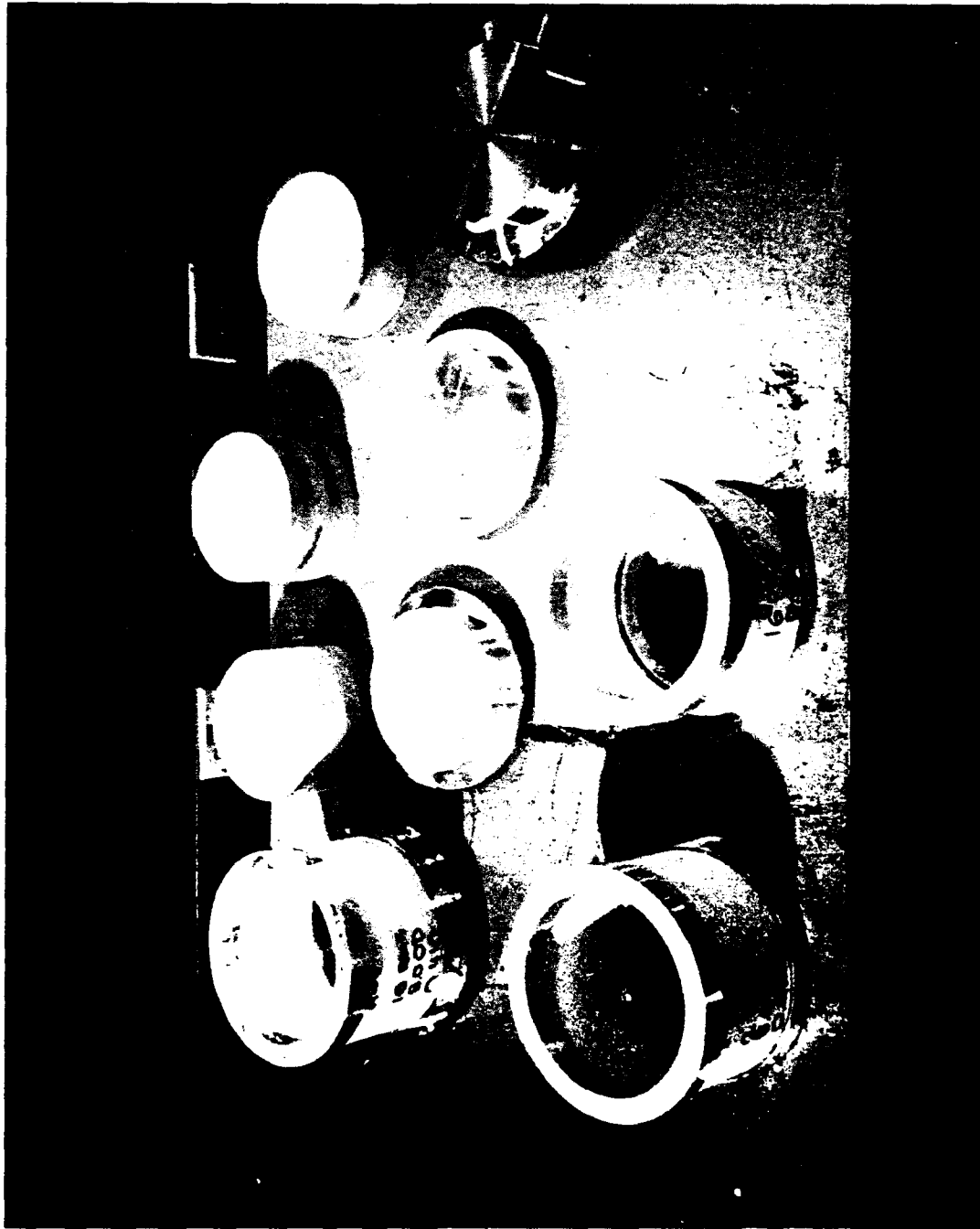


Figure C-12. Components of the test rack for cylindrical test specimens.

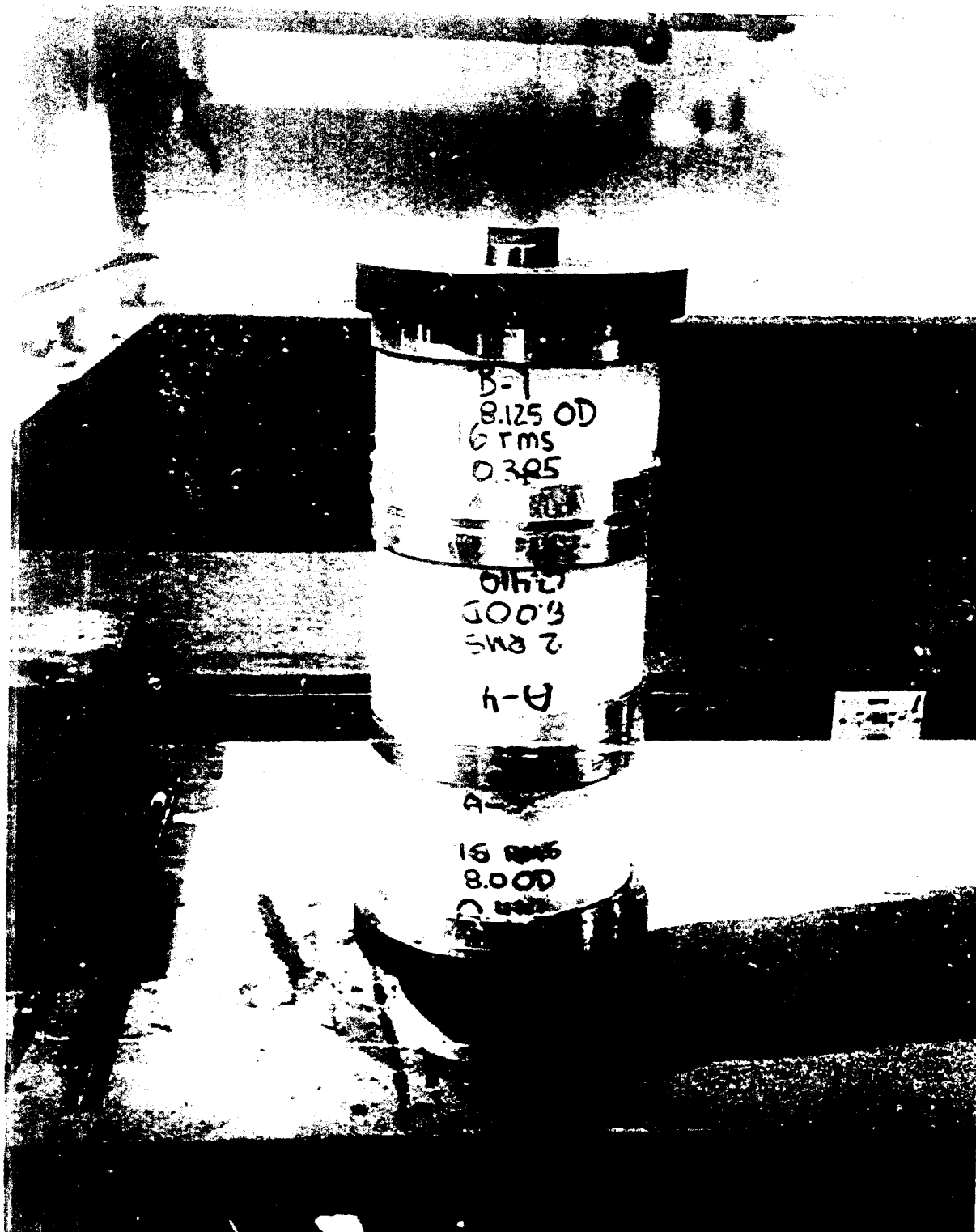


Figure C-13. Test rack assembly of cylindrical test specimens.



Figure C-14. Jig for removal of bonded end caps from ceramic cylinders that were pressure cycled.



Figure C-15. Fatigue cracks on the surface of ceramic cylinders after 310 pressure cycles generating 64,000 psi bearing stress on the 0.2-inch-thick steel gasket.

FEATURED RESEARCH

Table C-1. Test results of NRaD gasket material study.

<u>CYLINDER</u>	<u>BEARING INTERFACE</u>	<u>TEST DURATION</u>	<u>RESULT</u>
1A	2 RMS ceramic surface 0.25 in epoxy layer	1 cycle	End cap split
2A	16 RMS ceramic surface 0.25 in alumina powder	1 cycle	End cap split
2B	16 RMS ceramic surface 0.25 in epoxy plate G-10 glass fiber reinforced	2 cycles	End cap split
3B	16 RMS ceramic surface 0.25 in DELRIN plate	1 cycle	End cap split
6A	2 RMS ceramic surface 0.02 in steel gasket on 0.01 in epoxy layer	310 cycles	*Axial cracks on ceramic bearing surfaces
3A	16 RMS ceramic surface 0.01 in epoxy layer	310 cycles	*Axial cracks on ceramic bearing surfaces
4A	2 RMS ceramic surface 0.01 in epoxy layer	310 cycles	*No cracks on ceramic bearing surfaces
4B	As-fired ceramic surface 0.01 in epoxy layer	57 cycles	Failure of cylinder
5A	16 RMS ceramic surface 0.04 in graphite fiber reinforced PEEK gasket	310 cycles	*No cracks on ceramic bearing surface
5B	16 RMS ceramic surface 0.03 in glass fiber reinforced epoxy gasket G-10	310 cycles	*Axial cracks on ceramic bearing surfaces

NOTES: A Models - 127,000 psi max bearing pressure
OD = 8.0 in, L = 5.875, t = 0.410 in.

B Models - 150,000 psi max bearing pressure
OD = 8.125 in, L = 5.0 in, t = 0.385

*Observation of ceramic bearing gasket made after removal of metallic end cap.

**APPENDIX D: EFFECT OF
SACRIFICIAL END RINGS ON CYCLIC
FATIGUE LIFE OF CERAMIC
COMPOSITES**

FIGURES

- D-1. Cross-section of a Mod 1 end cap fitted with a sacrificial ceramic end ring.
- D-2. Cylindrical housing test assembly with a 12-inch OD 94-percent Al_2O_3 cylinder protected on one end with a sacrificial end ring.
- D-3. Dimensions of the ceramic components in the cylinder assembly.
- D-4. Components of the cylinder test assembly.
- D-5. Jig utilized in the removal of end caps from the ceramic cylinder.
- D-6. Typical cyclic fatigue crack observed on the bearing surface of the cylinder **protected** by a sacrificial ring after 534 pressure cycles to 10,000 psi.
- D-7. Fragments of the sacrificial ceramic ring after removal from the Mod 1 end cap.
- D-8. Typical cyclic fatigue crack observed on the bearing surface of the same cylinder **not protected** by a sacrificial ring.
- D-9. Ultrasonic C-scan of the cylinder end **not protected** by the sacrificial end cap.
- D-10. Ultrasonic C-scan of the cylinder end **protected** by the sacrificial ring.

APPENDIX D: EFFECT OF SACRIFICIAL END RINGS ON CYCLIC FATIGUE LIFE OF CERAMIC COMPOSITES

INTRODUCTION

Subsequent to the completion of the assembly and testing of the scale-model housing, a second housing utilizing a spare scale-model ceramic cylinder was assembled and tested to further investigate the fatigue life of ceramic components used in under-water pressure housings. The 500 cycles to 9,000 psi without failure achieved by the alumina-ceramic model housing hemispherical bulkhead using GFRP end gaskets was considered a very satisfactory performance. Yet, an alternative approach to the increasing cyclic life of ceramic housing components was developed that also was deemed worthy of investigation.

It has been shown that the fatigue life of ceramic hulls used for deep-submergence pressure housings is limited by circumferential cracks that originate from ceramic bearing surfaces and propagate axially into the ceramic shell wall. The structural integrity of the ceramic hull is compromised only when these cracks have propagated to the point where flakes of the ceramic wall spall off, allowing leakage and a reduction in the amount of material in the shell wall that can bear a compressive load. These cracks appear to originate on the bearing surfaces at the ends of ceramic hull components and are accentuated by tensile stresses that occur at this location due to the geometric and material discontinuities that exist between the ceramic hull and its metallic end cap rings.

There are several approaches that can be used to address this spalling phenomenon. One approach is to use materials with high-fracture toughness that are not susceptible to crack-growth-type problems. Another approach is to perform a detailed structural analysis of the joint region to reduce tensile stresses in the bearing surfaces of ceramic components by controlling the design variables that might cause the cracks to initiate. Yet another approach, as discussed in appendix C, is to employ gasket materials such as GFRP to protect

the bearing surfaces from which the circumferential cracks originate.

A new technique for limiting the effects of the spalling phenomenon is to bond a sacrificial ring to the end of the ceramic hull before assembly with a NOSC type Mod 1 (hereafter called Mod 1) end cap, as shown in figure D-1. This aids in isolating the region of the shell wall through which cracks propagate. Cracks that originate on the bearing surface between the ceramic ring and the metallic end cap are allowed to propagate through the ceramic ring, but are stalled at an epoxy interface between the ceramic ring and the remainder of the ceramic hull. Since the ceramic ring is entirely encapsulated by the metallic end cap ring, cracks are limited from propagating into any portion of the ceramic hull outside the end cap which reduces the chance for spalling to occur. This use of an interface as a crack barrier is a potentially effective means for providing extended fatigue life to a structure even if it is composed of brittle constituents such as ceramic and epoxy.

TEST ASSEMBLY

The ceramic ring and cylinder used in the assembled housing shown in figure D-2 were obtained by cutting a 0.50-inch-wide ring off one end of a 12.047-inch OD by 15.373-inch L by 0.434-inch-thick scale-model ceramic cylinder as shown in figure D-3, and then regrinding the new ceramic bearing surfaces. The bonding procedures for the Mod 1 metallic end cap rings were similar to those used for the scale-model housing, except that GFRP gaskets were not incorporated. Rather, a 0.10-inch-thick layer of epoxy was inserted between the metallic joint ring and bearing surface on the sacrificial ceramic ring. Similarly, a 0.10-inch-thick layer of epoxy was used to separate the other bearing surface on the sacrificial ceramic ring from the bearing surface on the ceramic cylindrical hull. These 0.010-inch-thick separations were obtained by placing 125-pound nonreinforced 0.010-inch-thick manila stock spacers between adjacent components during the epoxy bonding procedure. The opposite end of the ceramic hull did not have a sacrificial ceramic end ring, but was encapsulated with a Mod 1 end cap with a 0.010-inch-thick epoxy layer between the ceramic bearing surface and the metallic end cap.

Figure D-4 shows the sacrificial ceramic ring, ceramic cylinder, and both metallic end cap rings prior to assembly. Pressure testing of the hull assembly was performed using flat-steel bulkhead end closures as shown in figure D-2. Sealing of the entire assembly was maintained by O-ring face seals between the metallic end cap rings and steel end closures that were preloaded together using four external tie rods. Pressure testing of the assembled housing was performed in tap water at ambient room temperature. The pressure test consisted of 500 pressure cycles to an external pressure of 10,000 psi. After pressure testing, the housing was removed from the pressure vessel and disassembled for inspection.

TEST RESULTS

After removal from the pressure vessel, the metallic end caps were removed from the ceramic hull using the fixture shown in figure D-5. Removal of the end cap from the hull end with the sacrificial ceramic ring resulted in the sacrificial ceramic ring remaining embedded inside the end cap ring. Visual inspection of the embedded ceramic ring revealed that substantial circumferential cracks had propagated through the full thickness of the sacrificial ceramic ring up to surface of the 0.010-inch-thick epoxy layer. Visual inspection of the bearing surface of the ceramic cylinder adjacent to the sacrificial ring did not disclose any cracks. Later, with the aid of die penetrant, a single circumferential crack was discovered on the bearing surface of the ceramic cylinder adjacent to the sacrificial ceramic ring as shown in figure D-6. Thus, for the 500 pressure cycles completed, the 0.010-inch-thick layer between the ceramic ring and ceramic cylinder appears adequate enough to have isolated the main hull from the relatively high level of crack propagation that occurred in the sacrificial end ring.

The sacrificial ceramic ring was eventually removed from the Mod 1 end cap to determine the extent of the circumferential cracks that had formed during pressure cycling. The sacrificial ring contained enough circumferential cracks that it could be separated into the annular segments

shown in figure D-7 after its removal from the metallic end cap.

The Mod 1 end cap was removed from the other end of the ceramic cylindrical hull that was not protected by a sacrificial ceramic ring. Inspection of this end disclosed numerous circumferential cracks on the bearing surface of the cylinder as shown in figure D-8.

After removal of both metallic end caps, ultrasonic NDT of the ceramic cylinder was performed. The largest crack present at the cylinder end that had no sacrificial ceramic ring protection was found to extend to an axial depth of 5.5 inches into the shell wall from its bearing surface. Conversely, at the cylinder end adjacent to the sacrificial ring, the depth of the crack detected with die penetrant was determined to be approximately only 1 inch. Ultrasonic NDT indicated the presence of other smaller circumferential cracks at the protected end which could not be seen with the aid of die penetrant. Figures D-9 and D-10 represent ultrasonic C-scan results of both the cylinder end protected with a sacrificial ring and the cylinder end not protected with a sacrificial ring.

Comparison of figures D-9 and D-10 reveals the extent to which the sacrificial ring reduced the amount of crack damage at the cylinder end to which it was bonded. The total area of internal separations detected by ultrasonic C-scan was measured to be 30-square inches for the unprotected end, and 8.8-square inches for the protected end of the ceramic cylinder. The circumferential length of the deepest crack at the unprotected end was four times greater than the circumferential length of the deepest crack at the cylinder end protected with the sacrificial ceramic ring. At the same time, the depth of the crack on the unprotected end of the cylinder was five-and-one-half times greater than that at the protected end. This implies that the circumferential cracks had extended well out of the portion of the ceramic shell that was encapsulated by the end cap at the end where no sacrificial ceramic ring was present. The presence of substantially deeper cracks at the cylinder end that was not protected by a sacrificial ceramic ring implies that spalling and associated leakage of water would occur at this end first, as opposed to

the cylinder end that is protected by a sacrificial ceramic ring.

CONCLUSIONS

The use of sacrificial ceramic end rings in Mod 1 end caps shows promise as a technique that can be used to increase the number of pressure cycles to design depth that underwater pressure housings made from brittle materials, such as ceramics, can withstand without spalling.

RECOMMENDATIONS

Further tests should be performed to verify the results of this first test assembly. Additional tests should include not only scale-model cylinders with

12-inch outer diameters, but also full-size cylinders made of alumina ceramic. Since extensive pressure cycling data exists from prior testing programs conducted by NOSC on 20-inch OD ceramic cylinders, it is recommended that a 20-inch OD cylindrical test assembly be equipped with sacrificial ceramic rings and pressure cycled to failure. These tests would provide a relative comparison of the cyclic fatigue life that can be achieved by 20-inch OD housings to 9,000 psi design depths, both with and without sacrificial ceramic end rings. Periodic ultrasonic inspections of the cylinder ends during pressure cycling will provide information on the rate and extent of fracture plane growth for protected and unprotected ends.

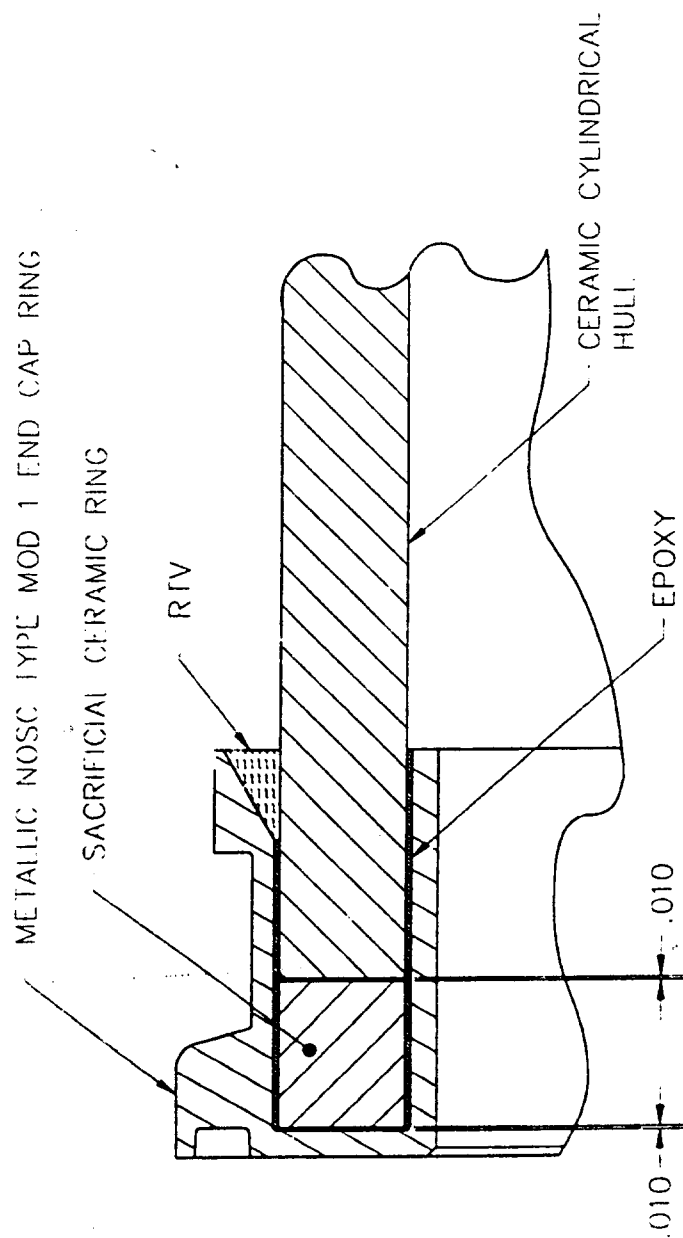


Figure D-1. Cross-section of a Mod 1 end cap fitted with a sacrificial ceramic end ring.

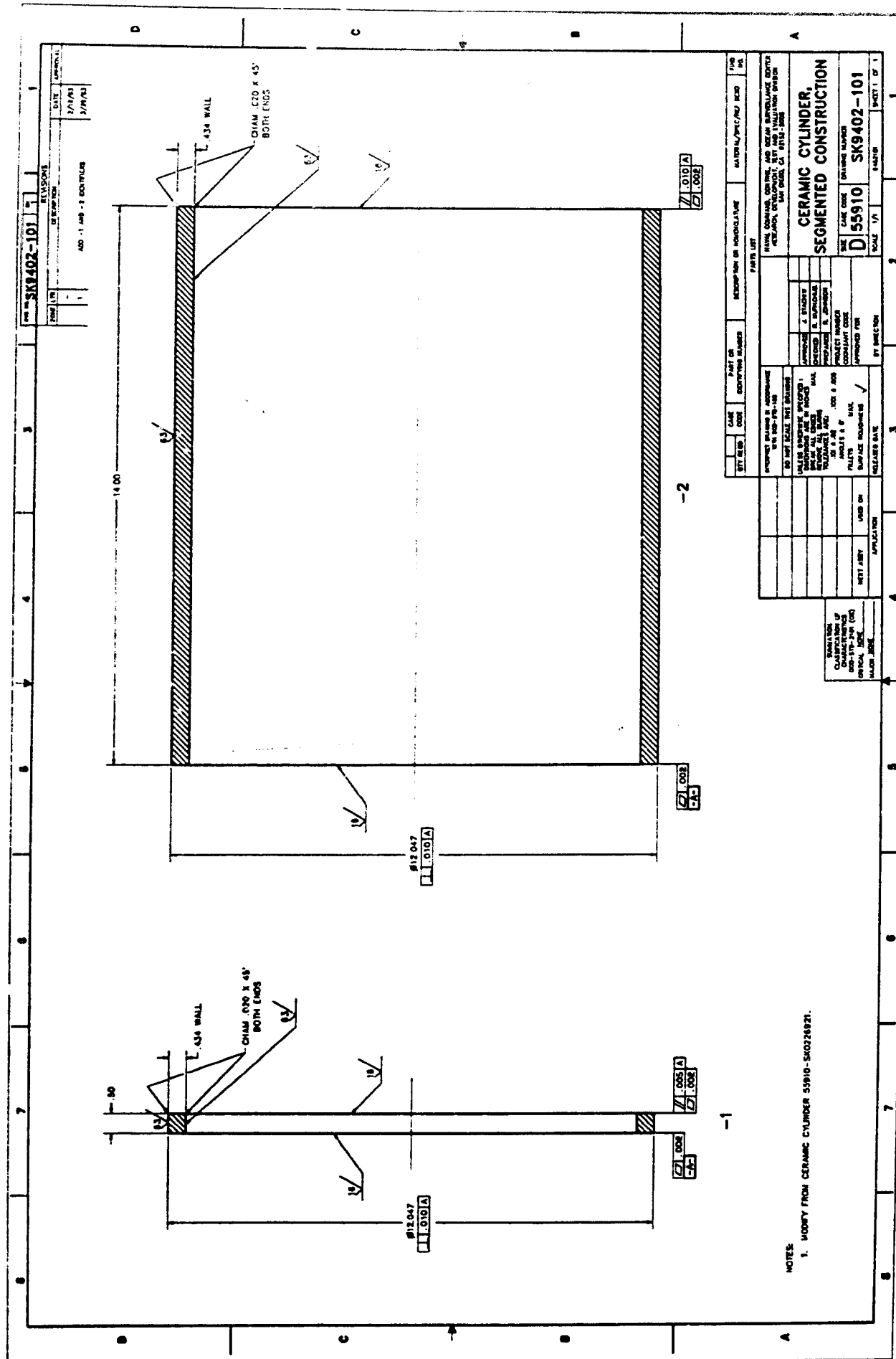


Figure D-3. Dimensions of the ceramic components in the cylinder assembly.

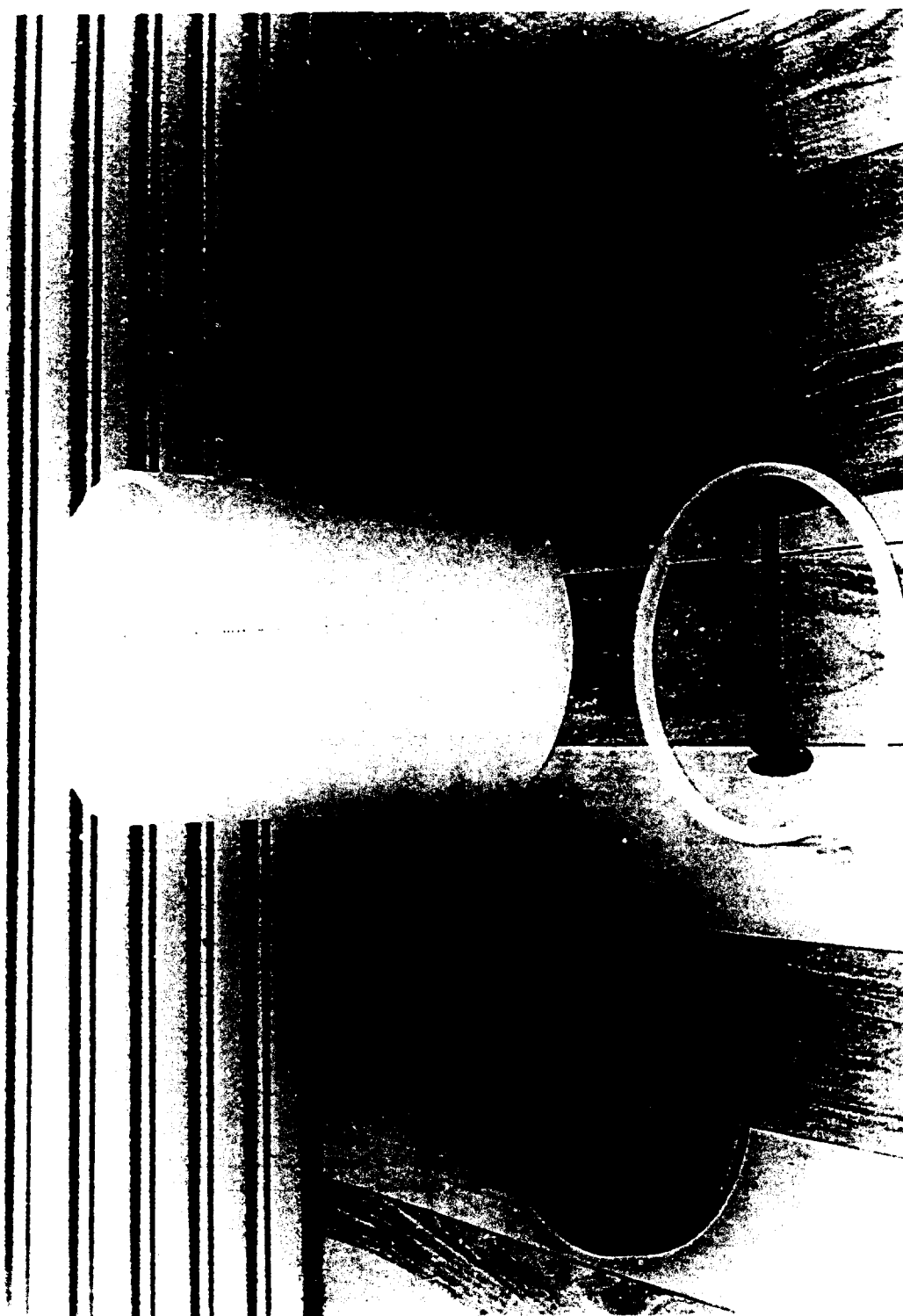


Figure D-4. Components of the cylinder test assembly.

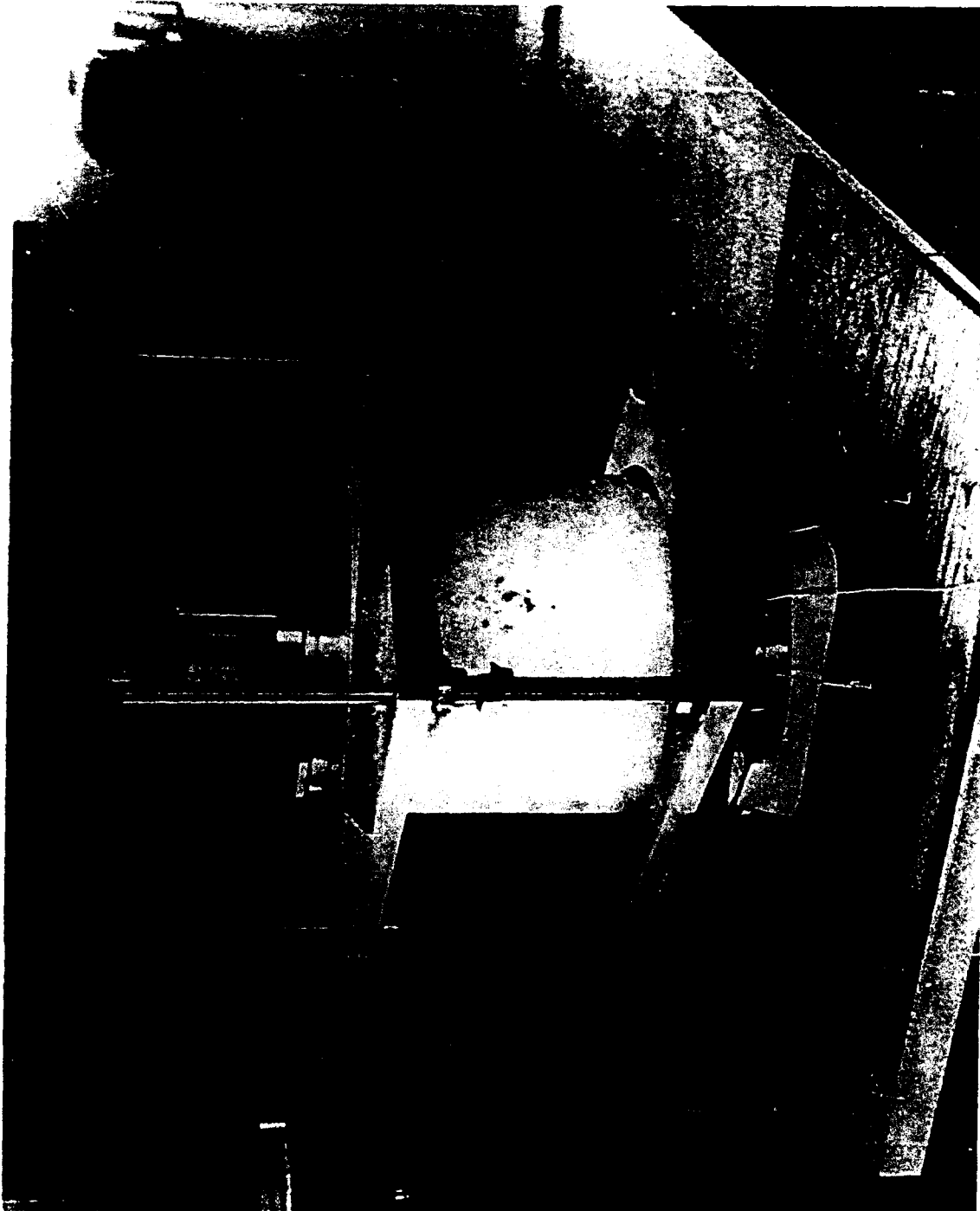


Figure D-5. Jig utilized in the removal of end caps from the ceramic cylinder.



Figure D-6. Typical cyclic fatigue crack observed on the bearing surface of the cylinder protected by a sacrificial ring after 534 pressure cycles to 10,000 psi.

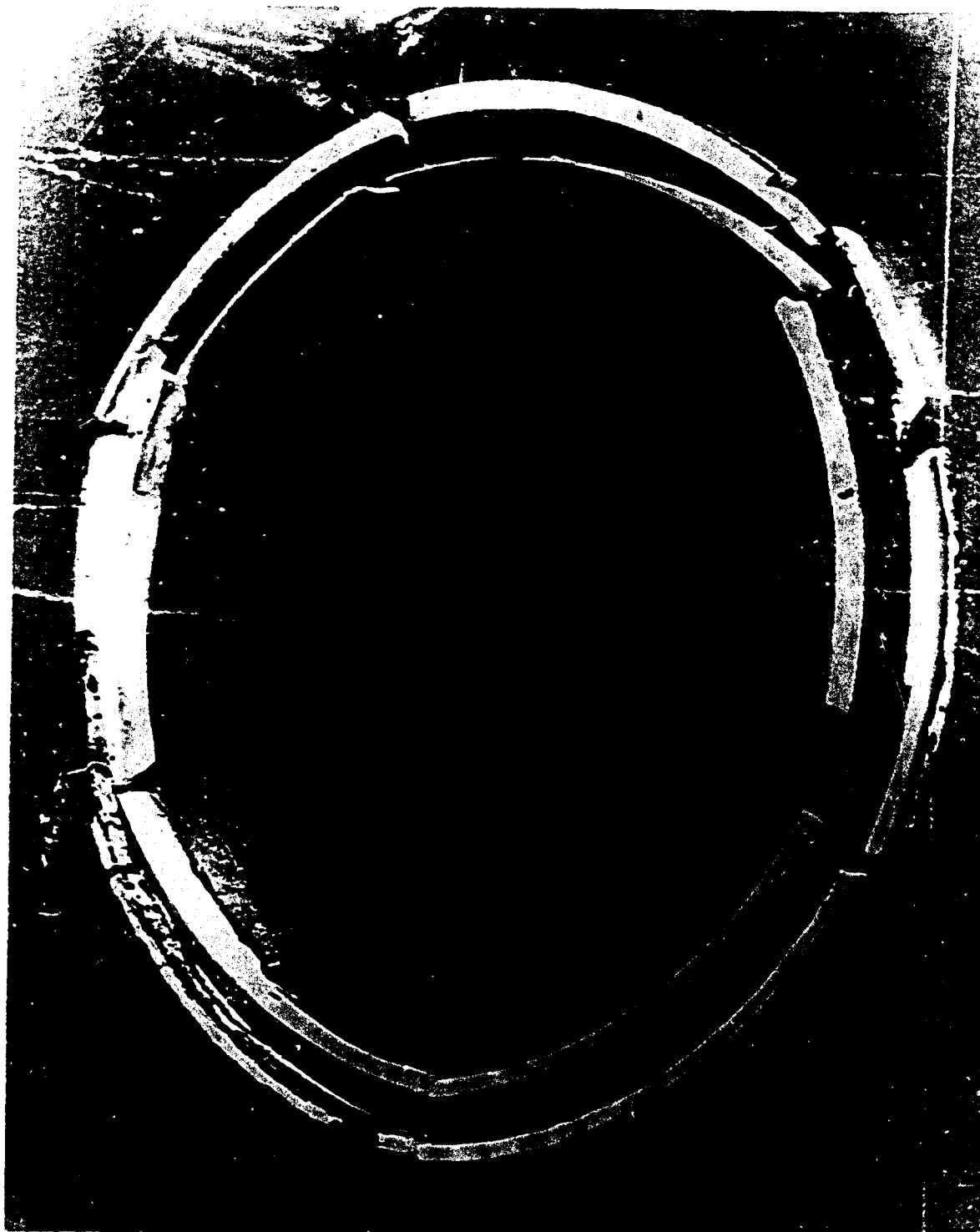


Figure D-7. Fragments of the sacrificial ceramic ring after removal from the Mod 1 end cap.



Figure D-8. Typical cyclic fatigue crack observed on the bearing surface of the same cylinder not protected by a sacrificial ring.

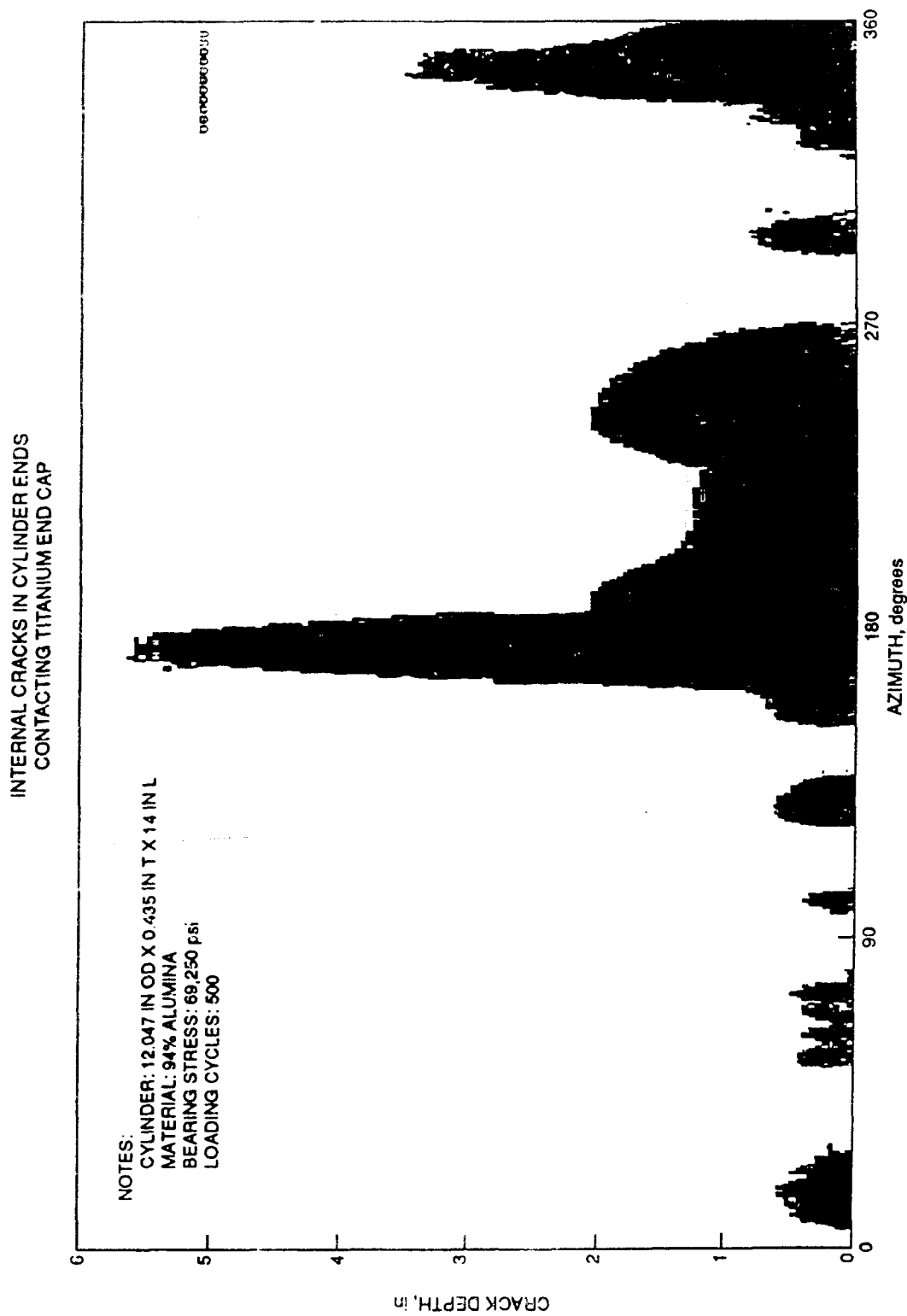


Figure D-9. Ultrasonic C-scan of the cylinder end not protected by the sacrificial end cap. Each degree of azimuth equals 0.1 of an inch on the external surface of cylinder.

INTERNAL CRACKS IN CYLINDER END
RESTING ON SACRIFICIAL CERAMIC RING

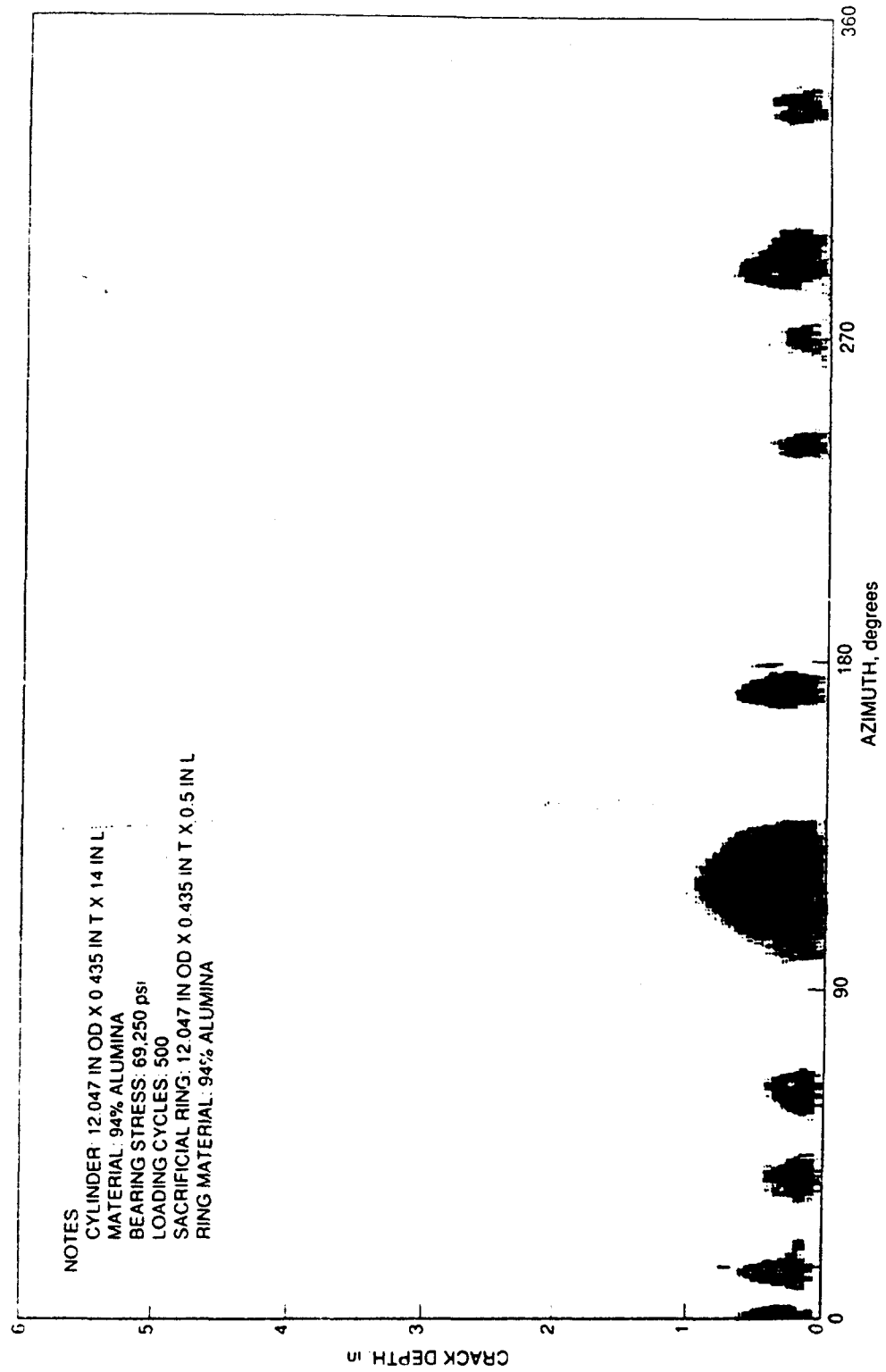


Figure D-10. Ultrasonic C-scan of the cylinder end protected by the sacrificial ring.

REPORT DOCUMENTATION PAGE

Form Approved
OMB No. 0704-0188

Public reporting burden for this collection of information is estimated to average 1 hour per response, including the time for reviewing instructions, searching existing data sources, gathering and maintaining the data needed, and completing and reviewing the collection of information. Send comments regarding this burden estimate or any other aspect of this collection of information, including suggestions for reducing this burden, to Washington Headquarters Services, Directorate for Information Operations and Reports, 1215 Jefferson Davis Highway, Suite 1204, Arlington, VA 22202-4302, and to the Office of Management and Budget, Paperwork Reduction Project (0704-0188), Washington, DC 20503.

1. AGENCY USE ONLY (Leave blank)		2. REPORT DATE March 1993		3. REPORT TYPE AND DATES COVERED Final	
4. TITLE AND SUBTITLE EVALUATION OF SCALE-MODEL CERAMIC PRESSURE HOUSING FOR DEEP SUBMERGENCE SERVICE Fifth Generation Housings				5. FUNDING NUMBERS PE: 0603713N PROJ: S0397 ACC: DN302232	
6. AUTHOR(S) J. D. Stachiw, R. P. Johnson, and R. R. Kurkchubasche					
7. PERFORMING ORGANIZATION NAME(S) AND ADDRESS(ES) Naval Command, Control and Ocean Surveillance Center (NCCOSC) RDT&E Division San Diego, CA 92152-6152				8. PERFORMING ORGANIZATION REPORT NUMBER TR 1582	
9. SPONSORING/MONITORING AGENCY NAME(S) AND ADDRESS(ES) Naval Sea Systems Command Washington, DC 20362				10. SPONSORING/MONITORING AGENCY REPORT NUMBER	
11. SUPPLEMENTARY NOTES					
12a. DISTRIBUTION/AVAILABILITY STATEMENT Approved for public release; distribution is unlimited.				12b. DISTRIBUTION CODE	
13. ABSTRACT (Maximum 200 words) The scale model of a 26-inch OD pressure housing assembly for service to a 20,000-foot (6,096-meter) depth was designed, subjected to structural analysis, fabricated from 94-percent alumina ceramic, instrumented with strain gages, and tested to destruction. The scale model consisted of two 12.047-inch OD by 15.375-inch L by 0.434-inch t (30.59-centimeter OD by 39-centimeter L by 1.1-centimeter t) monocoque cylinders of 94-percent alumina ceramic, joined by a titanium coupling with an integral T-ring stiffener, and closed off with two ceramic hemispherical bulkheads. The hemispherical bulkheads incorporated a short cylindrical skirt the thickness of which matched the wall thickness of the cylinders. The ends of both the cylinders and hemispheres were enclosed in Naval Ocean Systems Center (NOSC) Type Mod 1 titanium end caps bonded to the ceramic surfaces with epoxy adhesive. The scale model housing assembly successfully withstood a proof test to 10,000 psi (69 MPa) and 100 pressure cycles to 9,000 psi (62 MPa). In a separate test, one of the ceramic hemispheres from the housing was pressure cycled by itself 500 times to 9,000 psi (62 MPa) without appearance of surface spalling. When pressurized to destruction, the scale-model housing imploded at 11,933 psi (82.3 MPa). The scale-model housing assembly is capable of supporting in seawater a payload of 69 pounds. The structural design, selection of materials, fabrication process, and assembly procedure resulted in a ceramic pressure housing with a 0.61 weight/displacement ratio, acceptable for service to 20,000 feet (6,096 meters). The cyclic fatigue life of the ceramic components exceeded 500 pressure cycles to design depth. A titanium housing assembly with identical interior dimensions and safety margin at design depth would be approximately 42 percent heavier. The payload capacity of the ceramic housing is three times greater than that of the titanium housing assembly. Based on the structural performance of the 12-inch-diameter scale-model housing, the designs of the 25-inch-diameter structural components in the full-scale 26-inch-diameter external pressure housing assembly is considered to have been validated.					
14. SUBJECT TERMS ceramics external pressure housing ocean engineering				15. NUMBER OF PAGES 147	
				16. PRICE CODE	
17. SECURITY CLASSIFICATION OF REPORT UNCLASSIFIED	18. SECURITY CLASSIFICATION OF THIS PAGE UNCLASSIFIED	19. SECURITY CLASSIFICATION OF ABSTRACT UNCLASSIFIED	20. LIMITATION OF ABSTRACT SAME AS REPORT		

UNCLASSIFIED

21a. NAME OF RESPONSIBLE INDIVIDUAL J. D. Stachiw	21b. TELEPHONE (include Area Code) (619) 553-1875	21c. OFFICE SYMBOL Code 9402

THE AUTHORS



DR. JERRY STACHIW is Staff Scientist for Marine Materials in the Ocean Engineering Division of the Engineering Department. He received his undergraduate engineering degree from Oklahoma State University in 1955 and graduate degree from Pennsylvania State University in 1961.

Since that time he has devoted his efforts at various U.S. Navy Laboratories to the solution of challenges posed by exploration, exploitation, and surveillance of hydrospace. The primary focus of his work has been the design and fabrication of pressure resistant structural components of diving systems for the whole range of ocean depths. Because of his numerous achievements in the field of ocean engineering, he is considered to be the leading expert in the structural application of plastics and brittle materials to external pressure housings.

Dr. Stachiw is the author of over 100 technical reports, articles, and papers on design and fabrication of pressure resistant viewports of acrylic plastic, glass, germanium, and zinc sulphide, as well as pressure housings made of wood, concrete, glass, acrylic plastic, and ceramics. His book on "Acrylic Plastic Viewports" is the standard reference on that subject.

For the contributions to the Navy's ocean engineering programs, the Navy honored him with the Military Oceanographer Award and the NCCOSC's RDT&E Division honored him with the

Lauritsen-Bennett Award. The American Society of Mechanical

Engineers recognized his contributions to the engineering profession by election to the grade of Life-Fellow, as well as the presentation of Centennial Medal, Dedicated Service Award and Pressure Technology Codes Outstanding Performance Certificate.

Dr. Stachiw is past-chairman of ASME Ocean Engineering Division and ASME Committee on Safety Standards for Pressure Vessels for Human Occupancy. He is a member of the Marine Technology Society, New York Academy of Science, Sigma Xi and Phi Kappa Honorary Society.



RICHARD P. JOHNSON presently is an engineer with the Structural Mechanics, Analysis and Design Branch and Ocean Technology Branch. He has held this position since 1987. Before that, he was a Laboratory Technician for the Ocean Engineering Laboratory, Uni-

versity of California at Santa Barbara from 1985-1986, and Design Engineer in the Energy Projects Division of SAIC from 1986-1987. His education includes a B.S. in Mechanical Engineering from the University of California at Santa Barbara in 1986, and an M.S. in Structural Engineering from the University of California, San Diego, in 1991. He has published "Stress Analysis Considerations for Deep Submergence Ceramic Pressure Housings," *Intervention '92*, Marine Technology Society. He is a member of the Marine Technology Society.



RAMON R. KURKCHUBASCHE is a Research Engineer at the Naval Command, Control and Ocean Surveillance Center, RDT&E Division and has worked since November 1990 in the field of deep submergence pressure housings fabricated from ceramic materials. His education includes a B.S. in Structural Engi-

neering from the University of California at San Diego, 1989; and an M.S. in Aeronautical/Astronautical Engineering from Stanford University in 1990. His experience includes conceptual design, procurement, assembly, testing, and documentation of ceramic housings. Other experience includes buoyancy concepts utilizing ceramic, non-destructive evaluation of ceramic components. He is a member of the Marine Technology Society, and has published "Elastic Stability Considerations for Deep Submergence Ceramic Pressure Housings," *Intervention '92*, Marine Technology Society.